TEMPORAL-SPATIAL FUNCTIONAL ANALYSIS OF THE

CLASS-IIa1 MOTION DETECTION CELL OF THE FLY

<u>CALLIPHORA PHAENICIA</u>

Thesis by

Michael Yih-Hwa Jin

In Partial Fulfillment of the Requirements

for the Degree of

Doctor of Philosophy

California Institute of Technology

Pasadena, California

1981

(Submitted September 23, 1980)

ACKNOWLEDGEMENTS

ABSTRACT

The physiology of the horizontal motion detection cell class-IIa1 of the fly _Calliphora phaenicia_ was studied by extracellular recording. The receptive field was treated as a multi-input single output system such that Volterra-Wiener functional formalism could be used to describe the input-output relation. The present work has three objectives: (1) To study the functional of a subunit called the basic motion detection unit. Interpretation of the kernel's features was obtained by comparing it with the results of transient type stimuli. (2) To investigate the organization of the nonlinear spatial interactions in relation to the hexagonal array of visual elements along the horizontal and vertical lines of symmetry. Two sets of experiments were done to find the difference in the organizations of this interaction under light and dark adapted conditions. (3) To investigate the binocular interaction between two class-IIa1 cells each located in different lobes.

The basic motion detection unit could be modeled by two first and second order self kernels, which are associated with their two channels, and a cross kernel. The modeling response of a single channel is dominated by the contribution from the second order self kernels, because the receptive field is of on-off type. The cross kernel predicts the multiplication-like directionally selective motion response. Both white noise and transient type stimuli confirmed that an excitatory effect as well as an inhibitory effect exist when stimulus patterns move in the forward direction and backward direction, respec-

tively. The cross kernel model can be thought of as a correlation model which has delay type linear filters (instead of differential and integration type filters). An inhibition model with four types of inhibitory interactions was developed which adequately explained the function of this basic motion detection unit.

Horizontally and vertically aligned eight-stripe white noise patterns were used to investigate the receptive field organization. Under dark adapted conditions the interaction was limited to six adjacent columns and rows. The horizontal cross kernels reveal directionally selective characteristics and have significant 'weights' for those describing the interactions between one column and the nearest four adjacent columns. The vertical cross kernels show a mutually excitatory effect, which could be the evidence of neural pooling of photoreceptors. Under light adapted conditions two major differences appeared. They are: (1) Only two horizontal cross kernels, which describe the interactions between one column and the nearest two columns, have significant 'weights'. The interactions outside this range show reversed directionally selective characteristics. (2) All horizontal and vertical cross kernels have negative diagonal components which indicate a mutually inhibitory effect. This could be a nonlinear sensitivity control mechanism. All the above results were studied with monocular preparation.

The binocular interaction was studied by stimulus patterns located both within the binocular region and outside it. The results confirmed that a mutually inhibitory relationship exists between the class-IIa1 cell and its mirror image in the opposite lobe.

TABLE OF CONTENTS

CHAPTER I

INTRODUCTION

The visual system, an integration of the sensory and information processing systems, is responsible for transmitting environmental information for animals. The sensory part transduces the absorbed photon energy into electrical signals, which is the projection of the visual environment. The rest of the system abstracts 'features' from them.

Due to different needs of animals, each visual system has its own types of 'features'. However, there are common types among them also; one type which exists from insect to vertebrate is the directionally selective motion detection unit. These units have been found in the cerebral cortex of cats (Hubel, 1959; Hubel and Wiesel, 1959), the optic tectum of frogs (Lettvin, et al., 1959), the retinae of rabbits and pigeons (Barlow and Hill, 1963; Maturana and Frenk, 1963), and the optic lobe of flies and locusts (Bishop and Keehn, 1966; Horridge, 1965). The term directionally selective means that the unit responds when a pattern moves in one direction, whereas when a pattern moves in the other direction, it elicits little or no response (Barlow and Levick, 1965). In addition to the directional selectivity, these units were also sensitive to the velocity or the contrast frequency (ratio of velocity to spatial wavelength) (Bishop and Keehn, 1966; Eckert, 1980).

It has been known that directionally selective units may function to control behavioural reactions. There are several correlations between the optomotor response and the activity of these units in fly. Both of them are sensitive to the direction of movement of an

object, have a similar dependence upon light intensity, and show a similar variation with moving velocity and spatial wavelength of patterns (Bishop and Keehn, 1966). In other experiments with mammals it also appears that units found in superior colliculus function to coordinate the eye or head movements to follow the moving object (Gordon, 1972). Therefore, the importance of this common 'feature' is obvious without further emphasis.

A photosensory element, thought of as a single input to these units, has the ability only to sense the temporal information of the light flux. To detect movement, it is necessary to process the temporal-spatial information with at least two inputs. The question is, how do they process this information? The earliest functional model was suggested by Hassenstein and Reichardt (Reichardt, 1961) through the behavioural experiments on the insect Chlorophanus. This model was based on the correlation mechanism; the model was comprised of two linear filters (integration type and differential type), a multiplicative interaction, and an averager (Fig. 1.1).

Barlow and Levick (1965) also worked on the mechanism and stated that sequence-discrimination results primarily from an inhibitory mechanism. They also related the functional organization to the anatomical organization. Their data indicated that the inhibitory mechanism is nonlinear. In fact, both the correlation model and inhibition model are based on a multiplication-like interaction. Linear processing by summing or subtracting signals of the two inputs could not elicit a motion response (Poggio and Reichardt, 1973a)
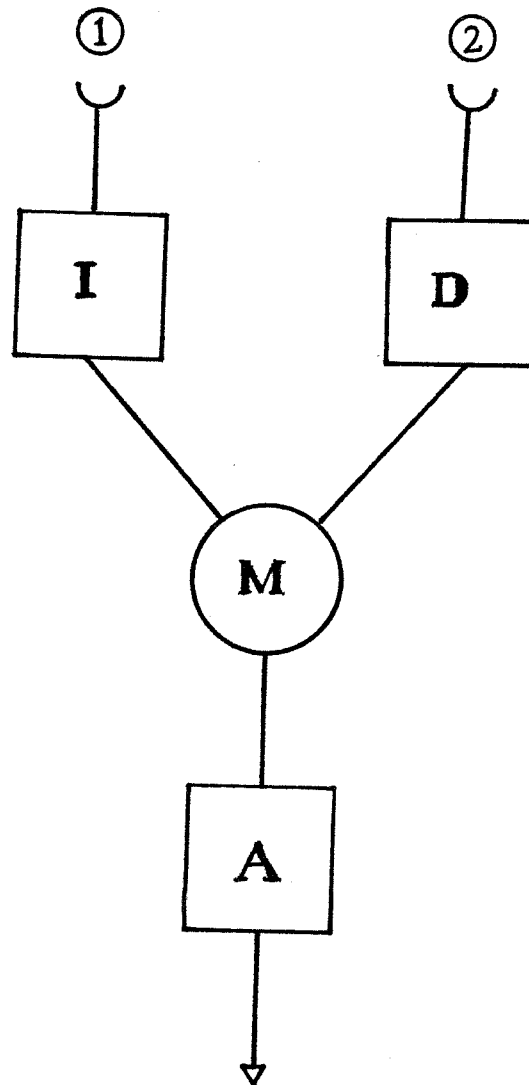
Fig. 1.1 Basic configuration of a correlation
model. 1 and 2 inputs. I linear filter
of the integration type. D linear
filter of the differential type. M
multiplicative interaction. A averager.

Mathematical modeling of this nonlinear system, as approached by parametric techniques, is almost impossible because of its complexity. Marmarelis and McCann (1973) used a nonparametric technique called the Wiener method to model the dynamics of the motion detection cell of fly. This model was found to have nonlinearity limited to second order. Until then the basic directionally selective model (the two input minimum-configuration model) was functionally well described (This model was able to predict all experiments accurately), but the relationships between this model and the correlation model or the inhibition model were not stated.

In compound eye research, one interesting question is how the subunits of a large field motion detection cell are organized in comparison with the geometry of the retina. Understanding of the sampling distance of two inputs, their angle relative to the retina coordinate, and the strength of each unit, may lead to insights into the mosaic arrangement of the ganglion cells along the pathway of such a large field cell. Buchner (1976) solved this problem by measuring the averaged optomotor turning responses to a traveling sinewave grating, which varied with moving velocity and direction, then factoring out the weight of each unit by analyzing the fourier coefficients of the responses and decomposing a matrix equation.

The second question arises from a general phenomenon that the spatial resolution of a directionally selective unit changes with the light intensity of the surroundings. Under light adapted conditions, a cell is relatively able to perceive a fine grating moving with fast

speed. But under dark adapted conditions, both the spatial and temporal resolution of the cell are decreased (McCann and MacGinitie, 1965; Barlow, 1972).

Dvorak and Snyder (1978) worked on this problem by taking the responses from a directionally selective unit and measuring the sensitivity versus the spatial wavelength of the stimulating sinewave. They suggested that the change of spatial acuity could arise from an increase of the acceptance angle of photoreceptors and neural pooling of signals from neighbouring receptors with different visual axes. Using the same method described by Buchner (1976), Pick and Buchner (1979) factored out the weights of each subunit of the motion detection cell along the horizontal line of symmetry under both light adapted and dark adapted conditions. The results indicated that under dark adapted conditions about five adjacent columns interact as motion detection subunits, while under light adapted conditions only two neighbouring columns have significant interaction. Thus, they made a more quantitive description of the subject and gave one more suggestion on the mechanism of the neural recruitment of movement detectors. However, their work has several disadvantages. First, under light adapted conditions the sinewave may introduce higher harmonic terms due to saturation within the retina level. Second, their theory was based on an assumption that all the contributions to the response were from two input subunits. No consideration was made on the effect from subunits with more than two inputs. These two points would affect the accuracy of the weight coefficients. Besides, because their experiments were studied only for one contrast frequency, the experiments have to be re-

peated for different contrast frequencies.

Within this thesis, the research work on the above questions uses the nonlinear identification method that was previously used by Marmarelis and McCann (1973). The functional of the basic motion detection unit was studied by three steps. First, the second order cross kernel of the system was obtained. Second, by eliminating the possibility of the existance of higher order kernels, the predicted impulse responses were theoretically related to the second order cross kernel. Then, another set of experiments using transient type stimuli (equivalent to the assembly of impulse type stimuli) were used to confirm the predicted impulse responses of the system. Both the correlation model and the inhibition model were used to compare with the above results. Finally, an inhibition model was developed to meet the functional of the basic motion detection unit of the fly.

The recently developed nonlinear identification method by the Volterra-Wiener approach is a general system theory, and it is directed toward the study of the above problems. The Volterra series expansion for multi-input system has the following form, according to Poggio and Reichardt (1976).

$$y(t) = g_0 + \sum_{k=1}^{N} g_k * x_k + \sum_{k,j}^{N} g_{kj} *^2 x_k x_j + \dots$$

$$+ \sum_{k_1 \dots, k_n}^{N} g_{k_1, k_2, \dots, k_n} *^n x_{k_1} \dots x_{k_n} + \dots$$

where

$$g_{k_1 \ldots k_p} *^p x_{k_1} \ldots x_{k_p} = \int_{-\infty}^{\infty} \int_{-\infty}^{\infty} g_{k_1 \ldots k_p}(\tau_1, \cdots, \tau_p)$$

$$\cdot \prod_{j=1}^{p} x_{k_j}(t-\tau_j) d\tau_1 \ldots d\tau_p$$

and $y(t)$ is the system response. The $x_k(t)$ $(k=1,\cdots,N)$ are the inputs of the system. The terms $g_{k_1,\ldots,k_n}(\tau_1,\cdots,\tau_n)$ are called kernels; these are nonparametric descriptors of the system. When all the sub-scripts are identical (i.e., $k_1=k_2=\ldots=k_n=r$) $g_{k_1,\ldots,k_n}(\tau_1,\cdots,\tau_n)$ is called the nth order self kernel of channel r, otherwise $g_{k_1,\ldots,k_n}$ $(\tau_1,\cdots,\tau_n)$ is called the nth order kernel of channel k_1 through k_j (j is the number of nonidentical subscripts). Thus, the response associated with a single channel r could be described by a first order kernel $g_r(\tau)$, a second order kernel $g_{r,r}(\tau_1,\tau_2)$, and all higher order kernels. The response due to two channels i and j could be described by a second order kernel $g_{i,j}(\tau_1,\tau_2)$, third order kernels $g_{iij}(\tau_1,\tau_2,\tau_3)$ and $g_{ijj}(\tau_1,\tau_2,\tau_3)$, a fourth order kernel $g_{iijj}(\tau_1,\tau_2,\tau_3,\tau_4)$, and the rest of the higher order kernels. The response from interactions of more channels could be listed in a similar way. A system is called p-order n if the cross kernel contribution is limited to the interaction of up to n channels. For a basic directionally selective unit

with two inputs, the cross kernel $g_{i,j}(\tau_1,\tau_2)$ is the key kernel to be identified.

The experiments dealt with the horizontal motion detection cell class-IIal of the fly <u>Calliphora phaenicia</u>. Temporal-spatial white noise stimuli were used as stimulus patterns which were placed within the receptive field. Kernel computing programs were used to compute the first three p-order 1 kernels, the first four p-order 2 kernels, and the first one p-order 3 kernel. Modeling programs were used to predict the responses by computed kernels.

Another set of experiments were designed to investigate the mutually inhibitory mechanism of two class-IIal cells, which was studied previously by Dill (1970). Again, the Volterra-Wiener approach was applied to this subject to study the binocular interaction under stimulated condition.

The contents of each chapter are listed as follows:

Chapter 2: An overview of the fly visual system is presented. The physiology and anatomy of the class-IIal cells are treated in a more detailed way. The scheme for generating temporal-spatial white noise patterns, experimental methods, data collection, and signal processing are described.

Chapter 3: Wiener kernels are introduced as the device for non-linear system modeling. The relationships between the type of nonlinearity and the kernel components are interpreted. Different types of white noise, their properties, and the criterion for choosing the white noise which is needed, are reviewed.

Chapter 4: The basic motion detection unit is studied by using both white noise and transient type stimuli. Experiments included are one output and two-input system identification and tests under different light conditions. The second order cross kernel did show temporal integration and dark adapted conditions.

Chapter 5: Multiple stripe patterns were used to investigate the interactions between columns and rows of visual elements. The variance of the weight coefficients in the spatial domain are shown under dark and light adapted conditions. A negative response was observed from experiments with both a multiple stripe and a two stripe patterns.

Chapter 6: The mutual inhibitory interaction between two class-IIa1 cells is described. Wiener kernels of binocular and monocular systems are compared to provide insight into the mechanism. The cross kernel between two eyes show a directionally selective interaction.

Chapter 7: A summary is made of the results of chapter 4, 5, and 6. All kernel models are linked with the corresponding ganglia of the visual system. An inhibition model with four types of inhibitory interactions was developed. Suggestions for further research are made.

CHAPTER II

THE PHYSIOLOGY OF THE FLY EYE

AND EXPERIMENTAL METHODS

2.1 Introduction

The compound eye of the fly is a favorable object for a neuro-physiological approach for several reasons. First, the structure of the fly's visual system is of reasonable complexity. The numbers of photoreceptors and visual interneurons are relatively small (267,000 interneurons in Musca; Strausfeld, 1976) compared with vertebrate. The photoreceptors are well separated anatomically from other classes of higher order neurons. The ganglia tend to be clearly separated; this allows the study of units in identifiable ganglia. From retina to third order ganglion, lobula and lobular plate, all have a highly-ordered geometry and a periodic columnar structure. Second, despite the compound eye's simple appearance, its function is complex enough to be interesting.

Behavioural studies indicate that the fly has well defined turning and landing responses. Collett and Land (1975) also indicate that the fly's eye must serve certain functions for chasing behaviour. More recent results reveal the ability to make figure-ground discrimination (Poggio and Reichardt, 1976a; 1979). Besides, the receptor cells and first order ganglion cells have been extensively studied both in anatomy and physiology. With a more stable recording method, the acceptance angles of receptors and monopolar cells were obtained more accurately (Hardie, 1979). Last, the experimental prep-

aration is simple and the fly is readily available.

2.2 The Fly Visual System

The visual system of the fly consists of two eyes, two optic lobes, and part of the brain (Fig. 2.1). Each eye is of a hemispherical shape and consists of a hexagonal array of ommatidia. The number of ommatidia is about 5,000 for the fly Calliphora (Beersma, et al., 1977). Each ommatidium consists of a transparent lense (the dioptric apparatus), photoreceptors, and pigment cells. There are eight photorecptors (R1-6, R7/8) grouped in a compact cylindrical bundle named the retinula. Along its inner surface, there is a particular formation called the rhabdomere, which is usually united with other rhabdomeres in a compact form called a rhabdom. The rhabdom is composed of tightly packed microvilli which contain visual pigment for absorbing light. The pigment cells contain pigment granules which vary their congregation around the rhabdom to regulate illumination. Within one ommatidium the optical axes of eight rhabdomeres are different, but the angular separation of their axes matches the interommatidia angles such that seven (or eight) different rhabdomeres are 'looking' at the same point in the visual field. (Braitenberg, 1967) R7 and 8 are thinner, compared with R1-6; this is part of the reason that there are differences in spectral sensitivity among the photoreceptors (waveguide effect; Kirschfeld and Snyder, 1976). R1-6 have a spectral sensitivity peak at 353 nm (UV) and 486 nm. R7 is a UV receptor (Meffert and Smola, 1976). R8 has maximum sensitivity at 486 nm and lower UV sensitivity (Jarvilehto, 1976). Although it was thought
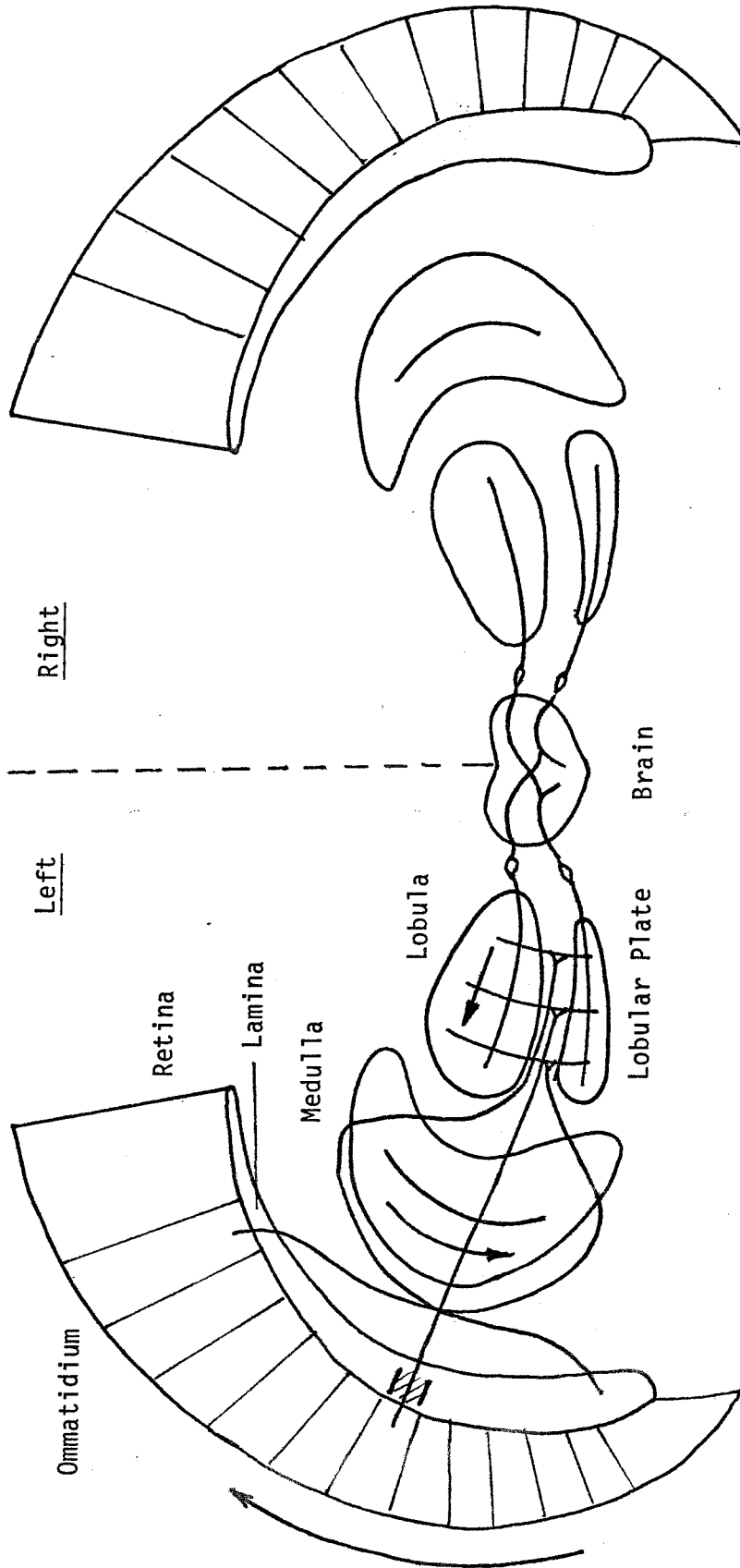
12

Fig. 2.1 Horizontal section of fly's head.

that there are two visual pigments responsible for these two peaks, only one rhodopsin (visual pigment) with a peak at 480 nm has been found (Hamdorf, Paulsen, and Schwemer, 1973).

The optic lobes consist of four synaptic neuropils: lamina, medulla, lobula, and lobular plate. The lamina shows a periodic columnar structure of elements called cartridges. Each cartridge is formed by first order ganglion cells and the axons of six retinular cells (R1-6), which have the same optical axes. Thus, every cartridge is mapped from one point in the visual field. There are five monopolar cells of which L1-2, called large monopolar cells (LMC), receive their primary inputs from receptors. L2 is presynaptic to receptors and to the L1 monopolar cells. Interconnections between cartridges are mediated by amacrine cells and L4 monopolar cells (Strausfeld and Campos-Ortega, 1977). On the chiasma, an on-center off-surround organized cell named on-fiber was found by extracellular recordings (Arnett, 1971). There has been no evidence that motion detection units exist either in the lamina or in the outer chiasma. The R7 and 8 retinular cells pass through this cartridge without making synaptic contacts (Braitenberg, 1967; Braitenberg and Strausfeld, 1973; Strausfeld, 1971).

The second order ganglion, the medulla, has a regular columnar structure also. Each medulla column arises from a lamina cartridge (with L cells) and R7 and 8 cells which represent the same visual point. Both the lamina cartridge and R7 and 8 cells end at different levels of a medulla column and synapse with third order neurons (amacrine and tangential cells). The medulla column and the third order neuron layers

are orthogonal to each other and form a matrix structure. Small field units containing direction selective units have been found in this region (McCann and Dill, 1969; Devoe and Ockleford, 1976). Due to the complex structure and large number of interneurons, the medulla has been thought as the region where much information processing takes place. Within the medulla, superficial tangential cells are connected, through the posterior tract, to the tangential cells of the opposite lobe, determining a direct medulla-medulla connection.

The third order ganglion, the lobula and the lobular plate, also have a periodic columnar structure (Strausfeld, 1976). These regions receive cartridge input from the medulla. The lobula has mainly small field intercolumnar fibers which integrate a small number of medulla cartridge inputs. The lobular plate shows two sets of giant fibers (Pierantoni, 1973) which integrate (sum) a large number of incoming cartridges to form a partial or full eye visual field unit. There are four sets of horizontal layer fibers connecting medulla and opposite lobula, medulla and lobular plate, medulla and opposite lobula (again), and lobula and lobular plate. Details concerning giant fibers will be given in section 2.4.

The function of the lamina is related to sensitivity control (light adaptation mechanism; Laughlin and Hardie, 1978) and basic form integration (Arnett, 1971). The medulla contains more complex functional units including directionally selective units. The lobula and lobular plate provide vertical and horizontal motion information for the motor circuits of the thoracic compound ganglion. They may also

provide position information (Poggio and Reichardt, 1976b).

2.3 Receptive Field Projection in the Visual System

The fly Calliphora has a visual field covering almost 360° of the surroundings, expecting a small caudal region. There is binocular overlap of the visual fields of both eyes around the frontal and caudal midlines (Franceschini, 1975). For Calliphora, the male fly has an enlarged dorso-frontal overlap compared with female fly (Beersma, et al., 1977). The hexagonal array has three axes, x, y, and z, along its ommatidia columns. At the frontal part of the eye this array is stretched along the z axis. Normally, there are seven rhabdomeres within different ommatidia 'looking' in the same direction, but in the horizontal midline there are nine rhabdomeres. The rhabdomeres in the lower part of the eye form a mirror image of those in the upper part of the eye. The boundary between the superior and the inferior regions is defined by this horizontal midline.

Within the frontal part of the eye, the interommatidia angle $\Delta\phi_h$ is approximately 1.25^o, which gradually increases to the value of 2.5^o in the lateral part of the eye. The acceptance angle $\Delta\rho$ (defined by its gaussian shaped spatial sensitivity distribution) of R1-6 is about 1.6^o, whereas $\Delta\rho$ of R7 and 8 is about 1.3^o. Fig. 2.2 shows the mosaic structure of the ommatidia with the above data, large and small circles representing $\Delta\rho$ of R1-6 and R7/8, respectively. As the lamina cartridge passes the first chiasma to the medulla, the horizontal field projection is inverted such that the frontal parts of the medulla
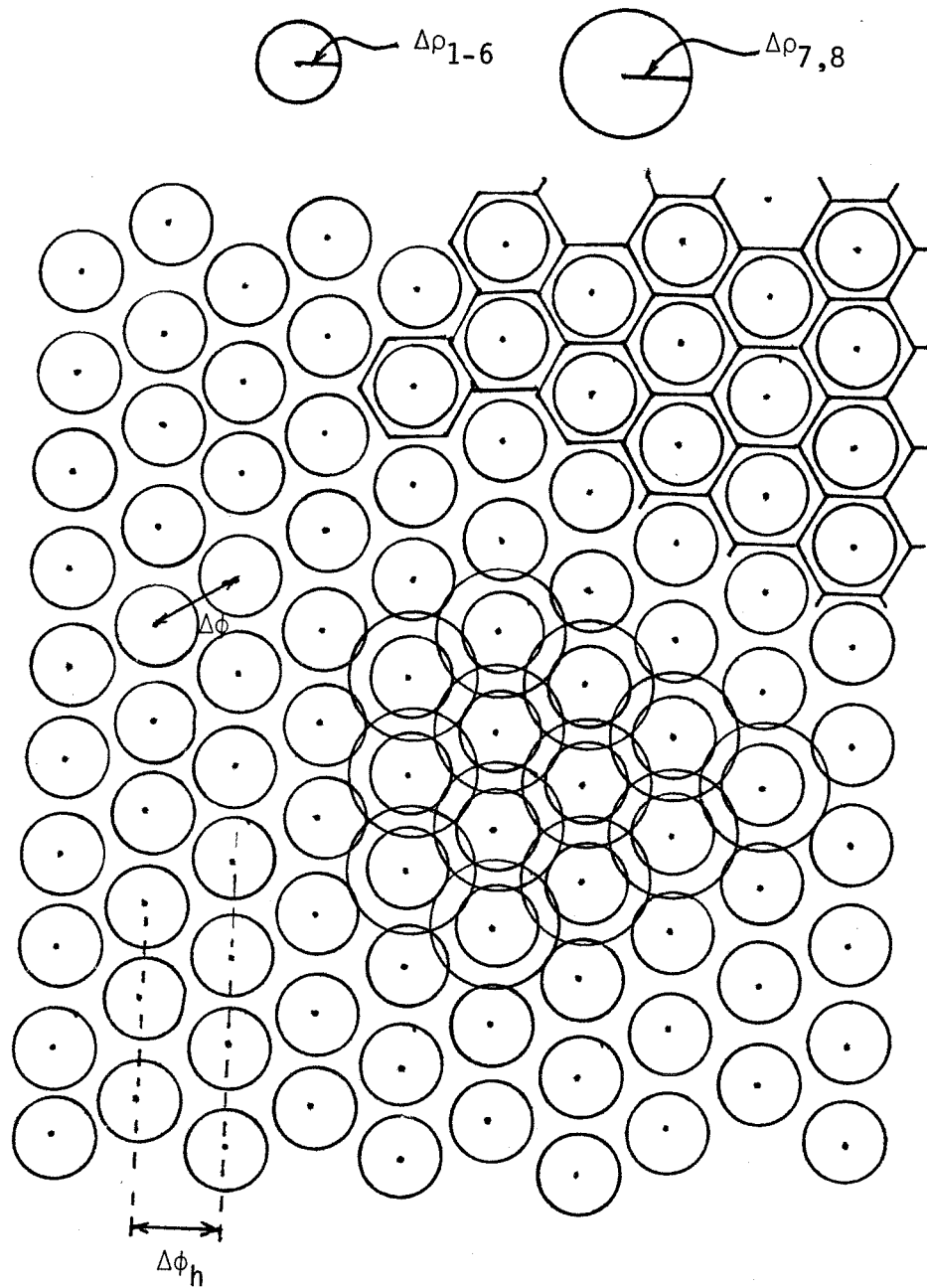
Fig. 2.2 Mosaic structure of the ommatidia in the frontal part of the eye of the fly. Each dot represents the optical center of a facet lens. The facet lenses constitute a pattern of regular hexagons(upper half, right). The inter-ommatidial angle $\Delta\phi$ is the angle between the optical axes of neighbouring ommatidia and $\Delta\phi_h$ is the 'effective' inter-ommatidial angle as measured in the horizontal direction.

correspond to the caudal-lateral eye region and vice versa. Within the lobula and lobular plate, the distal parts of the two lobulae represent the frontal eye region and vice versa, the dorsal parts represent the dorsal eye region and vice versa. The columns corresponding to the frontal eye region have the largest volume, indicating the existence of a kind of 'neural fovea'.

2.4 Class-II Cells

The function of motion detection units was investigated by Bishop, Keehn, and McCann (1968); McCann and Dill (1969); and McCann and Foster (1971). These units were studied and located by extracellular probing and marking techniques. They were classified by the anatomical location, field of view, and the selective motion detection. Classes II and III refer to units found in the lobula-lobular plate region and the brain, respectively. Within each region there are units with receptive fields of the ipsilateral side or contralateral side, named b or a units. Selective motion directions include inward (along z axis), outward, upward (perpendicular to z axis), and downward types, these types were represented by indices 1, 3, 4, and 2. Thus a contralateral inward unit found in the lobula-lobular plate was named class-IIal unit. All these units responded maximally to motion in their specific direction and were inhibited (firing rate was less than that for no motion) for the opposite direction of motion. If the spatial wavelength (λ) of the pattern is smaller than twice the interommatidial angle $\Delta\phi$, i.e., $\Delta\phi<\lambda<2\Delta\phi$, these units will detect motion as appearing to be on the reverse of its true direction (recently by Eckert, 1980). Class II

cells had their receptive field sizes either full eye or about 60°. Fig. 2.3 shows a contour map of a class-IIa1 cell, responding to small moving pattern.

Anatomical identification by recordings and dye-injections were done by Pierantoni (1973), Dvorak, et al., (1975), and Hausen (1976). They described a set of lobular plate 'giant' interneurons having the same function as the motion detection units studied by extracellular recording. These cells were wide-field elements which connect the dendritic fan of the lobular plate with the input region in the photo-cerebrum, from which descending neurons originate. There were eight classes which can be divided into two systems: a horizontal movement processing system and a vertical movement processing system. A cell named H1 has been thought to be identical with the class-IIa,b1 cells (Hausen, 1976). The H1 cell has its dendrites covering almost the whole anterior lobular plate surface, and its axon passing the lobula in a dorso-frontal direction to cross the midbrain. After entering the opposite lobe its axon projects on the lobular plate (Fig. 2.4). It responds selectively to ipsilateral horizontal forward motion. Simultaneous extracellular double recordings from the axon of both H1 cells in each lobe revealed that they are mutually inhibited by each other.

In summary, by electrophysiological and anatomical studies, the lobular plate interneurons integrate the motion information over particular part of the ipsilateral visual field and transmit this information into the contralateral lobular plate. After comparing the
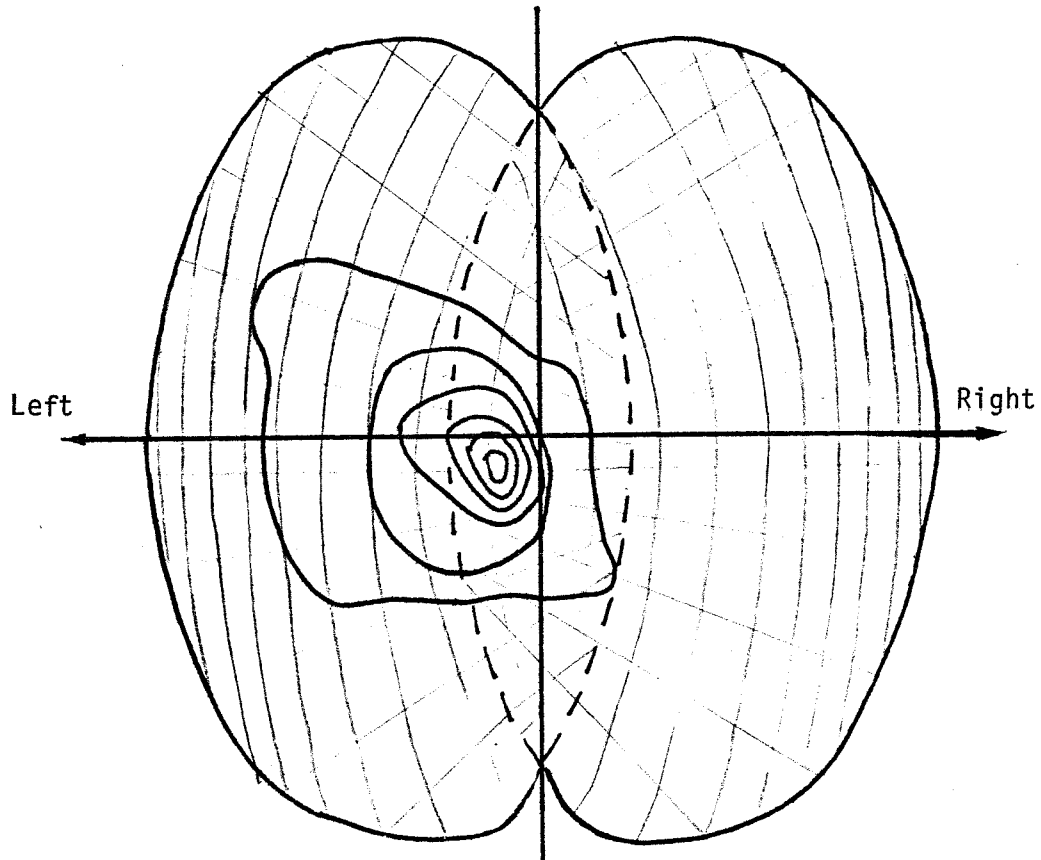
Fig. 2.3 Contour map showing response of class-IIa1
unit as function of pattern position. Coordinate
system represents orientation of rows and columns
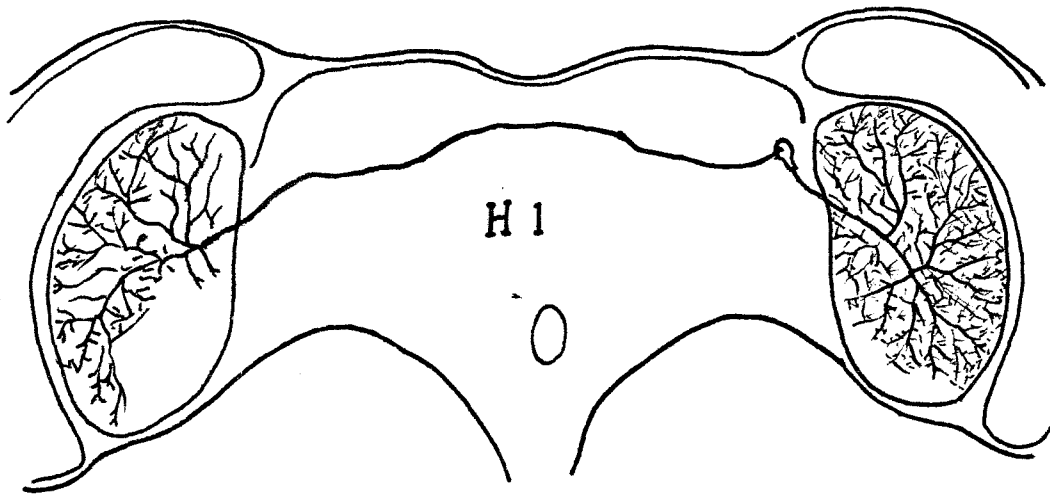of ommatidial facet array. Spacing is approximately
20 degrees.

Fig. 2.4 An H1-Cell shown in vertical section of fly optical lobe.

motion information from both eyes, they send the information to the motor system via descending neurons. The function of this system has been thought to be for the effective flight and navigation control.

2.5 Visual Acuity and Dark Adaptation

The compound eye of Calliphora is of the type called apposition, which means that each photoreceptor is optically isolated from the other. The perceived object image is spatially quantized by its ommatidia or to the reciprocal of interommatidia angle. In general, the structure of the compound eye is nonuniform. It is neither spherical, nor is it composed of the same size facets. In many insects there is a fovea region where the interommatidia angles tend to be the smallest, whereas in the peripheral region these angles become larger. There are two parameters determining the size of interommatidia angle, $\Delta\phi$, the facet size D and the eye radius R, (Fig. 2.5a). Their relationship is (Snyder, 1977):

$$\Delta\phi = D/R.$$

Within the fovea region (frontal region) the curvature of facets is flatter (larger eye radius) and the facet size is relatively larger (Horridge, 1977).

In each ommatidium, the acceptance angle $\Delta\rho$ (Fig. 2.5b) is mainly determined by the diameter of the rhabdom d_{Rh} and the distance from the distal tops of the rhabdomeres to the posterior nodal point $\underline{f}$, as follows (Snyder, 1977)

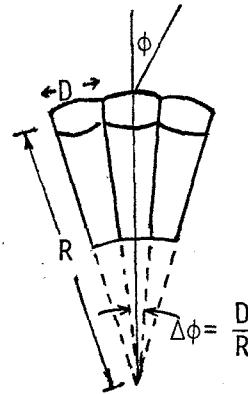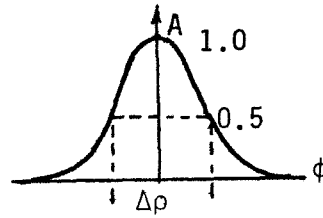$$\Delta\rho = \frac{d_{Rh}}{f} .$$

Fig. 2.5a Right. The acceptance angle and cross section of ommatiadia. D is the facet diameter, R the eye radius. $\Delta\phi$ the interommatidial angle, $\Delta\rho$ is the width of the function at 50% sensitive.
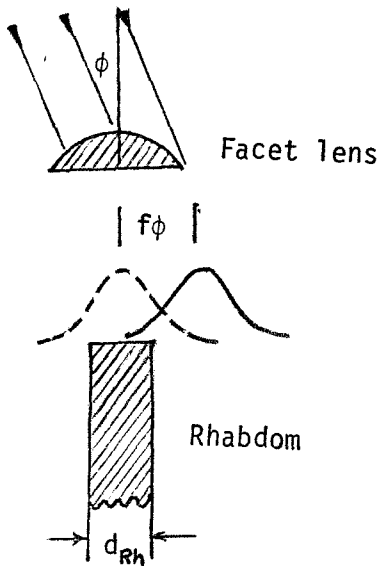

Fig. 2.5b Left. Displacement of the lens pupil intensity function. f is the distance from the distal tips of the rhabdomeres to the posterior nodal point.

For such a lens system, both $\Delta\phi$ and $\Delta\rho$ would limit the perception of a static sinewave grating by their high spatial cut off frequencies. When the compound eye is utilized to perceive a moving sinewave grating, due to the uncertainty from position shift within a certain time interval, the resolving power is further decreased. Thus, both $\Delta\phi$ and $\Delta\rho$ give the limitation of visual acuity.

In the dark adapted condition the compound eye, however, is no longer concerned with maintaining a high visual acuity. The most important function of the eye is to optimize the capture of all available photons. In a dark environment, the rare incoming photons cause 'quantum bump' of the receptor potential, which is therefore a noisy signal. The signal to noise ratio is proportional to the standard deviation of photon counts which is $\bar{N}^{1/2}$ (because the photon count is a poisson process) and $\bar{N}$ is the mean number of photons computed by a photoreceptor perintegration time. To increase the signal to noise ratio, the receptor has to increase the number of photons captured. This could be performed in two ways. Neural pooling is one mechanism, which cause noise reduction by superposing signals from neighbouring receptors. The factor of improvement is the square root of the number of pooling receptors. Another way is by increasing the acceptance angle of each receptor (Franceschini and Kirschfeld, 1976). The mechanism of this is associated with movement of screening pigment. Under light adaptation the pigment granules move toward the rhabdomeres to vary the waveguide property such that a part of light energy is propagated outside the rhabdom and scattered and absorbed by the pigment. In the dark adapted

condition, the pigment granules are away from the rhabdom and light within the acceptance angle is propagated by total internal reflection.

Another suggestion for the increasing sensitivity of movement perception is the neural recruitment of the movement specific units. This is a higher ganglion level integration mechanism by which the neural processes have to be done behind the retinal level.

2.6 Light Adaptation

The neural principle of vision in the light adapted condition is different from that in the dark adapted condition. As mentioned in the last section, in the dark adapted state, the information to be pre-ceived by the visual system is the small number of photons and the retinal neurons code it by a proportional magnitude of voltage. But in the light adapted condition, if the coding scheme is not modified, the background light intensity would saturate the neurons such that further increase of light intensity would not be represented.

Electrophysiological studies on light adaptation have found that there is significant functional change of the receptors and the LMCs. The receptor decreases its sensitivity as the background intensity increases; this makes the light adapted receptor respond over a dynamic range of 7 log units, which is 2 log units higher than dark adapted receptor. At least two mechanisms are associated with this functional change. One works by changing the waveguide property, which is mentioned in the last section. The other consists of a decrease in the number of conductance channels opened by each photon (Laughlin, 1975b). Compared with receptors, the LMCs have a greater sensitivity

change in the light adapted condition. The LMC has a fast light adaptation mechanism by which the background intensity signal is no longer represented at its membrane. Besides, LMCs give an off transient (hyperpolarization) for coding contrasts darker than the average background. The mechanism is suggested as four vertical (with one cartridge) negative feed-backs or feed-forwards loops acting in the lamina on the retinula cells and the LMCs (Laughlin, 1975a). There is also a possibility of the spatial distribution of sensitivity control via intercartridge amacrine cells.

2.7 Stimulus

The stimulus was provided by a closed circuit TV monitor (Conrac 9sp4) with parallel video inputs either from a TV camera, which faced at patterns generated on the oscilloscope screen, or from a PDP-11 minicomputer with digital stimulus tapes. Horizontally and vertically moving spots or lines were the major patterns on the oscilloscope screen, and these were used to characterize cells. Those stimulus signals from the PDP-11 were basically used for studying the cell. The highest rate of the TV monitor was 60 frames/sec which does not cover the spectral range of the class-II cell. However, judged by its spectrum (P. Marmarelis and McCann, 1973) the loss of accuracy is very small.

The image patterns from the digital stimulus tape consisted of a large square subdivided into 16x16 subunits. The size of each subunit could be set from 1 to 32^2 times the pixel's size. A concave lense with 20 mm aperture and 35 mm focal length was put in front of the TV

monitor to decrease the image size and also bring the distance between the image and the fly's eye down to 30 mm. This reduced image had a fairly linear range about 10 mm (25°) within the center region. The maximum intensity measured by a S.E.I. exposure meter was about 50 cd/m^2. There were two ways to vary the maximum intensity for the needs of various experiments. One was by using gray filters. The second was established by writing certain levels of data into digital stimulus tape. The stimulus signal within the digital stimulus tape provided 16 levels of magnitude, within which the upper 10 levels were uniformly distributed from 0 cd/m^2 to 50 cd/m^2. The phosphorus material on the monitor screen was a p^4 type (Fig. 2.6 shows its spectrum), which covered the spectral peak of the fly's R1-6 photoreceptor system.

There were two types of stimuli, transient type and white noise, for experiments. Fig. 2.7 shows two pairs of transient stimuli to stimulate forward and backward motions for a two-input basic motion detection unit. Ternary and binary white noise were used for two input and multi-input studies.

2.8 Preparation

The animals used were adult red eyed (wild type) specimens of both sexes of the blowfly Calliphora phaenicia. The specimens between 5 and 15 days were used for experiments. The fly was mounted on a piece of dental wax, by using a hot wire, in such a way that respiratory movements were not restricted. The head was tilted forward with respect to the thorax and fixed on the base, via a wax bridge, to expose the back of the head. The exoskeleton of one lobe was cut open and some of the air
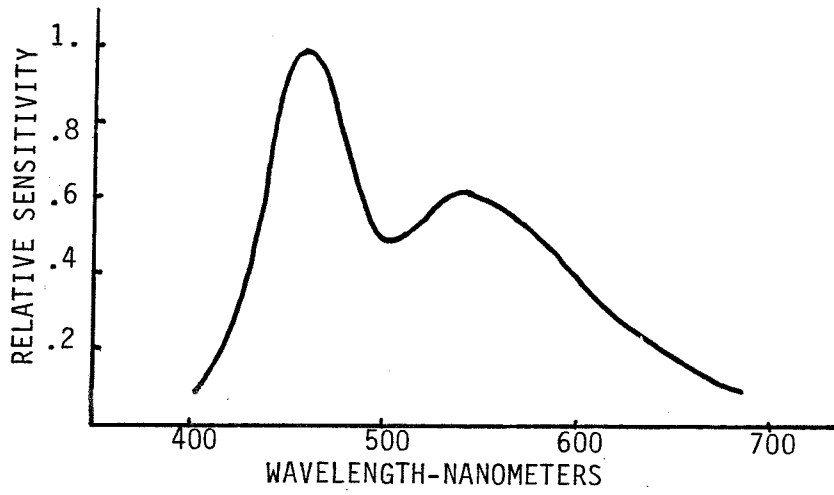
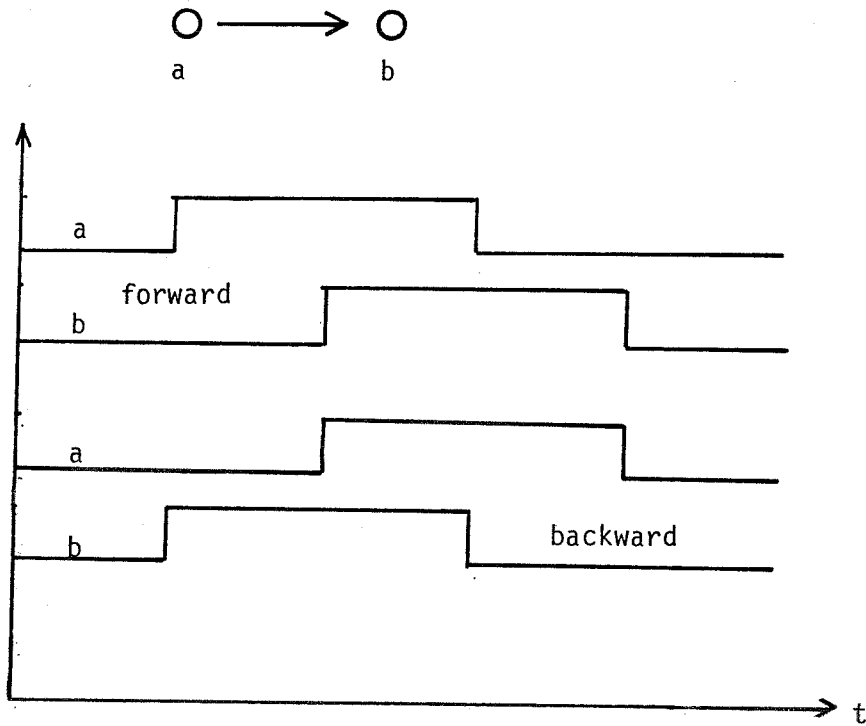Fig. 2.6 Spectral characteristics of
the display screen.

Fig. 2.7 Transient stimuli simulating
forward and backward motions.

sacs removed to permit access to the brain tissue. A platinum indifferent wire was inserted into the opening, contacted the tissue fluid, and hooked the exoskeleton boundary.

After preparation as described above, the fly with the wax base was put on a microprobing platform. The animal's position was aligned to make the center of ite visual field correspond to the coordinate system of the screen image by the following procedure. First, the microprobing platform was put on an optical system (Fig. 2.8), the position of the wax base was adjusted to let the horizontal and vertical axes of the fly eye align well with the cross hairs within the microscope ocular. Then, the microprobing platform was put in front of the TV monitor, and the position of the lens was adjucted so that the center of the screen image met the center of cross hairs of the telescope.

Extracellular recording electrodes were made with tungsten wires. The preparation method is the same as Arnett's (1971) technique. Briefly, the electrode was sharpened by dipping into sodium nitride solution repeatedly and checking through the microscope until the tip size was approximately 1 micron. The tip was then plated with gold and platinum and coated by epoxy (Hysol AC4396) and baked to dry. The insulation was then removed by passing current through it. The electrode had a d-c impedance of 2-10 Megohms.

2.9 Data Collecting

A moving bar generated by an oscilloscope and a manually controlled test board were used to characterize the selected direction and field
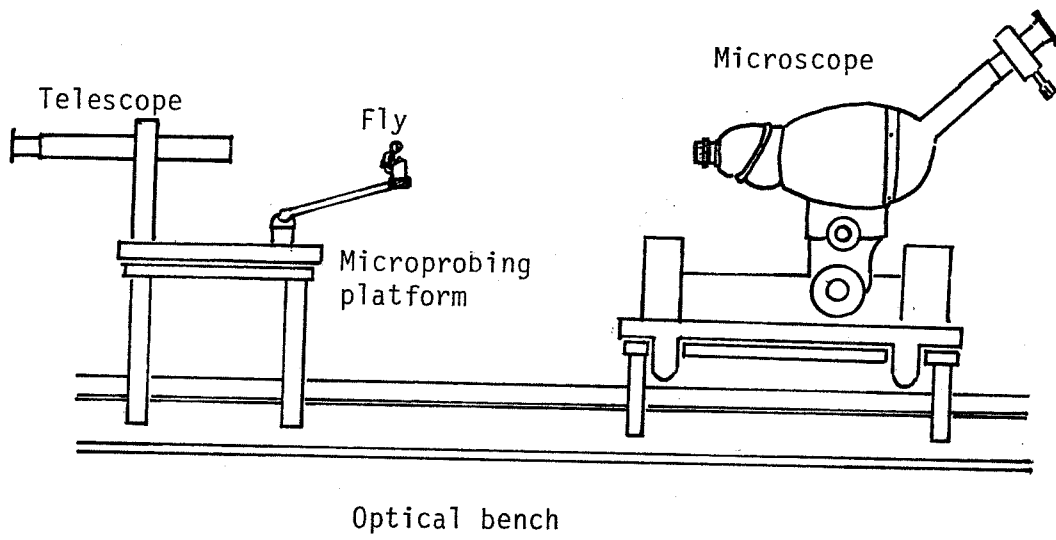
Fig. 2.8 Optical system for aligning
fly's head position.

size of the cell. Usually, spikes of the class-IIa1 cells were immedi-
ately obtained after penetration. The recordings were very stable and
lasted for several hours.

The spikes from the tip were about 100 to 400 UV depending on the
electrode tip size and the recording. Overall signal processing is
shown in Fig. 2.9. The signal was first amplified by a high impedance
preamplifier NFI (Biomedical Instruments) in series with another ampli-
fier FM 122 (Tektronix) with overall gain 1000. A bandpass filter with
250 HZ low cut off frequency and 10 KHZ high cut off frequency was used
to filter out the 60 cycle noise. The final stage was a model 121
window discriminator (W-P Instruments) for triggering clean spikes by
setting the threshold above the noise level. This processed response
signal and the synchronous signal from the TV were recorded by the FM
tape recorder (Ampex) then transferred into digital tapes via a PDP-
11/20 minicomputer with LAB software support, or recorded directly
onto digital tapes without analog tape recordings.

2.10 Signal Processing

Both the response and the synchronous signals recorded on digital
tape were of the time of event mode (TOE). In this mode, the data con-
tained the times of spikes which were read from digital clocks running
at 50 KHZ rates. The synchronous signal was a 60 HZ spike train. In
order to compute the kernels, the response has to be converted from
TOE mode into a continuous signal (it is sampled at certain rate, not
really continuous); this was done by using the synchronous signal as
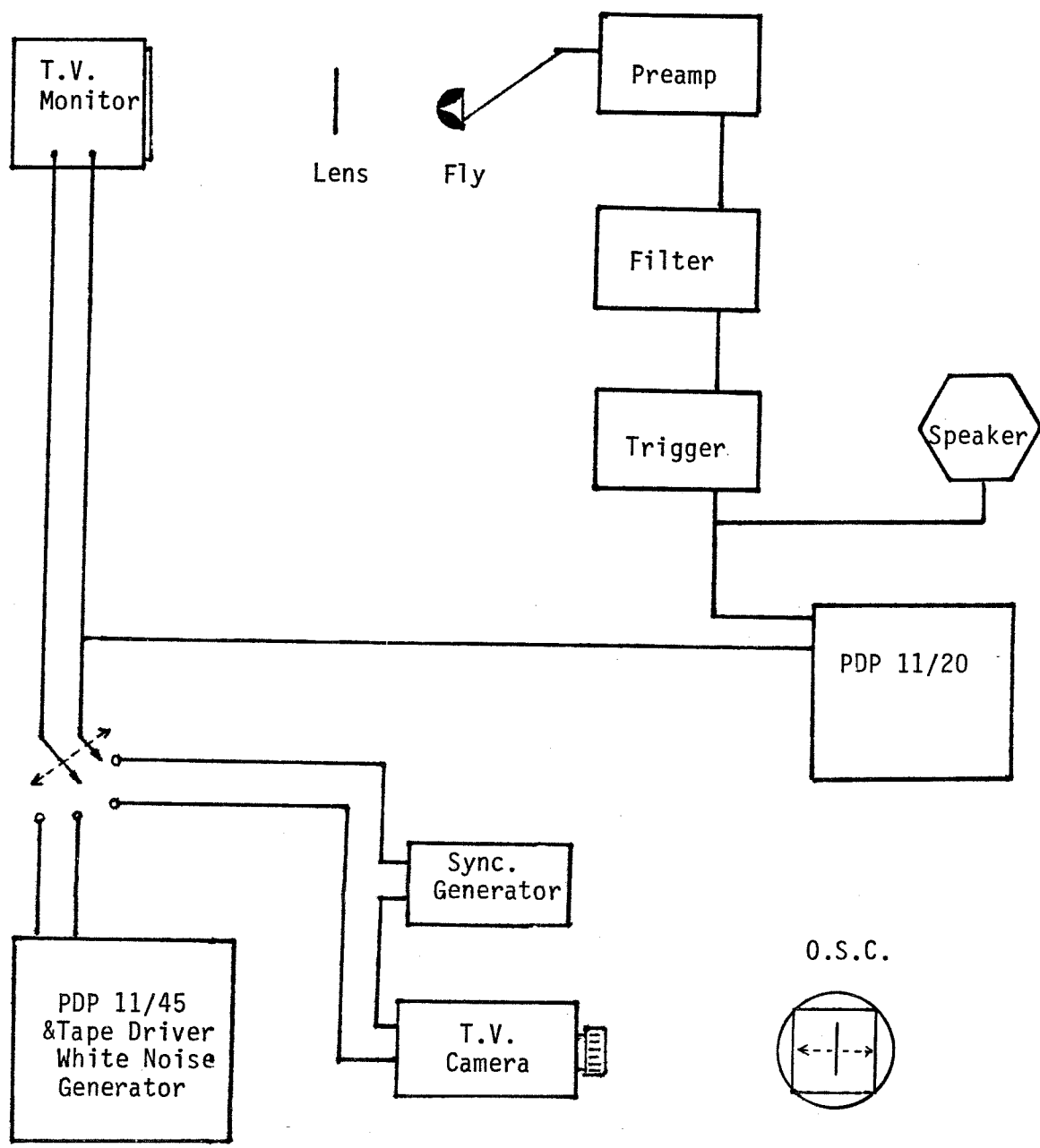a reference. The stimulus signals were also converted into continuous

Fig. 2.9 Experimental setup: stimulus and data collection configuration.

signals from the stimulus tape. Normally, both prepared response and stimulus signals had 60 HZ rate (16.6 msec binwidth). According to Marmarelis and McCann (1973), kernels computed by a re-binned signal with smaller binwidth had higher accuracy. Thus usually kernels were computed with 16.6 msec binwidth first. If the results were acceptable (unacceptable means noisy or error being made during processing) then signals were re-binned at 180 HZ (5.53 msec binwidth) and kernels were recomputed from them. Note that the re-binning procedure has to start from the synchronous signal. Furthermore, before kernel computing a low pass filter could be used to filter out the high frequency part, since the spectrum of the cell is within 50 HZ.

There are two types of encoding schemes for spike data, encoding by spike density and by instantaneous frequency. Their differences are not significant, especially for re-binned data (Sheby, 1978). A spike density encoding scheme was used for the data presented in the next chpaters.

2.11 Kernel Computing and Display

Although the video signal is synchronous with the synchronous signal, there is a delay time about 7.5 msec. This was remedied by shifting the time coordinate of the stimulus during kernel computing.

GAS (General Analysis System software in laboratory) provided programs for computing the self kernels up to the third order, and cross kernels of second order. Third, fourth order p-order 2 and third order p-order 3 programs were written to expand this capability

(see chapter 3). All the kernel data presented later were normalized by assigning +1 for <u>on</u> light level, -1 for <u>off</u> light level, and 0 for mean light level. For this reason the kernel has units of spikes per second. The units of light intensity was disregarded in kernel computing.

CHAPTER III

VOLTERRA AND WIENER KERNELS

AN ANALYTICAL REVIEW

3.1 Introduction

Mathematical description of systems is usually a relatively effi-
cient method in information communication because of its accuracy and
concise language structure. In recent years more mathematical methods
have been applied to biological systems. Visual systems, like most bio-
logical systems, have two common properties. One is their complex non-
linearity in nature, such that the well developed linear system analysis
techniques can not fulfill the requirements in modeling the system
behaviour. Secondly, there is no known analytical form for them, espe-
cially in the pioneering area of neurophysiology; 'Black Box' is the
general concept to apply to these systems.

The Volterra functional formulism introduced in chapter 1 is con-
fined to a class of systems which exhibit three basic characteristics:
stationary, finite memory, and analytic. It can approximate the input-
output relation of a wide class of nonlinear system. Volterra func-
tional series has the simplest form (i.e., one kernel contained in one
multiple integral term only) compared with other functional forms, and
it has been taken as an analytical tool. Unfortunately, there is no
method to measure the Volterra kernels yet.

3.2 Wiener Functional Expansion and Kernel Evaluation

Wiener (1958) derived an orthogonal functional series from the
Volterra functional series to allow the mathematical measurement of

the kernels. This is the so called Gram-Schmidt method, based on the correlation properties of a gaussian noise. For a one-input system it could be written as:

$$y(t) = \sum_{n=0}^{\infty} G_n[h_n;x(t)]$$

in the above equation, the output $y(t)$ is expanded by all functional terms G_n, within which h_n is the nth order Wiener kernel. The input $x(t)$ is a gaussian white noise with power level p, and two functional terms are orthogonal to each other. This is expressed by:

$$\overline{G_m[h_m;x(t)] \cdot G_n[h_n;x(t)]}^t = 0 \qquad m \neq n.$$

Within the above equation, the autocorrelation functions of the gaussian white noise determine the coefficients of each functional term. The nth order autocorrelation could be derived from the characteristic function of a gaussian process:

$$E[x(t-\tau_1) \cdot x(t-\tau_2)...x(t-\tau_n)]$$

$$= 0 \qquad \text{if n is odd}$$

$$= \binom{n}{2} p^2 \prod_{i,j=1}^{n} \delta(\tau_i - \tau_j) \qquad \text{if n is even}$$

By taking zero order Volterra kernel for the zero order Wiener kernel h_0, we start building the first order functional term G_1 by assigning the form

$$G_1[h_1;x(t)] = \int_{-\infty}^{\infty} h_1(\tau)x(t-\tau)d\tau + k$$

the constant k has to meet the following equation:

$$\overline{G_1[h_1;x(t)] \cdot G_0} = 0$$

It is satisfied when k is equal to zero, hence:

$$G_1[h_1;x(t)] = \int_{-\infty}^{\infty} h_1(\tau)x(t-\tau)d\tau$$

Next, the second order functional term is assigned by:

$$G_2[h_2;x(t)] = \iint_{-\infty}^{\infty} h_2(\tau_1,\tau_2)x(t-\tau_1)x(t-\tau_2)d\tau_1 d\tau_2$$

$$+ \int_{-\infty}^{\infty} k_1(\tau)x(t-\tau)d\tau + k'$$

The first and zero order kernels $k_1(\tau)$ and k' have to meet the following two conditions:

$$\overline{G_2[h_2;x(t)] \cdot G_1[h_1;x(t)]} = 0$$

and

$$\overline{G_2[h_2;x(t)] \cdot G_0} = 0$$

The first equation leads to:

$$k_1(\tau) = 0$$

The second equation leads to:

$$k' = -p \int_{-\infty}^{\infty} h_2(\tau,\tau)d\tau$$

Thus the second order functional term is:

$$G_2[h_2;x(t)] = \int\!\!\int_{-\infty}^{\infty} h_2(\tau_1,\tau_2)x(t-\tau_1)x(t-\tau_2)d\tau_1 d\tau_2$$

$$- p \int_{-\infty}^{\infty} h_2(\tau,\tau)d\tau$$

By the same procedure, the third order functional term exhibits as:

$$G_3[h_3;x(t)] = \int\!\!\int\!\!\int_{-\infty}^{\infty} h_3(\tau_1,\tau_2,\tau_3)x(t-\tau_1)x(t-\tau_2)x(t-\tau_3)d\tau_1 d\tau_2 d\tau_3$$

$$- 3p \int\!\!\int_{-\infty}^{\infty} h_3(\tau_1,\tau_2,\tau_2)x(t-\tau_1)d\tau_1 d\tau_2$$

Lee and Schetzen (1965) developed a procedure of measuring the Wiener kernels by cross correlation techniques. A nth order Wiener can be evaluated by the following formula:

$$h_n(\tau_1,\ldots,\tau_n) = \frac{1}{n!p^n} E\{(y(t)- \sum_{m=0}^{n-1} G_m[h_m;x(t)])y_n(t)\}$$

where

$$y_n(t) = x(t-\tau_1)x(t-\tau_2)\ldots x(t-\tau_n)$$

Thus by Lee and Schetzen's method the Wiener kernel must be measured in sequence. In order to evaluate a high order Wiener kernel, the modeling response contributed by the lower order has to be subtracted from the total response. Hence,

$$h_o = E\{y(t)\}$$

$$h_1(\tau) = \frac{1}{p}\{E\ y(t)x(t-\tau)\}$$

$$h_2(\tau_1,\tau_2) = \frac{1}{2p^2}\ E\{(y(t)-h_0)x(t-\tau_1)x(t-\tau_2)\}$$

$$h_3(\tau_1,\tau_2,\tau_3) = \frac{1}{6p^3}\ E\{(y(t)- \int_0^\infty h_1(\tau)x(t-\tau)d\tau)x(t-\tau_1)$$

$$\cdot x(t-\tau_2)x(t-\tau_3)\}$$

3.3 Impulse Response of an One Input System

The Volterra and Wiener functional series is a generalized integral of 'impulse response' of the system. Its first order kernel is the integral of impulse response of the linear part of the system. The second order kernel has a diagonal component and off-diagonal components. The diagonal component modifies single impulse response with the second order nonlinear part. The off-diagonal component modifies double impulse response. These can be shown as follows. Suppose a system can be modeled by first and second order Wiener kernels. i.e.,

$$y(t) = \int_{-\infty}^\infty h_1(\tau)x(t-\tau)d\tau + \int\int_{-\infty}^\infty h_2(\tau_1,\tau_2)x(t-\tau_1)x(t-\tau_2)d\tau_1 d\tau_2$$

Let a single impulse be the input, i.e.,

$$x(t) = \delta(t)$$

The response due to such an impulse is

$$y_1(t) = h_1(t) + h_2(t,t)$$

Since the first term represents the linear part, it obeys the homo-

geneous property. As for the second term, it does not obey this property. If we give the input a negative impulse, i.e.,

$$x(t) = -\delta(t)$$

Then, the response is

$$y_2(t) = -h_1(t) + h_2(t,t)$$

Thus the sign of the linear term varies with the sign of the input while the sign of the second order nonlinear term does not. By the above equation, the following relationships can be observed.

$$h_1(t) = \frac{1}{2}(y_1(t)-y_2(t))$$

$$h_2(t,t) = \frac{1}{2}(y_1(t)+y_2(t))$$

These equations indicate that within such a second order system the first order kernel is equivalent to the average of the difference of its positive impulse response and negative impulse response, the diagonal component of the second order kernel is equivalent to the average of their summation. This also makes it clear that the diagonal represents the nonlinearity to impulses of different heights.

When the input contains two impulses, one follows the other with a delay time Δt, i.e.,

$$x(t) = \delta(t) + \delta(t+\Delta t)$$

The response is

$$y(t) = h_1(t) + h_1(t+\Delta t)$$
$$+ h_2(t,t) + h_2(t+\Delta t,t+\Delta t)$$
$$+ 2h_2(t,t+\Delta t)$$

In addition to the response from each single impulse there is

one more term $2h_2(t,t+\Delta t)$ arising from the interaction of two impulses.

This off-diagonal component and the diagonal component are shown in

Fig. 3.1.

As the order of nonlinearity increases the response due to a

set of impulses involves more and more terms from higher order non-

linearity.

3.4 Two-Input Systems and Cross Kernels

The Wiener functional expansion for a two-input system has

been derived by Marmarelis and McCann (1973). In order to apply Lee

and Schetzen's cross correlation algorithm to measure its kernels,

these two inputs have to be assigned two independent gaussian

white noise. The functional expansion with these two inputs each

with power spectral densities p_x and p_u has the following form:

$$y(t) = \sum_{n=0}^{\infty} G_n[h_n;x(t),u(t)]$$

Its first two functionals are

$$G_0[h_0;x(t),u(t)] = h_0$$

$$G_1[h_1;x(t),u(t)] = \int_{-\infty}^{\infty} h_{1x}(\tau)x(t-\tau)d\tau + \int_{-\infty}^{\infty} h_{1u}(\tau)u(t-\tau)d\tau$$

The second order functional is
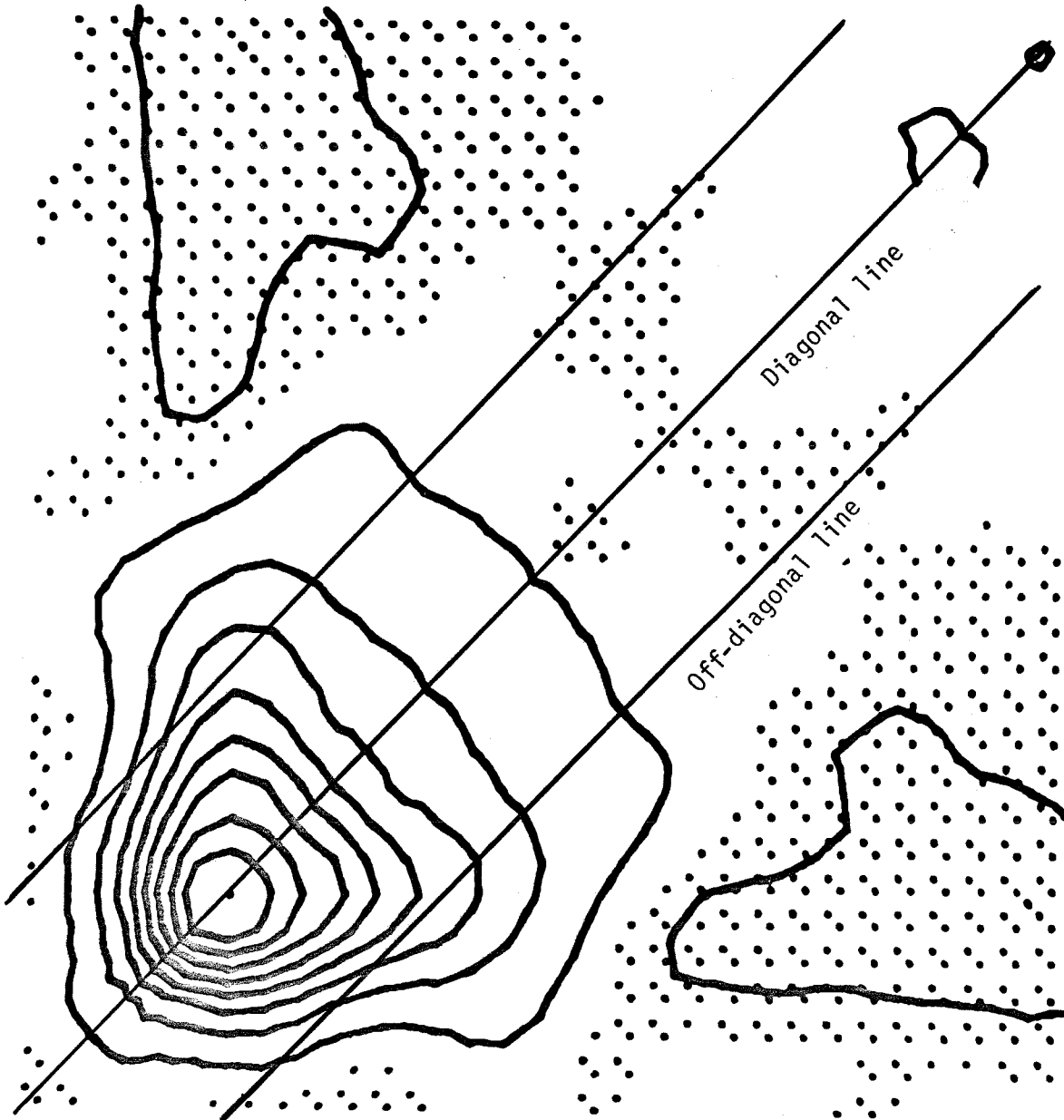
Fig. 3.1 Second order self kernel.
Diagonal line and off-diagonal line.

$$G_2[h_2;x(t),u(t)] = \int\int\limits_{-\infty}^{\infty} h_{2xx}(\tau_1,\tau_2)x(t-\tau_1)x(t-\tau_2)d\tau_1 d\tau_2$$

$$+ \int\int\limits_{-\infty}^{\infty} h_{2uu}(\tau_1,\tau_2)u(t-\tau_1)u(t-\tau_2)d\tau_1 d\tau_2$$

$$- p_x \cdot \int\limits_{-\infty}^{\infty} h_{2xx}(\tau,\tau)d\tau - p_u \cdot \int\limits_{-\infty}^{\infty} h_{2uu}(\tau,\tau)d\tau$$

$$+ \int\int\limits_{-\infty}^{\infty} h_{2xu}(\tau_1,\tau_2)x(t-\tau_1)u(t-\tau_2)d\tau_1 d\tau_2$$

The first order functional contains only self kernels h_{1x} and h_{1u}. The second order functional contains both self kernels h_{2xx}, h_{2uu} and cross kernel h_{2xu}. The self kernel h_{2jj} is symmetrical in the variables τ_1 and τ_2. The cross kernel h_{2xu}, in general, may have both symmetrical and asymmetrical components. The symmetrical part is directionally insensitive, while the anti-symmetrical part is directional sensitive. They can be represented as follows ($\bar{h}_{2xu}$: symmetrical; $\tilde{h}_{2xu}$: anti-symmetrical).

$$\bar{h}_{2xu}(\tau_1,\tau_2) = \frac{1}{2}\left[h_{2xu}(\tau_1,\tau_2)+h_{2xu}^T(\tau_1,\tau_2)\right]$$

$$\tilde{h}_{2xu}(\tau_1,\tau_2) = \frac{1}{2}\left[h_{2xu}(\tau_1,\tau_2)-h_{2xu}^T(\tau_1,\tau_2)\right]$$

T: Transpose operator

with,

$$\overline{h}_{2xu}(\tau_1,\tau_2) = \overline{h}_{2xu}^{\mathsf{T}}(\tau_1,\tau_2)$$

$$\tilde{h}_{2xu}(\tau_1,\tau_2) = -\tilde{h}_{2xu}^{\mathsf{T}}(\tau_1,\tau_2)$$

If the response contributed by the cross interaction (expressed by $y_{xu}(t)$) can be modeled with only one second order anti-symmetrical cross kernel, i.e.,

$$y_{xu}(t) = \int\!\!\!\int_{-\infty}^{\infty} h_{2xu}(\tau_1,\tau_2)x(t-\tau_1)u(t-\tau_2)d\tau_1 d\tau_2$$

then the impulse response due to a forward motion impulse (i.e., $x(t) = \delta(t)$, $u(t) = \delta(t+\Delta t)$ forward defined by $\Delta t > 0$) the response is:

$$y_{xu1}(t) = h_{2xu}(t,t+\Delta t)$$

While to a reverse motion impulse ($x(t) = \delta(t+\Delta t)$, $u(t) = \delta(t)$) the response is:

$$y_{xu2}(t) = h_{2xu}(t+\Delta t,t)$$

$$= -h_{2xu}(t,t+\Delta t)$$

Three other pairs of impulses also elicit an equivalent forward response; they are:

$$x(t) = -\delta(t), \qquad u(t) = -\delta(t+\Delta t)$$

or $\quad x(t) = \delta(t+\Delta t), \qquad u(t) = -\delta(t)$

or $\quad x(t) = -\delta(t+\Delta t), \qquad u(t) = \delta(t)$

Similarly, three other pairs of impulses elicit equivalent reverse responses. They are shown in Fig. 3.2 for the same
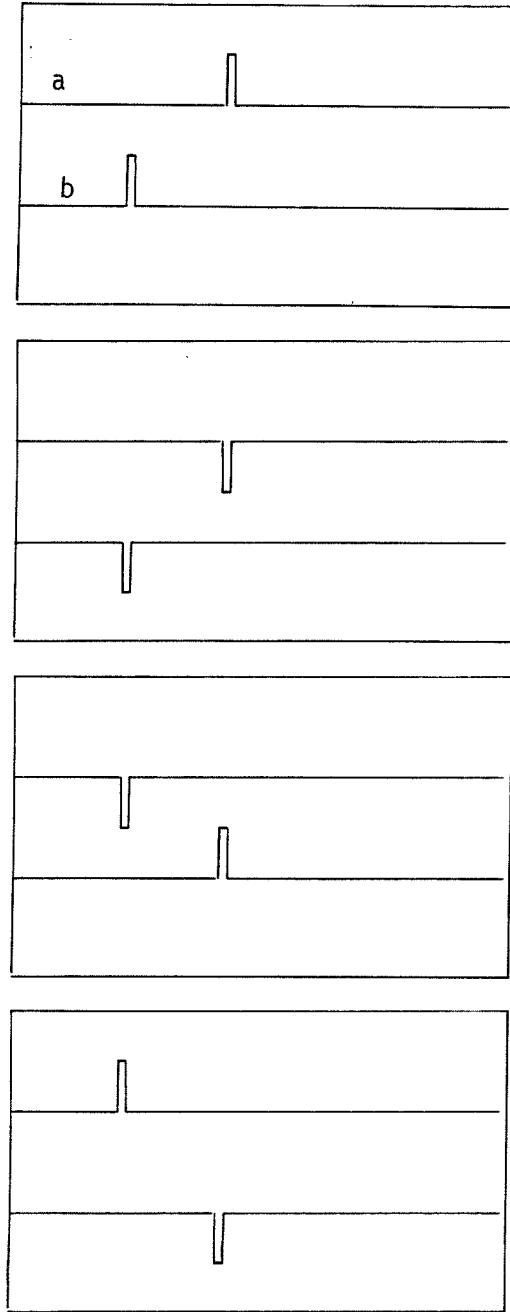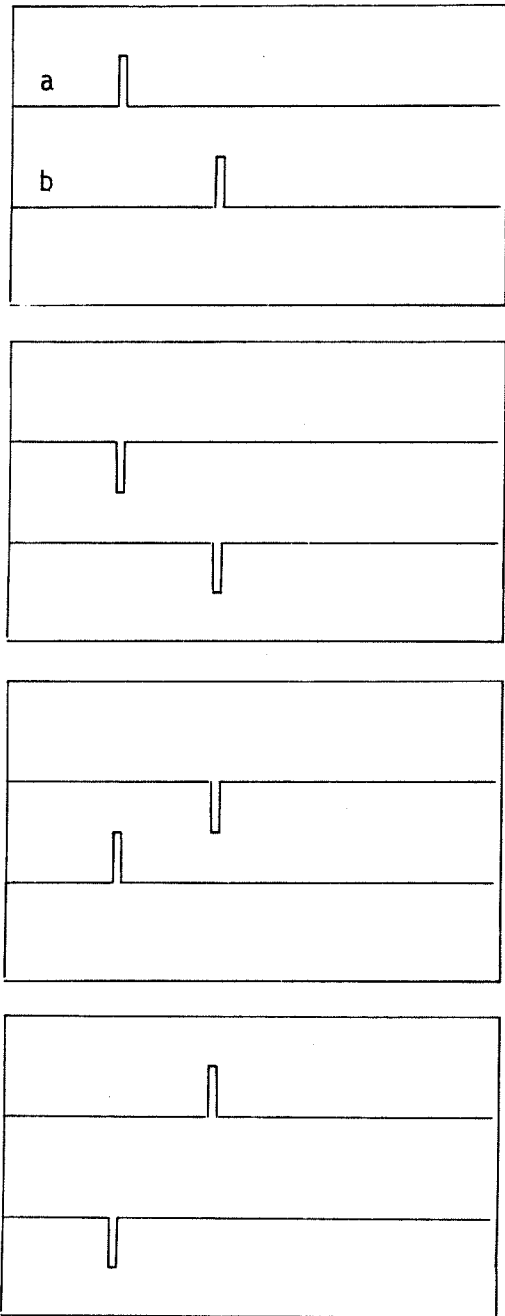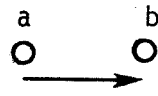
Fig. 3.2a Four pairs of impulses eliciting forward responses.

Fig. 3.2b Four pairs of impulses eliciting backward responses.
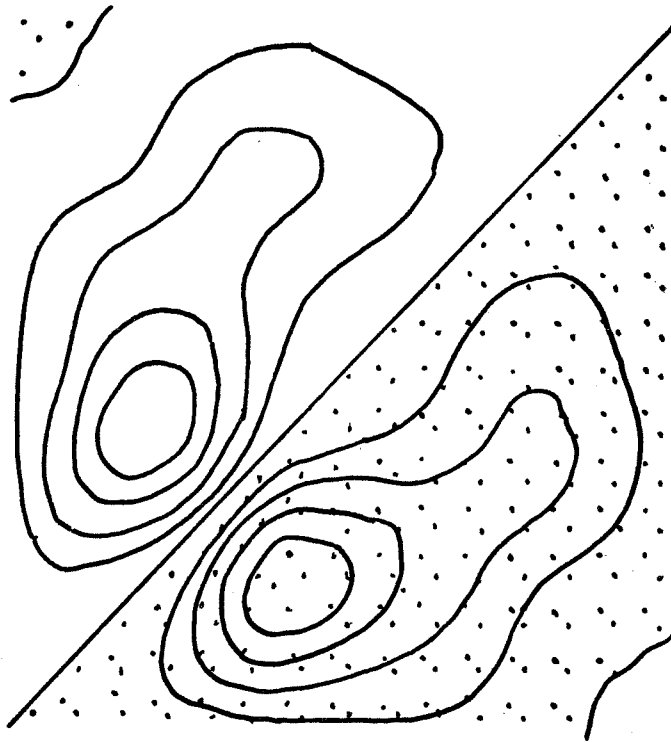
Fig. 3.3 Asymmetrical second order
cross kernel.Dots represent region
with negative values.

reason as the case of a single channel, the system may need higher order kernels to model the impulse responses when these responses are not equivalent. Fig. 3.3 is an example of the anti-symmetrical cross kernel.

The way to compute the second order cross kernel is (Marmarelis and Naka, 1974).

$$h_{2xu}(\tau_1,\tau_2) = \frac{1}{P_x P_u} E[y(t)x(t-\tau_1)u(t-\tau_2)]$$

The Wiener functional due to higher order cross kernels, such as the third order cross kernel, has the following form:

$$\iiint_{-\infty}^{\infty} h_{xuu}(\tau_1,\tau_2,\tau_3)x(t-\tau_1)u(t-\tau_2)u(t-\tau_3)d\tau_1 d\tau_2 d\tau_3$$

$$- P_u \iint_{-\infty}^{\infty} h_{xuu}(\tau_1,\tau_2,\tau_2)x(t-\tau_1)d\tau_1 d\tau_2$$

$$+ \iiint_{-\infty}^{\infty} h_{xxu}(\tau_1,\tau_2,\tau_3)x(t-\tau_1)x(t-\tau_2)u(t-\tau_3)d\tau_1 d\tau_2 d\tau_3$$

$$- P_x \iint_{-\infty}^{\infty} h_{xxu}(\tau_1,\tau_2,\tau_2)u(t-\tau_2)d\tau_1 d\tau_2$$

It is noted that there are two third order cross kernels h_{xuu} and h_{xxu}. The Wiener functional with the fourth order cross kernel has the form:

$$\iiiint_{-\infty}^{\infty} h_{xxuu}(\tau_1,\tau_2,\tau_3,\tau_4)x(t-\tau_1)x(t-\tau_2)u(t-\tau_3)u(t-\tau_4)d\tau_1 d\tau_2 d\tau_3 d\tau_4$$

$$- P_x \iiint_{-\infty}^{\infty} h_{xxuu}(\tau_1,\tau_1,\tau_2,\tau_3)u(t-\tau_2)u(t-\tau_3)d\tau_1 d\tau_2 d\tau_3$$

$$- P_u \iiint_{-\infty}^{\infty} h_{xxuu}(\tau_1,\tau_2,\tau_3,\tau_3)x(t-\tau_1)x(t-\tau_2)d\tau_1 d\tau_2 d\tau_3$$

$$+ P_x P_u \iint_{-\infty}^{\infty} h_{xxuu}(\tau_1,\tau_1,\tau_2,\tau_2)d\tau_1 d\tau_2$$
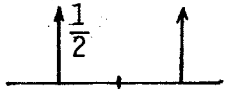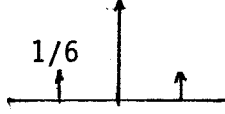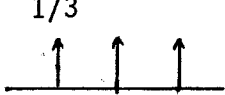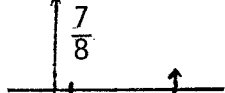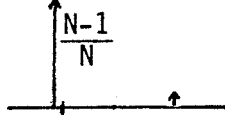
Poggio and Reichardt (1976a) suggested that within the fly's visual system a third order p-order 2 functional could arise from the mechanism of optomotor adaptation. A fourth order p-order 2 functional could be associated with the figure-ground discrimination, determination of behaviour mode, and optomotor adaptation.

In order to measure these high order kernels there are two difficulties to be overcome. One is that the experimental time should be long enough to give a high signal to noise ratio of the kernel. The other is on the evaluation of the diagonal points. Palm and Poggio pointed out that 'delta-like' measurement errors occur on these diagonals and they can be avoided by the use of some discrete time stochastic inputs (Palm and Poggio, 1977).

3.5 White Noise

48

The previous Wiener nonlinear identification theory was based

on gaussian white noise as input. However, a real white noise is

not feasible, for it has an infinite spectral range and infinite

levels of magnitude in time domain. When this theory is applied to

biological system, the spectral range could be reduced to an ex-

tent just covering the system bandwidth without loss of the informa-

tion of the system. The number of levels must also be reduced by

approximation or truncation. Besides, there are many different

types of white noise; they are different in their amplitude pro-

bability distributions and their generation statistics.

Several commonly seen types are binary, ternary, poisson, and

CSRS (the constant-switching-pace-symmetric random signals). Each

of them has different autocorrelation functions of all orders.

These lead to different powers and different functional forms.

Usually these differences are the two factors by which we could

make the choice of which stimuli to use. If the magnitude difference

between the highest level (bright) and the lowest level (dark)

is 2, then the powers of all types of white noise could be listed as

in Table 1. Among them the binary stimulus has the maximum power,

while the gaussian stimulus has the minimum power. Another aspect

is the existence of the diagonal of kernels. From Krause

(1975) it is known that the second order kernel of a poisson

stimulus does not have its diagonal. As for the binary stimulus,

there is no way to measure the diagonal. The meaning of the second

order diagonal component has been interpreted (section 3.3) as the

anti-symmetrical term of the impulse response due to a positive impulse

	P1	P2	Probability Distribution
Gaussian	1/9	1/27	
Binary	1	1	$\frac{1}{2}$
Ternary	1/3	1/3	1/6
Ternary(CSRS)	2/3	2/3	1/3
Poisson 1/8	7/16	343/256	$\frac{7}{8}$
Poisson 1/N	$\dfrac{4(N-1)}{N^2}$	$\dfrac{16(N-1)^3}{N^4}$	$\frac{N-1}{N}$

$$P1 = \overline{X(t)^2} \qquad P2 = \overline{X(t)^4}$$

Table. 1 First and second autocorrelation functions of several white noises.

or a negative impulse. In the experiments of later chapters, the response elicited from an <u>off</u> level is as important as that from an <u>on</u> level. Therefore the considerations about the type of stimuli to be selected are: (1) The diagonal of kernels of the stimulus exist. (2) Stimulus has a high power. Thus, ternary is the best type for the choice. Since ternary has the same second order autocorrelation function as the gaussian stimuli, the second order kernel computing routine for gaussian stimuli needs no modification. Thus if an experiment is designed for studying the single input system, a ternary stimulus is selected. If it is designed for investigating the cross interaction of two inputs, binary stimulus is selected. Time profiles of these two stimuli are shown in Fig. 3.4.

3.6 <u>Weight Coefficient</u>

A sinewave grating has been used extensively in the study of spatial vision. By varying the spatial frequency and measuring the averaged response of a motion detection cell, a sensitivity curve could be constructed, by which the sampling distance of inputs and spatial organization of motion detection subunits could be evaluated. This section is concerned with a detailed treatment of the relationship between the strength of the averaged response and the nonlinear cross kernel. The weight coefficient is then introduced. Consider a sinewave grating moving in front of a n-equidistant receptors system with a direction parallel to them, as shown in Fig. 3.5. If we assume each receptor has a spatial sensitivity with the form of a delta function (needle-shaped function), then the signal sensed by
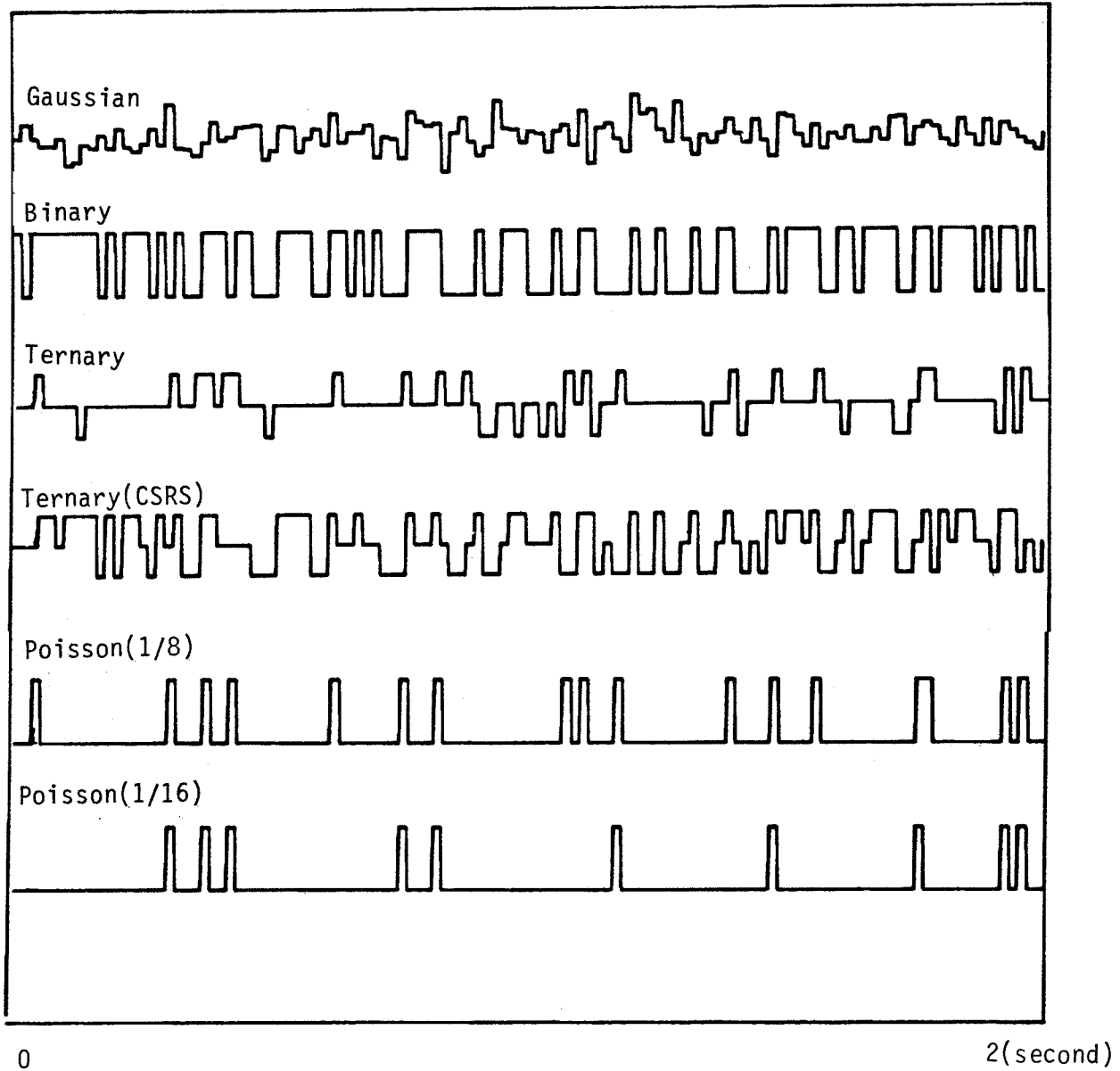
51

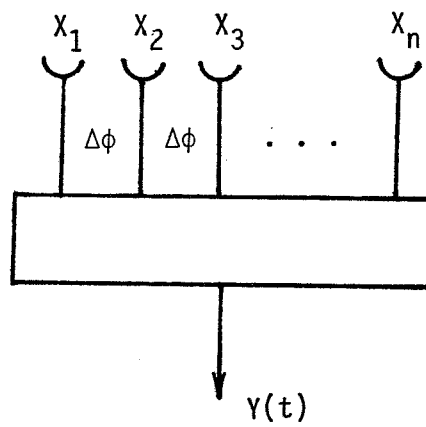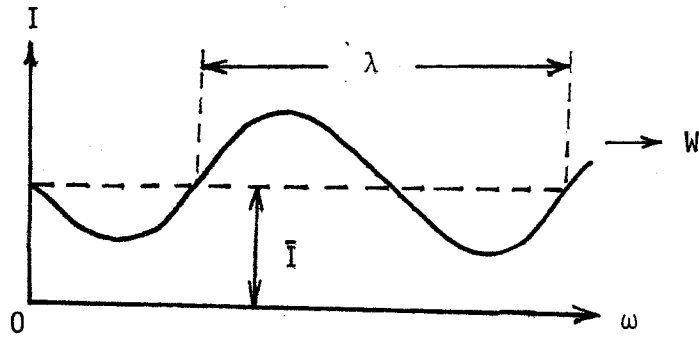Fig. 3.4 Several types of
White Noises.

Fig. 3.5 Illustration of the stimulus
situation for equally spaced receptors.

receptor i is given by:

$$x_i(t) = \bar{I} + \Delta I \sin \omega_0(t - i\Delta t)$$

$$\omega_0 = \frac{2\pi |w|}{\lambda}$$

$\Delta t = \Delta\phi/w$ denotes the time it takes the grating to move from one receptor to the next. The term $\Delta\phi$ is the distance between two receptors.

If an elementary motion detection unit has two inputs such as the ith and jth receptors in Fig. 3.5, and if this unit is modeled by a nonlinear cross kernel $g_{i,j}$, then the averaged response of this unit has the following form:

$$\bar{y}_{i,j} = E\left[\iint\limits_{-\infty}^{\infty} g_{i,j}(\tau_1,\tau_2) x_i(t-\tau_1) x_j(t-\tau_2) d\tau_1 d\tau_2\right]$$

or this could be written in frequency domain as:

$$\bar{y}_{i,j} = \frac{1}{T_0(2\pi)^2} \int_{-T_0/2}^{T_0/2} \iint\limits_{-\infty}^{\infty} G_{i,j}(\omega_1,\omega-\omega_1)$$

$$\cdot x_i(\omega_1) x_j(\omega-\omega_1) d\omega_1 e^{i\omega t} d\omega dt$$

where

$$G_{i,j}(\omega_1,\omega_2) = \iint\limits_{-\infty}^{\infty} g_{i,j}(\tau_1,\tau_2) e^{-i(\omega_1\tau_1 + \omega_2\tau_2)} d\tau_1 d\tau_2$$

$$x_j(\omega) = \int_{-\infty}^{\infty} x_j(t)e^{-i\omega t} dt$$

$$= 2\pi\overline{I}\delta(\omega) + i\pi\Delta I \;\; \delta(\omega+\omega_0)e^{ij\omega_0\Delta t} - \delta(\omega-\omega_0)e^{-ij\omega_0\Delta t}$$

The result was derived by Buchner (1976) with the following form:

$$\overline{y}_{i,j} = \overline{I}^2 G_{i,j}(0,0) + \frac{\Delta I^2}{2} \; ReG_{i,j}(-\omega_0,\omega_0)\cos(j-i)\omega_0\Delta t$$

$$+ \; ImG_{i,j}(-\omega_0,\omega_0)\sin(j-i)\omega_0\Delta t$$

Where $ReG_{i,j}$ and $ImG_{i,j}$ are the real and imaginary part of $G_{i,j}$

$$G_{i,j} = ReG_{i,j} + i\cdot ImG_{i,j}$$

Within the above results the term $ImG_{i,j}(-\omega_0,\omega_0)\sin(j-i)\omega_0\Delta t$

is varied with the direction of movement. This is because

changing the sign of velocity ω would effect the sign of ω_0

and also $\sin(j-i)\omega_0\Delta t$. The term $ImG_{i,j}(-\omega_0,\omega_0)$ is defined as

the 'weight coefficient' which measures the strength of the

averaged response to a sinewave. The following equations lead

to $ReG_{i,j}$ and $ImG_{i,j}$.

$$ReG_{i,j}(-\omega_0,\omega_0) = \iint_{-\infty}^{\infty} g_{i,j}(\tau_1,\tau_2)Re \; e^{-i(-\omega_0\tau_1+\omega_0\tau_2)} d\tau_1 d\tau_2$$

$$= \iint_{-\infty}^{\infty} g_{i,j}(\tau_1,\tau_2)\cos\omega_0(\tau_2-\tau_1)d\tau_1 d\tau_2$$

$$= \iint_{-\infty}^{\infty} \overline{g}_{i,j}(\tau_1,\tau_2)\cos\omega_0(\tau_2-\tau_1)d\tau_1 d\tau_2$$

$$\text{Im}G_{i,j}(-\omega_o,\omega_o) = \iint\limits_{-\infty}^{\infty} \tilde{g}_{i,j}(\tau_1,\tau_2)\sin\omega_o(\tau_2-\tau_1)d\tau_1 d\tau_2$$

Thus $\text{Re}G_{i,j}$ and $\overline{g}_{i,j}$ is one fourier pair, $\text{Im}G_{i,j}$ and $\tilde{g}_{i,j}$ is another

pair, where $\overline{g}_{i,j}$ is the symmetrical part of $g_{i,j}$ and $\tilde{g}_{i,j}$ is the

anti-symmetrical part of $\overline{g}_{i,j}$. These have been shown in section 3.4.

Note that the elementary motion detection unit with channels i and j

has its contributions to the averaged response with the j-ith har-

monic term. This is consistent with Reichardt's (1961) model and

such system will detect motion as appearing to be the reverse of

its true direction for $\Delta\phi \leq \lambda \leq 2\Delta\phi$.

CHAPTER IV

TWO-INPUT STUDIES ON BASIC

MOTION DETECTION UNITS

4.1 Introduction

Although in theory an experiment using temporal-spatial
white noise as the stimulus could quickly reveal a pretty detailed
description of a system, the author would rather start with the
simplest case which confines the stimulus to two inputs of a basic
motion detection unit (two inputs separated by 2.5°). There are
several reasons for this. First, since the whole system (class-IIa1
cell) is considered as a set of parallel connected subunits, by
working out a subunit model first we may get an idea of the system
properties, which include order of nonlinearity, memory, and mini-
mum experimental time for obtaining clean kernels. Second, in order
to give the explanation of the kernels, transient type stimuli were
applied to test the system. This would be manageable only if the
number of inputs is as few as possible. Third, by comparing the
kernels obtained from two channels with the kernels from multi-
channels, the possibility of p-order three interaction could be
observed without actually computing it.

Marmarelis and McCann (1973) have worked on this unit with two
$1/2^{\circ}$ spots separated by 2.5° aligned in the horizontal line. However,
the following experiments in this chapter were done by two $8^{\circ} \times 1/2^{\circ}$
vertical stripes. The signal to noise ratio of the response was
increased when larger areas are stimulated. The contour features of

the kernel are the same as those obtained by Marmarelis. These two stripes contain several two-spot systems. They are assumed to have the same characteristics. Within the next chapter this will be proved by the studies on vertical interactions. All the experiments of this chapter were done in R20-I10 contralateral eye field. The fly's head has to be tilted 15° left to make its z axis matched with the horizontal line of the stimulus system.

4.2 Single Channel Test

Fig. 4.1 is a set of intensity series of post stimulus time histogram (PST) with 200 msec pulse stimulated on a single channel ($1/2^{\circ}$ x 8° stripe area). Pulse intensity was from 50 cd/m^2 down to .08 cd/m^2. Off level intensity was half the pulse intensity. It could be observed that there are both transient on, transient off responses and a slowly decayed sustained on response. To examine the transient on/off responses more carefully, the next experiment was done by both positive pulse and negative pulse with pulse width 64 msec. Both responses revealed positive reaction (increase of firing rate) (Fig. 4.2). Thus, we know that the single channel of class-IIa1 cell is of the mixed type, sustained on and transient on/off unit.

Three sets of white noise experiments were designed and used to compare the results from transient stimulus experiments. Ternary white noise was used here, because it has three light levels and each could be related to on level, steady state level, and off level. Other advantages of ternary white noise are those given in
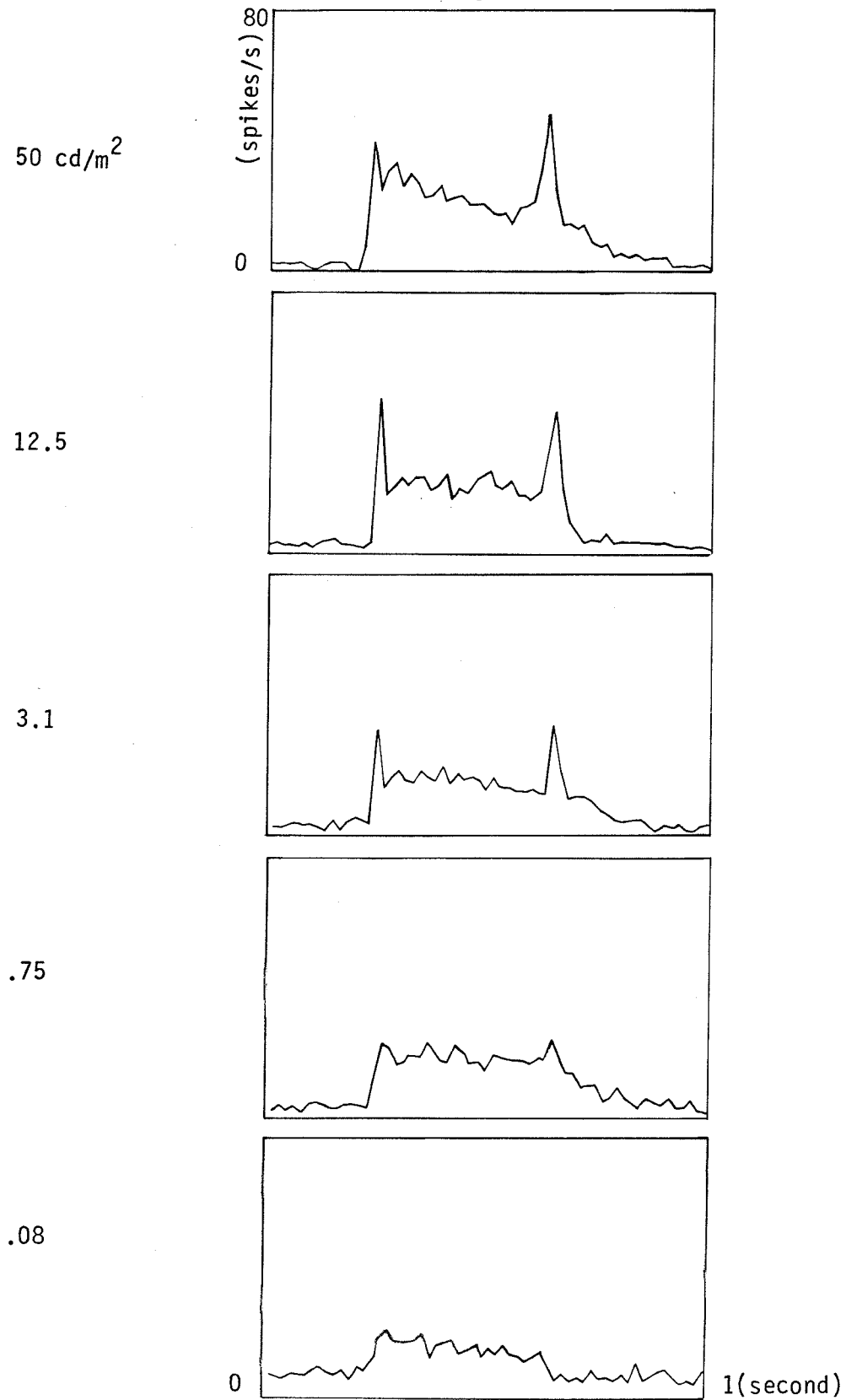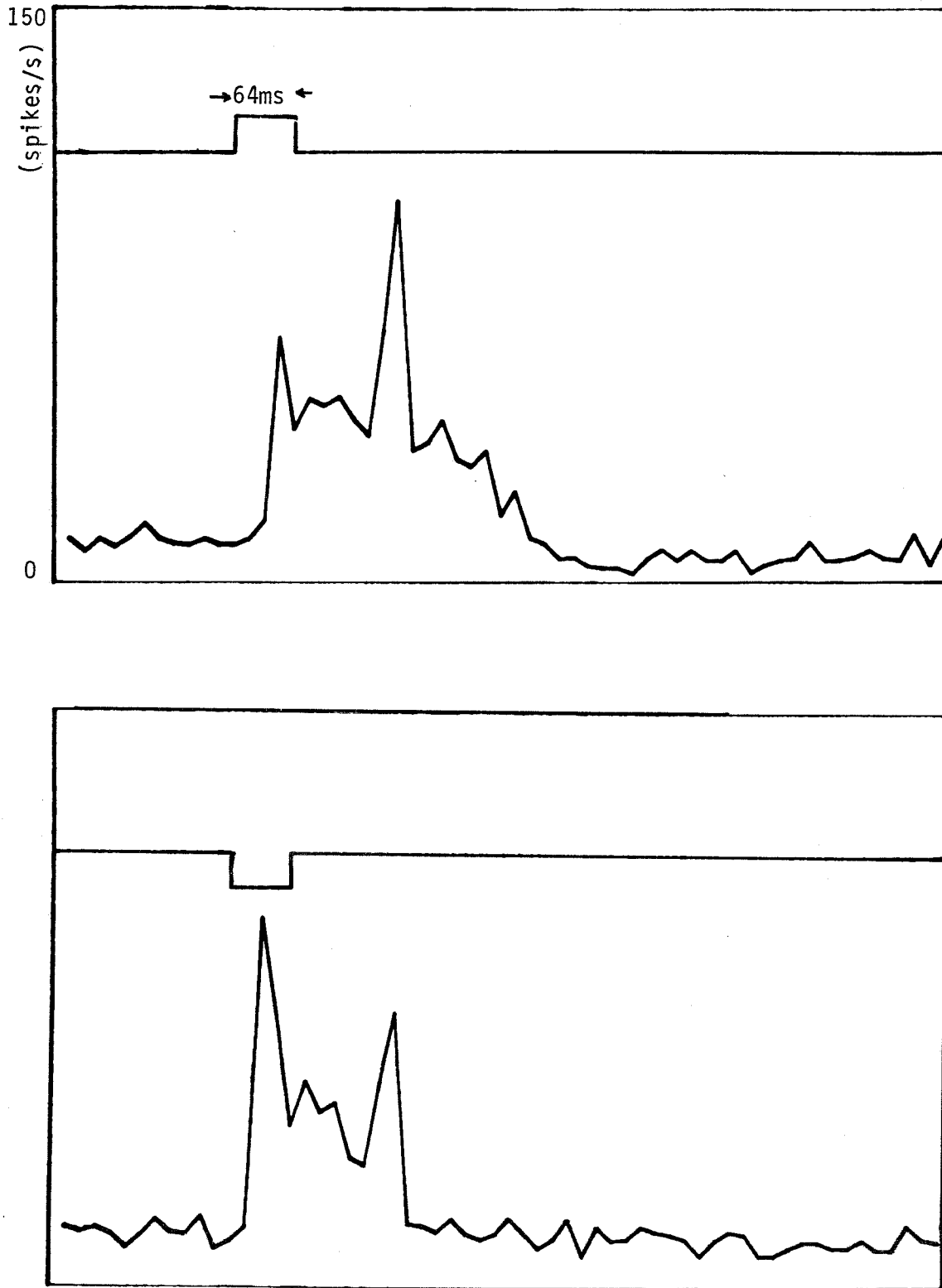
Fig. 4.1 Single channel intensity series.

Fig. 4.2 Positive and negative
pulse responses.

chapter 3 which are: (1) Fewer levels make computation fast. (2) The diagonal points of the second order self kernel exist. Set A is 100% modulated with .5 cd/m^2 on level intensity (low intensity set). Set B is 100% modulated with 50 cd/m^2 on level intensity (high intensity set). Set C is 10% modulated on maximum intensity 50 cd/m^2 (medium intensity with DC background).

Fig. 4.3a,b presents the first and second order kernels of results from experiments A, B, and C. By using kernels to model the white noise response, all these sets show that the second order kernel dominates the modeled response. Kernels of sets A and B are similar; both of their first order kernels have positive maxima and their second order kernels all have positive diagonal components which decay slowly. But kernels of set C are different Its first order kernel has negative maxima, and its second order kernel does not show a long lasting positive diagonal component. These differences are due to their different modulation widths. A white noise stimulus with 100% modulation width can test and model the system dynamics from totally dark to the maximum intensity. Thus, both sustained on and transient on/off responses could be modeled by the first and second order kernels . A white noise stimulus with 10% modulation width can model the system dynamics only within that 10% intensity range. In such a case the sustained response is mostly represented by the averaged firing rate, which is the zero order kernel. Therefore, the first and second order kernels of sets A and B contain information concerning sustained on term and their positive
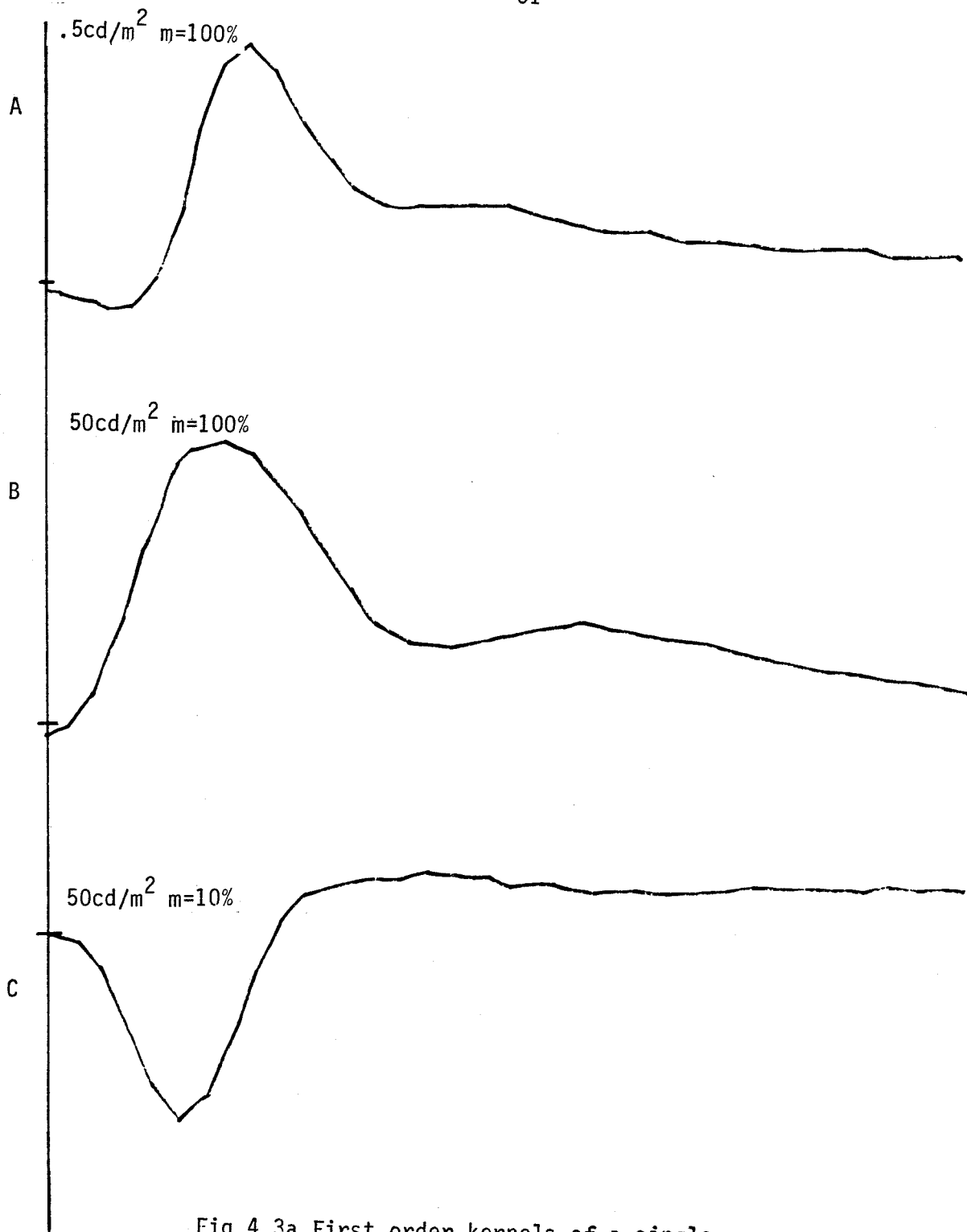
Fig 4.3a First order kernels of a single
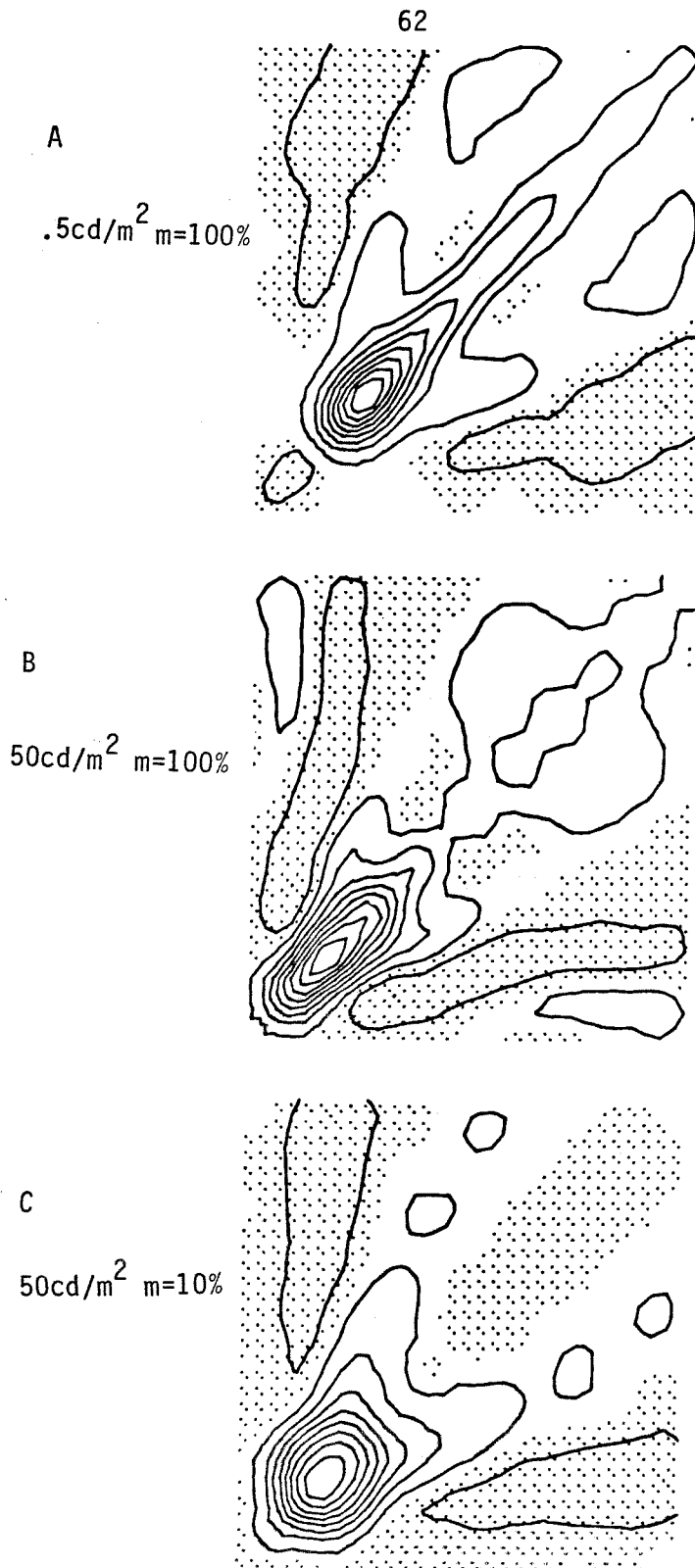channel system. Their peak values are (A)
18.75 (B) 23 (C) -12.5 spikes/sec^2.

A

.5cd/m^2 m=100%

B

50cd/m^2 m=100%

C

50cd/m^2 m=10%

Fig 4.3b Second order kernels of a single channel system. Each contour line represents a division of (A) 5.9 (B) 8.4 (C) 39 spikes/sec^3.

maxima of the first order kernels and slowly decaying positive diagonal components of the second order kernels are contributed by this term. The modeling responses of set B with a 200 msec pulse as input are shown in Fig.4.4. It is clear that the first order kernel models a sustained response, the second order kernel models a transient response. As for the negative maxima of the first order kernel with set C, it could be explained by two factors. First, the first order kernel reflects the average of the difference between a positive impulse response and negative impulse response. Second, with a DC light background the system is more sensitive to negative impulse.

There is a slight difference between sets A and B, which is the time delay of kernel peak. First order kernels of sets A and B have peaks at time delay 50 msec and 33 msec, respectively. Second order kernels also show that set B has less time delay to peak, which is 20 msec. The second order kernel of set C has more positive component further away from diagonal than sets A and B; this shows that the memory of the first impulse excitatory effect on the second impulse is longer under the condition with a DC background light.

The negative off-diagonal component of each case has an second order adaptation effect which would drive the transient response back to silence.

Third order kernel computation revealed that the third order contribution could be neglected. It is natural to think that other higher order kernels do not exist.
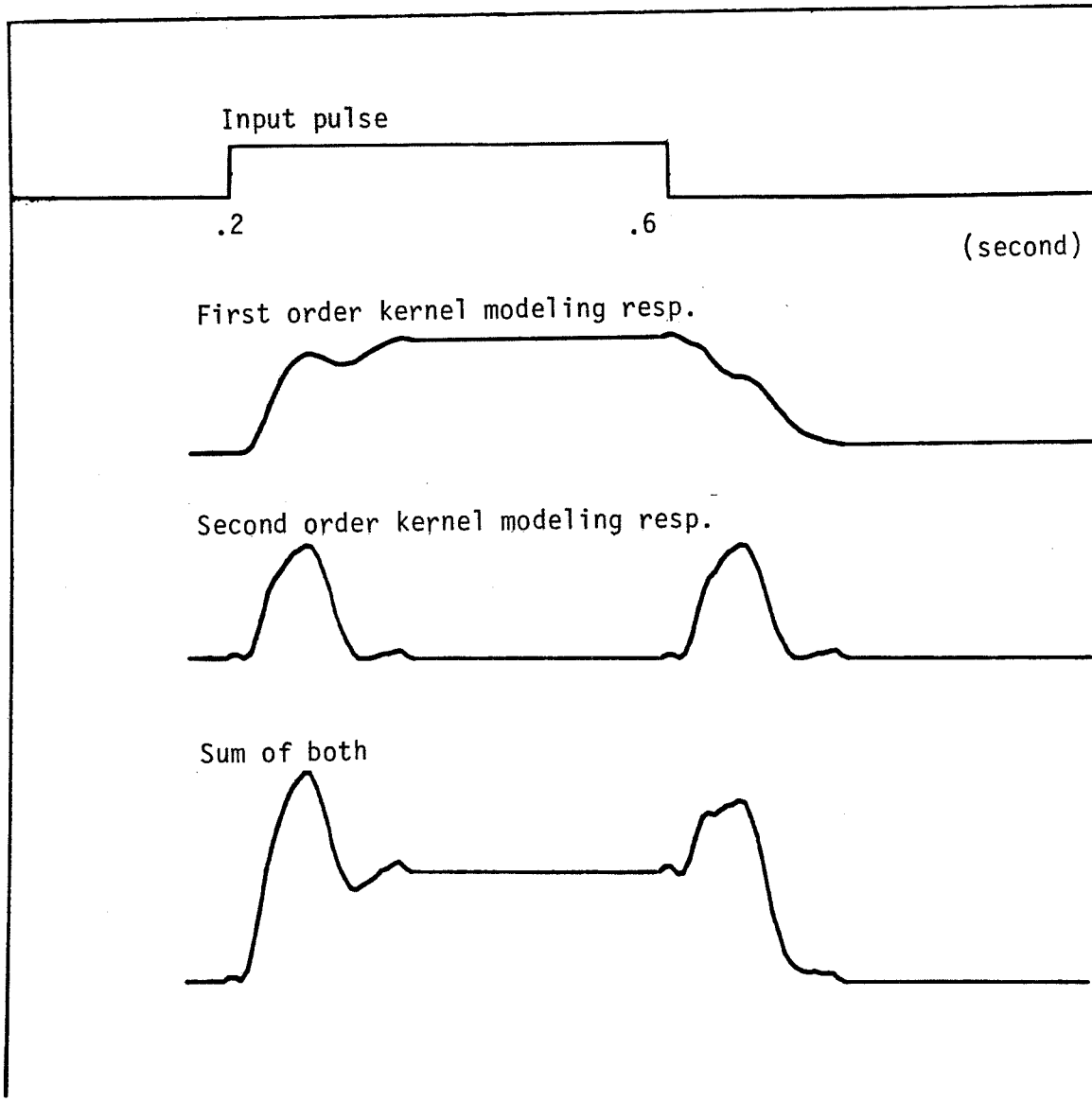
Fig 4.4 Model predicted response to a
pulse stimulus for a single channel system.

In what functions are sustained <u>on</u> term and transient on/off term involved? It is known that the fly has a phototaxic response (the fly usually gets close to a light source). Poggio and Reichardt (1976b) suggested that the fly's visual systems are able to compute the position by the second order self kernel. The sustained <u>on</u> term may be related to the phototaxic response. The transient on/off term may be related to position computation because the on/off term is the second order nonlinear term.

All the aspects considered above are summarized by a conceptualized model (Fig. 4.5) which is a parallel connected system with two pathways: one is the sustained <u>on</u>, the other is transient on/off. The sustained <u>on</u> pathway could be modeled by the zero order kernel and the first order kernel.

$$y_s(t) = k_0(m) + k_1(m) \cdot \int_{-\infty}^{\infty} h_{1s}(\tau, I_0) x(t-\tau) d\tau$$

The modulation width 'm' controls the distribution of each kernel component, increasing 'm' would result in larger k_0 and smaller k_1. Kernel h_1 depends on I_0, larger I_0 decreases the time delay of kernel peak. The transient on/off pathway could be modeled by the first and second order kernels.

$$y_t(t) = k_1'(m) \cdot \int_{-\infty}^{\infty} h_{1t}(\tau, I_0) x(t-\tau) d\tau$$

$$+ k_2'(m) \cdot \left[\int_{-\infty}^{\infty} h_{1t}(\tau, I_0) x(t-\tau) d\tau \right]^2$$
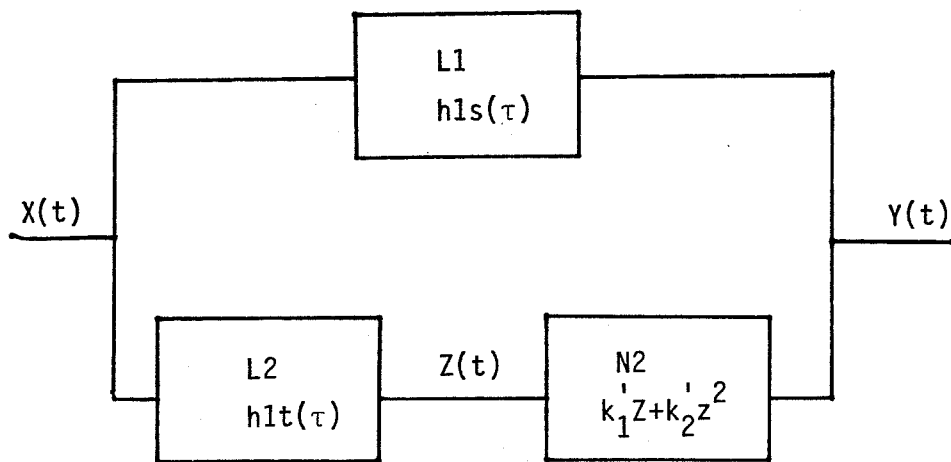
Fig. 4.5 Single channel conceptualized model with sustained channel(L1) in parallel with transient channel(L2,N2).

Both the sign and magnitude of k_1' and k_2' depend on 'm'; increasing

'm' would cause larger negative k_1'. Larger I_0 decreases the time

delay of kernel peak. Here the second order kernel is separated

by its first order kernels. Thus, this system is a linear system

cascaded with a zero-memory nonlinear system which includes a

quadratic term (square law device). The modeling response of the qua-

dratic term would double the input frequency. A series of sinewave

from 1 HZ to 16 HZ and the modeling responses are presented as in

Fig. 4.6.

The results of one channel experiments could be summarized as

follows:

1. To transient on and transient off stimulus the cell responds

   with transient increase of firing rate.

2. To sustained on stimulus the cell responds with sustained

   firing rate which decays slowly.

3. The memory of the system is about 100 msec.

4. The predicted response to white noise of the second order

   kernel dominates the total response with 62% contribution.

5. The first order kernel reflects the averaged effect on posi-

   tive impulse and negative impulse. The predicted white noise

   response of the first order kernel has 17% contribution.

6. The sustained on response is contained in the zero and the

   first order kernels.

7. The transient on/off response is involved with the first
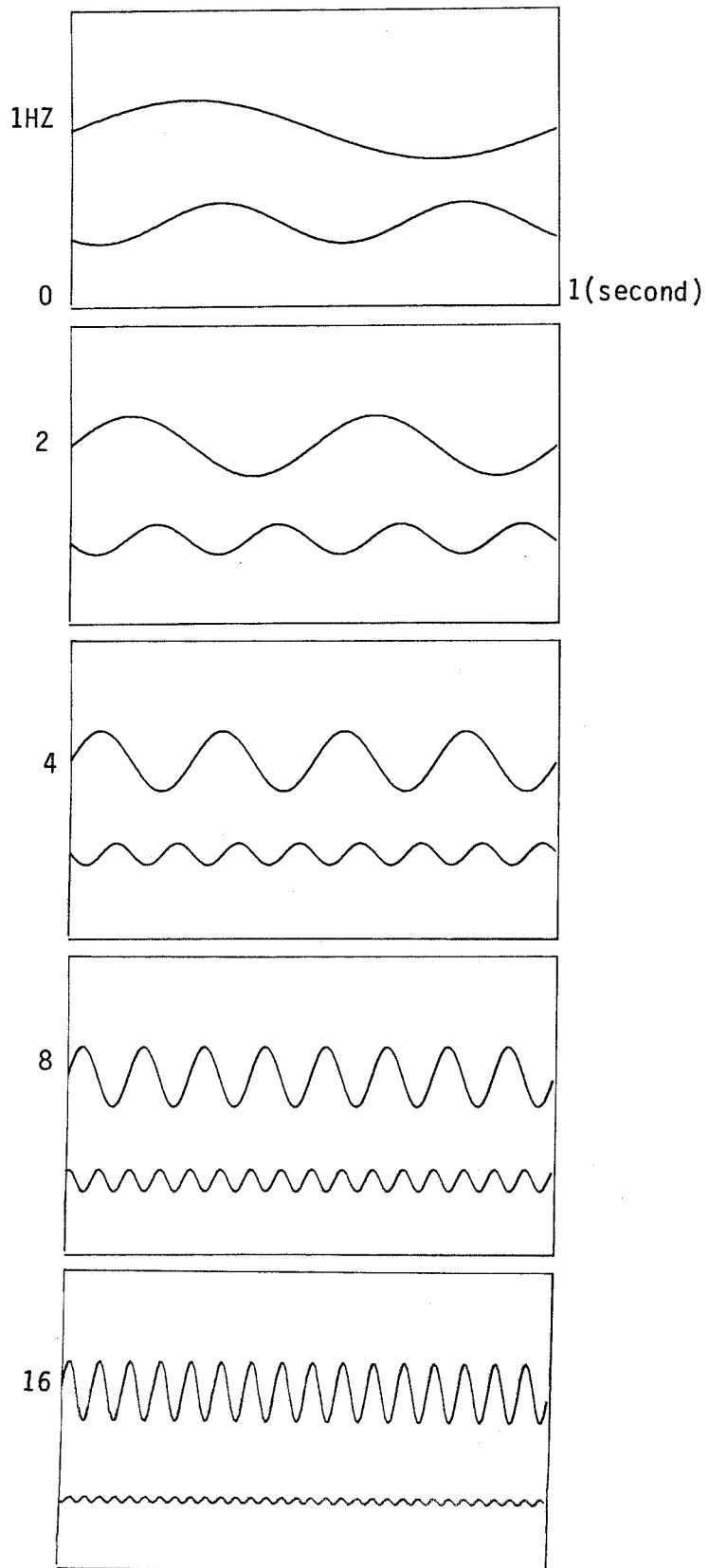
   and second order kernels.

Fig. 4.6 Single channel second order
kernel modeling responses with sinewave
as inputs.

8. The conceptualized system model is a parallel connected system with two pathways; one is the sustained <u>on</u>, the other is the transient on/off.

Other one-input experiments at certain intensity and modulation conditions reveal that within the receptive field of the class-II cell there is only one type of first and second order kernels (kernel features do not vary with receptive field). The next section shows that when two-input stimuli are used to study the receptive field, the first order kernels begin to be differentiated.

4.3 Two-Channel Self Kernel Studies

Reichardt's correlation model (1961) consists of two types of channels, one is of integrating type, the other is of differential type. The experiments in this section were designed to identify these properties and to find the underlying cause. Fig. 4.7 shows the stripe pattern of two channels stimulus with stripe 'a' at the leading site, and stripe 'b' at the trailing site. The first test used two 100% modulated ternary white noise stimuli. Fig. 4.7 shows that the first order kernel of channel 'a' has a negative peak which is different from that of channel 'b'. From the experiments of the last section, it is obvious that the change is due to the stimulus on the adjacent channel 'b'. But whether it is caused by the steady state intensity in channel 'b' or by the dynamics (Sheby, 1978) arising from white noise is unknown. Two more experiments were done for finding the answer. One set is with channel 'a' a ternary white noise and channel 'b' constant light, the other
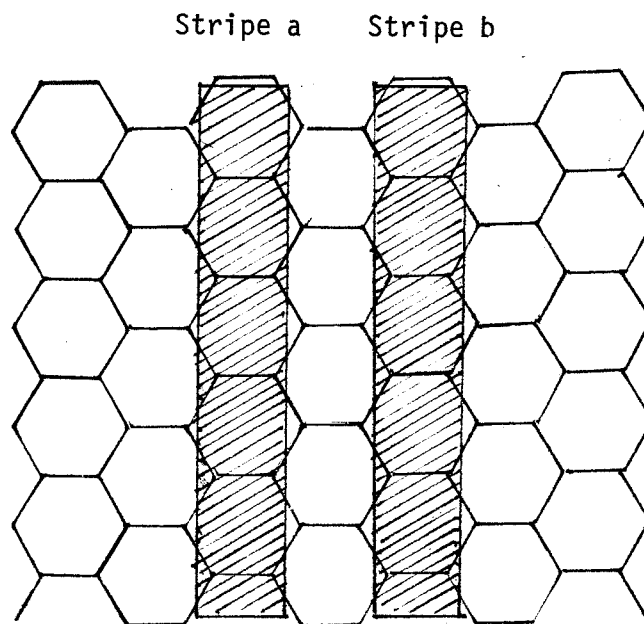
Stripe a   Stripe b

Fig. 4.7 The stripe pattern of two-channel
stimuli.

Single channel study

Hb

Ha

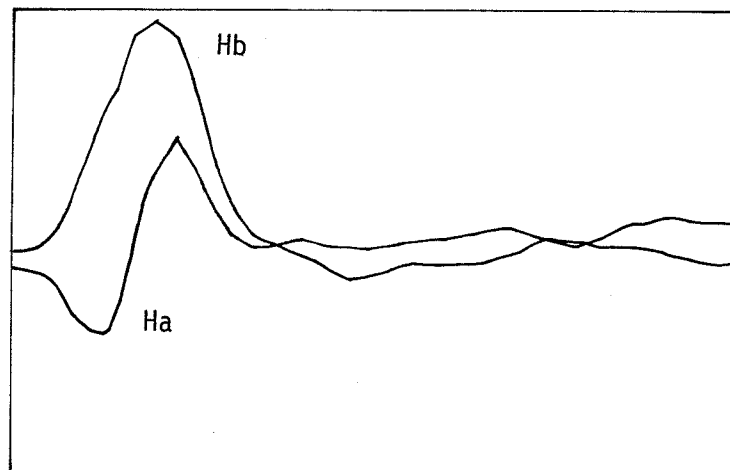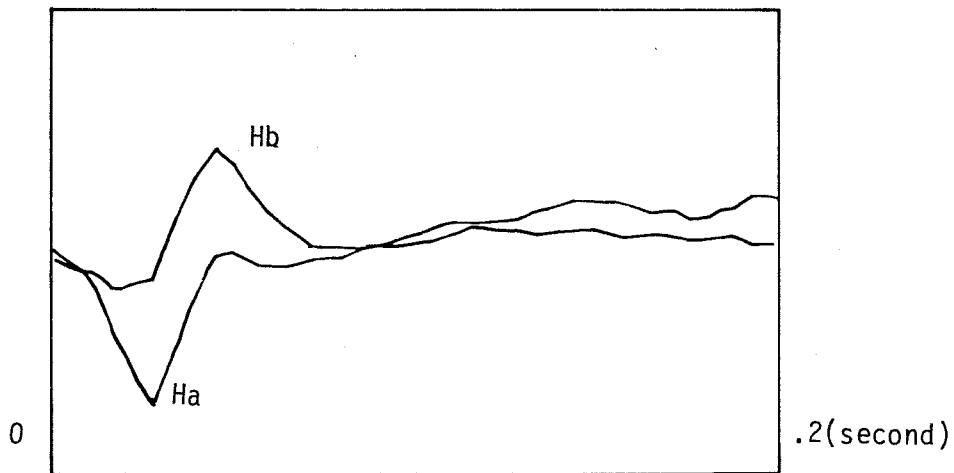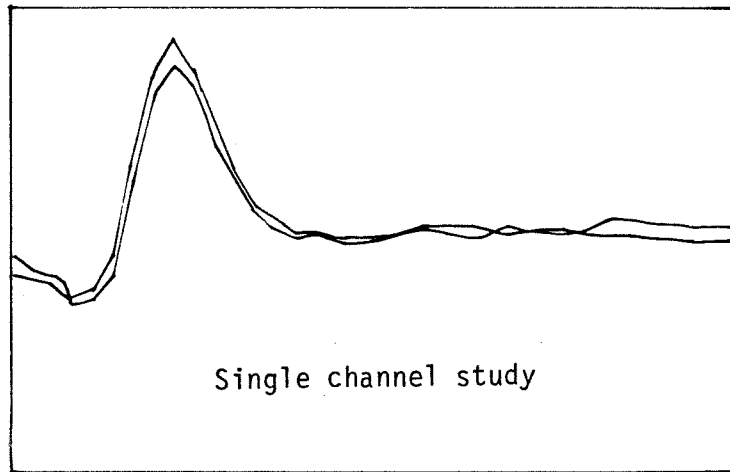0   .2(second)

Hb

Ha

Fig. 4.8 (middle) Two-channel white
noise study.

Fig. 4.9 (lower) One channel white
noise, the other channel constant light.

is with channel 'b' a ternary white noise and channel 'a' constant

light. The kernels computed from these experiments in Fig. 4.9 have

the same characteristics as above. Thus we know that the properties

of the leading channel could be changed by stimulating the trailing

channel with constant light. By examining the second order kernel

of all the above cases, no significant difference has been found.

The conclusion must be that channel 'a' has a stronger response to

transient off than to transient on when channel 'b' is on and channel

'b' has a stronger response to transient on than to transient off

when 'a' is on. This is satisfied even when the delay time of the later

transient is infinity.

4.4 The Mutual Interaction of the Basic Motion Detection Unit

To study the responses of a selective motion detection unit it is

conventional to use a transient stimulus on each channel with a proper

time delay. Such a stimulus would elicit a forward motion response if

the stimulus in the trailing channel has a delay relative to the leading

channel and a reverse motion response in the contrary case. Fig. 4.10

presents typical motion responses in each direction. It should be

noted that the stimulus could be viewed as an assembly of four

types of double pulses at the transitions as shown in Fig. 3.2.

This would help in explaining each of their excitatory and inhibi-

tory contirbutions to the cross kernel.

Fig. 4.11 is an intensity series of forward and reverse responses

to the transient stimulus. It could be observed that within intensity

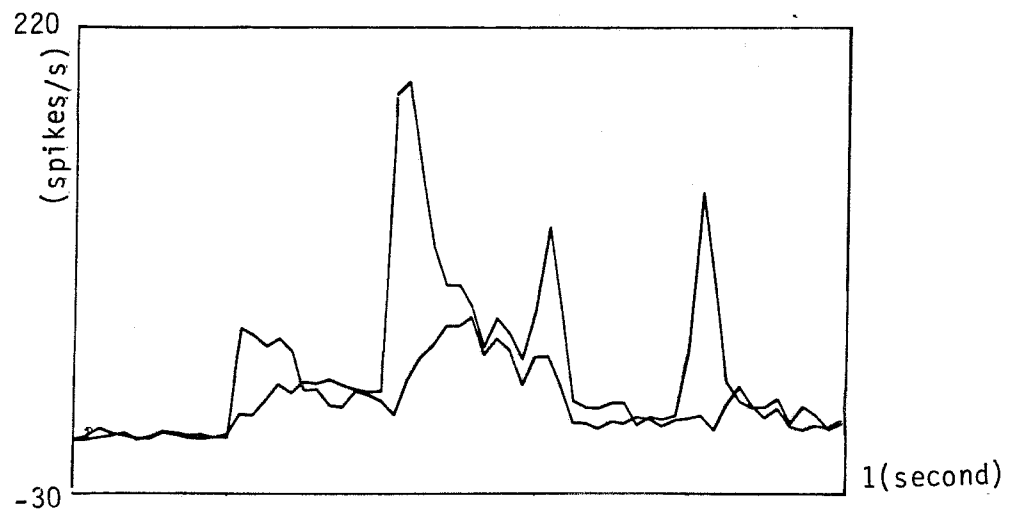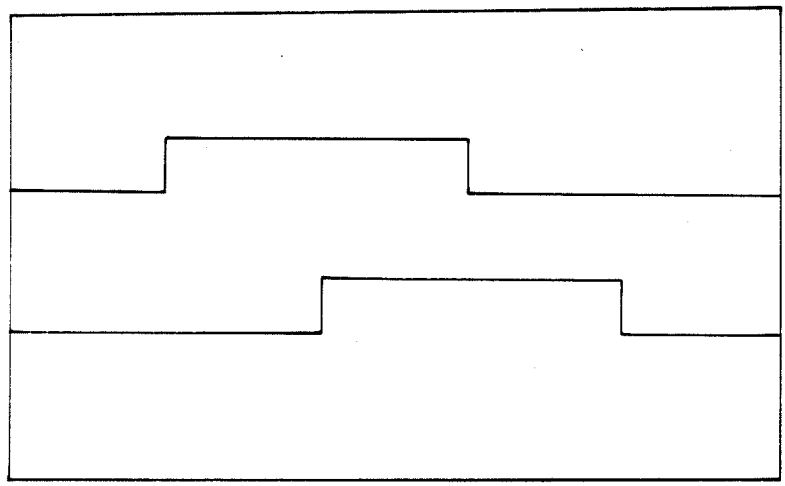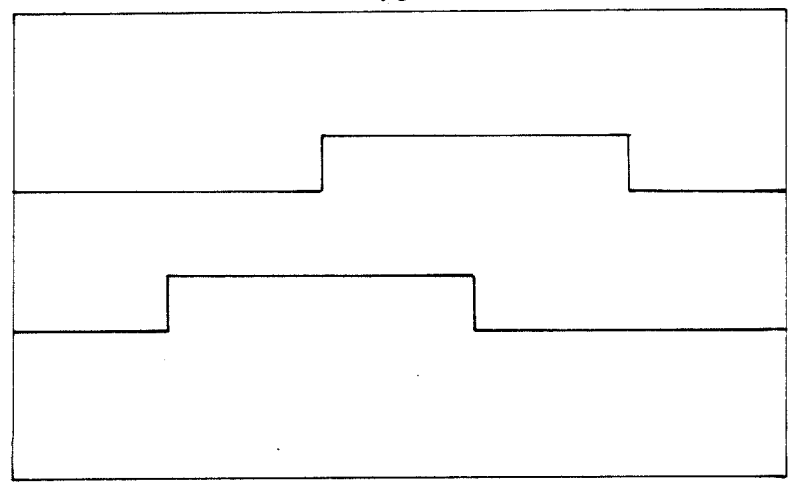range from 12 cd/m^2 to 3 cd/m^2 the directional selective effect is

Fig. 4.10 Typical motion responses
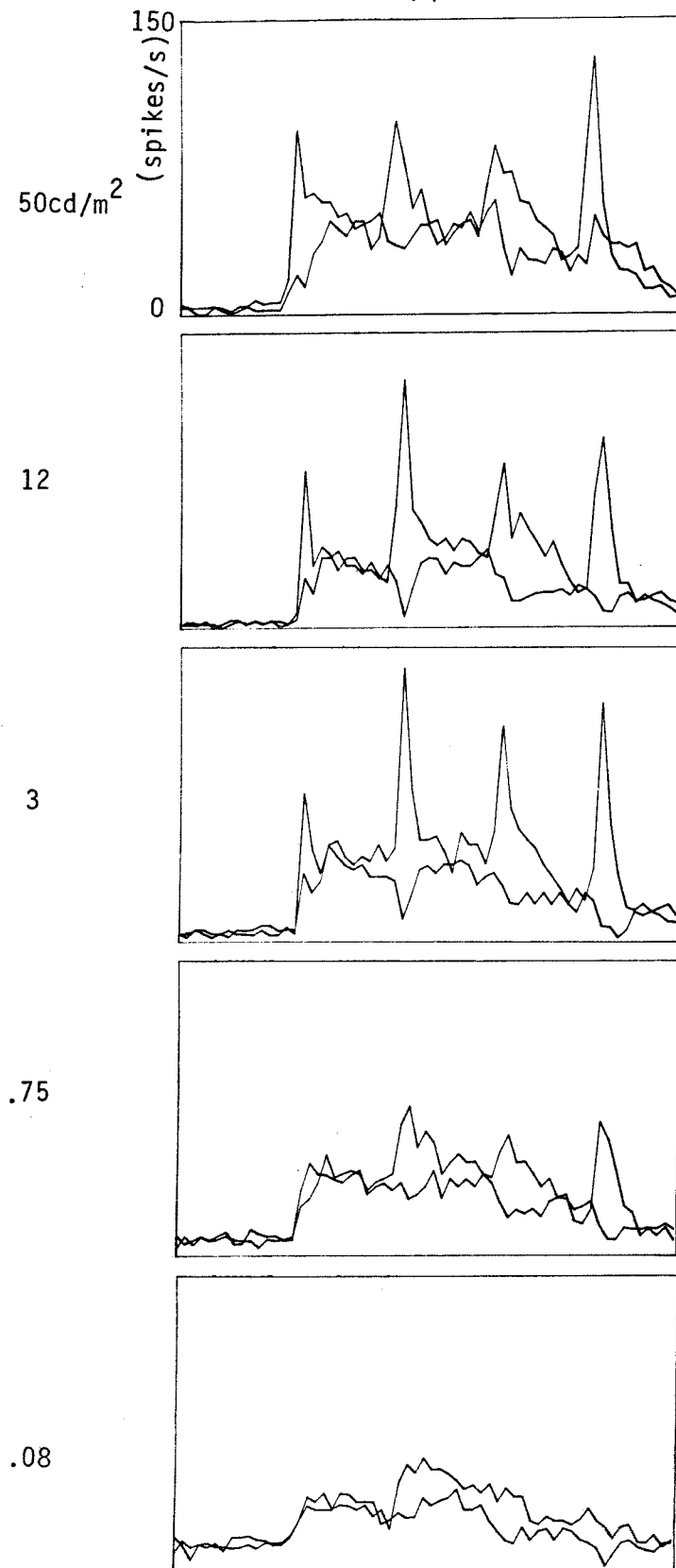of both directions.

Fig. 4.11 An intensity series of
forward and reverse responses.

more efficient than those outside the range. With these data sets, however, it is not possible to determine whether the forward (or reverse) responses are merely linear summation (or substraction) of the responses elicited by each channel alone. Is there a nonlinear contribution (Δ as illustrated by the following equations) for response on each direction?

R (forward) = R_a + R_b (with Δt delay) + Δ (excitation)

R (reverse) = R_b + R_a (with Δt delay) + Δ (inhibition)

Fig. 4.12 is a series of the nonlinear interaction terms obtained by subtracting responses of Fig. 4.2 from response of Fig. 4.11 (these data were from one cell). Except the lowest and highest intensity cases all show clear excitatory (or inhibitory) effect on three transient states. There is no excitatory or inhibitory contirbution from the first transit state, because R_a is equal to R (forward) and R_b is equal to R (reverse) here by the same adapted condition. At low intensity, there is very small contribution from this nonlinear interaction term. At high intensity (50 cd/m^2), a constant inhibition exists in both forward and reverse directions. This remarkable change exposes different mechanisms associated with the system at different intensity conditions. This will be discussed in later chapters.

A typical second order cross kernel is shown in Fig. 4.13. There is a positive region on one side of the diagonal line and a negative region on the other side. This matches with the results of transient stimuli shown above (in Fig. 4.12). The memory of this
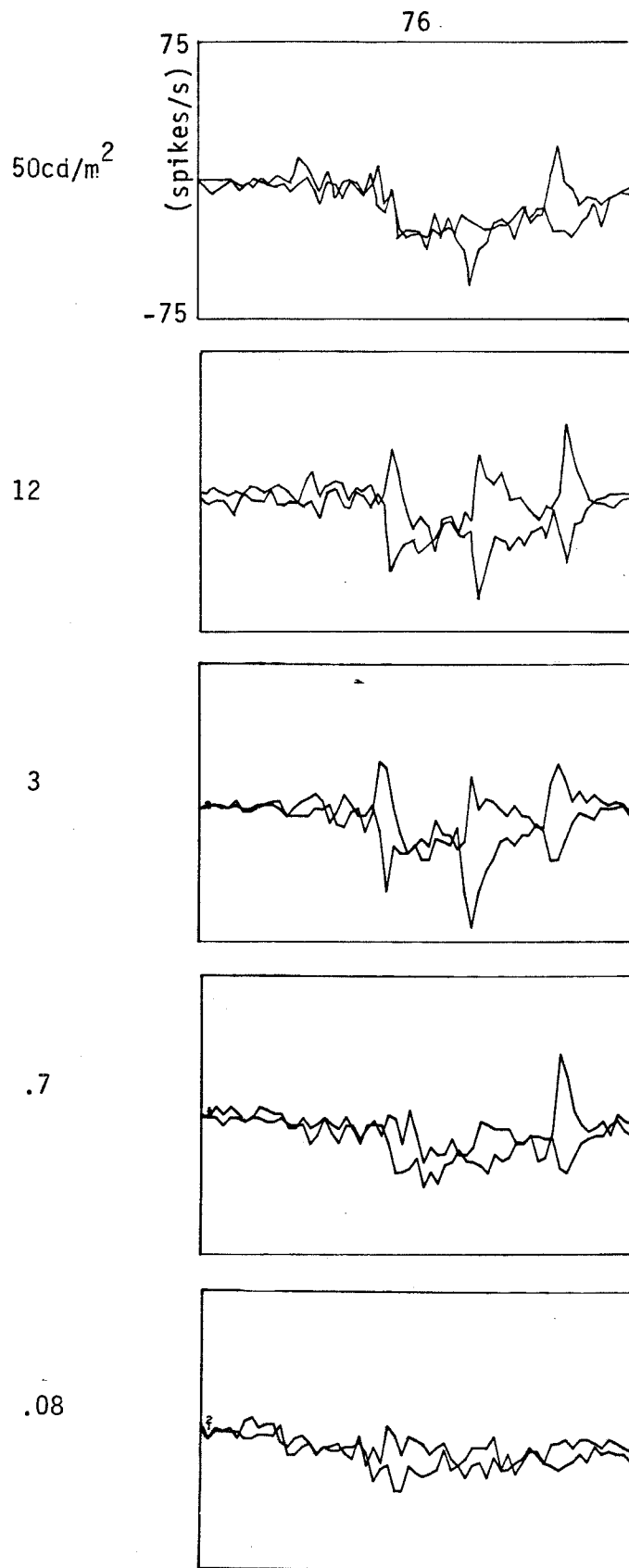
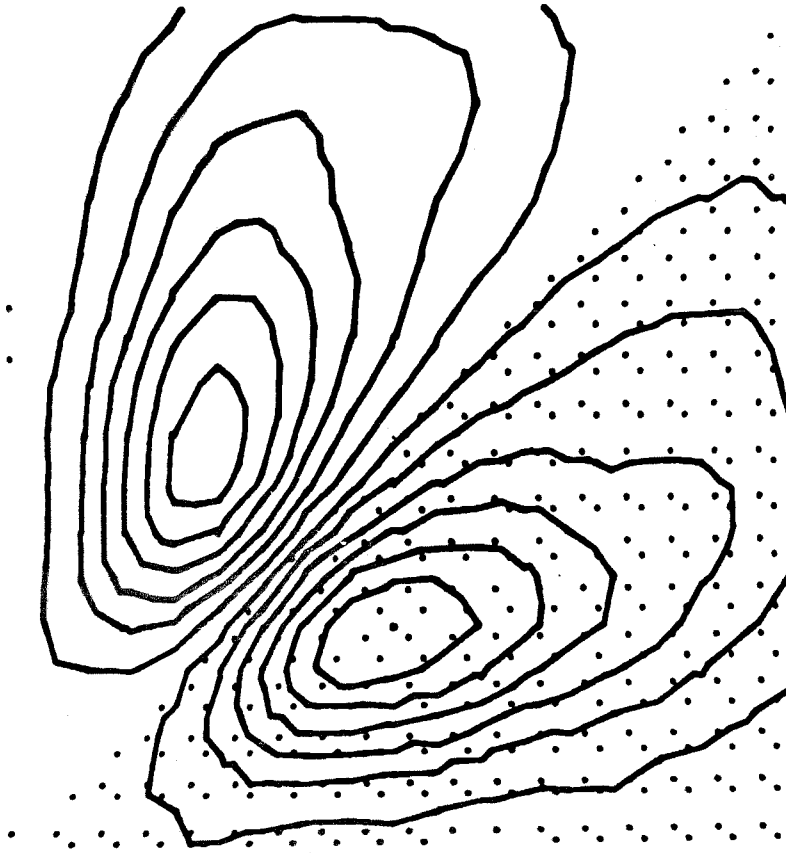Fig 4.12 An intensity series of the nonlinear term of forward and reverse responses.

Fig. 4.13   Typical second order
cross kernel.

kernel is about 100 msec. By the definition of this cross kernel, a positive region is built by the averaged responses from the stimulus shown in Fig. 3.2a, a negative region is built by that from the stimulus shown in Fig. 3.2b. For this system third and fourth order kernels were computed and they were small enough to be neglected. Therefore the second order cross kernel is able to model all the interaction cases of Fig. 3.2 with very high accuracy. Modeling responses to transient type stimuli by cross kernel are shown in Fig. 4.14. There are four positive peaks at each transition state of the forward motion and four negative peaks at each transition state of the reverse motion. This result is consistent with the impulse response analysis which was treated in section 3.4.

The correlation model suggested by Reichardt has the following form:

$$\overline{R(t)} = \frac{1}{T} \int_{-T/2}^{T/2} Y_1(t) \, Y_2(t) \, dt$$

$$Y_1(t) = I(x_1(t)), \qquad Y_2(t) = D(x_2(t))$$

where $x_1(t)$ and $x_2(t)$ are the input signals, I and D are the integration and differential type linear filters, respectively.

The second order cross kernel model obtained here is similar to the correlation model in that it has the multiplication-like interaction, but this model has delay type filters instead of I and D type filters. This model could be rewritten in the form:

$$R(t) = \int\limits_{-\infty,}^{\infty} \int\limits_{0}^{\infty} h_{2xu}(\tau_1, \tau_1 + \tau_2) \; x(t - \tau_1) \; u(t - \tau_1 - \tau_2) \; d\tau_1 d\tau_2$$

$$+ \int\limits_{0,}^{\infty} \int\limits_{-\infty}^{\infty} h_{2xu}(\tau_1 + \tau_2, \tau_2) \; x \; (t - \tau_1 - \tau_2) \; u(t - \tau_2) \; d\tau_1 d\tau_2$$

The first term measures the similarity (correlation) between x and u in one direction (u is in advance of x by time delay τ_2). The second term measures the similarity between u and x in the reverse direction (x is in advance of u by time delay τ_1). Since it is known that h_{2xu} is anti-symmetric; h_{2xu} is positive in one direction (one side of the diagonal), and is negative in the other direction. Thus this cross interaction gives a positive response if there is a correlation in one moving direction and gives a negative response if there is a correlation in the other direction.

Of particular importance are the cross kernels under different intensity and modulation conditions. From the temporal information of these kernels it is expected to get a clearer idea of the system. Fig. 4.15 are three cross kernels with (a) intensity .5 cd/m^2, 100% modulation (b) 50 cd/m^2, 10% modulation (c) 5 cd/m^2, 10% modulation. Experimental time of each set was 15 min. The relatively low frequency of (a) shows that under low intensity condition the interaction mechanism tends to have temporal integration. Besides, in (a) the time delay of peak is longer. With a DC steady state light in (c) the system is driven to respond faster and has less temporal integration.
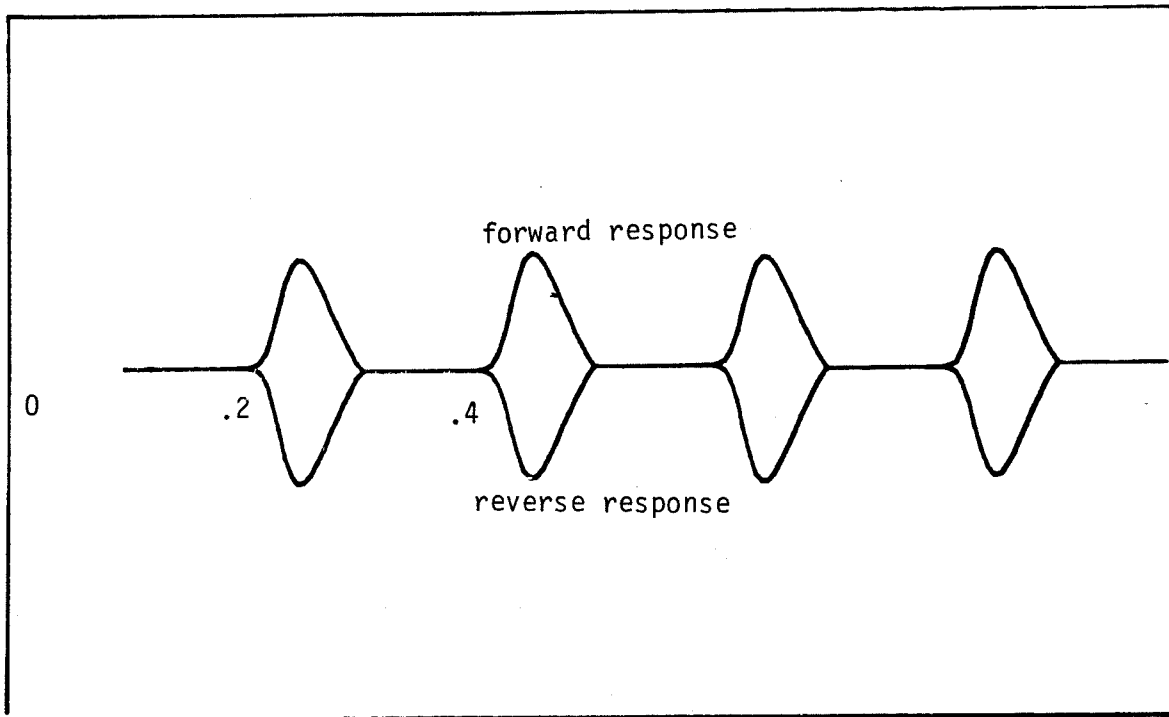
Fig. 4.14 Model predicted responses to the
transient type stimuli by the second order
cross kernel.

(a)

.5cd/m^2 m=100%

81

(b)

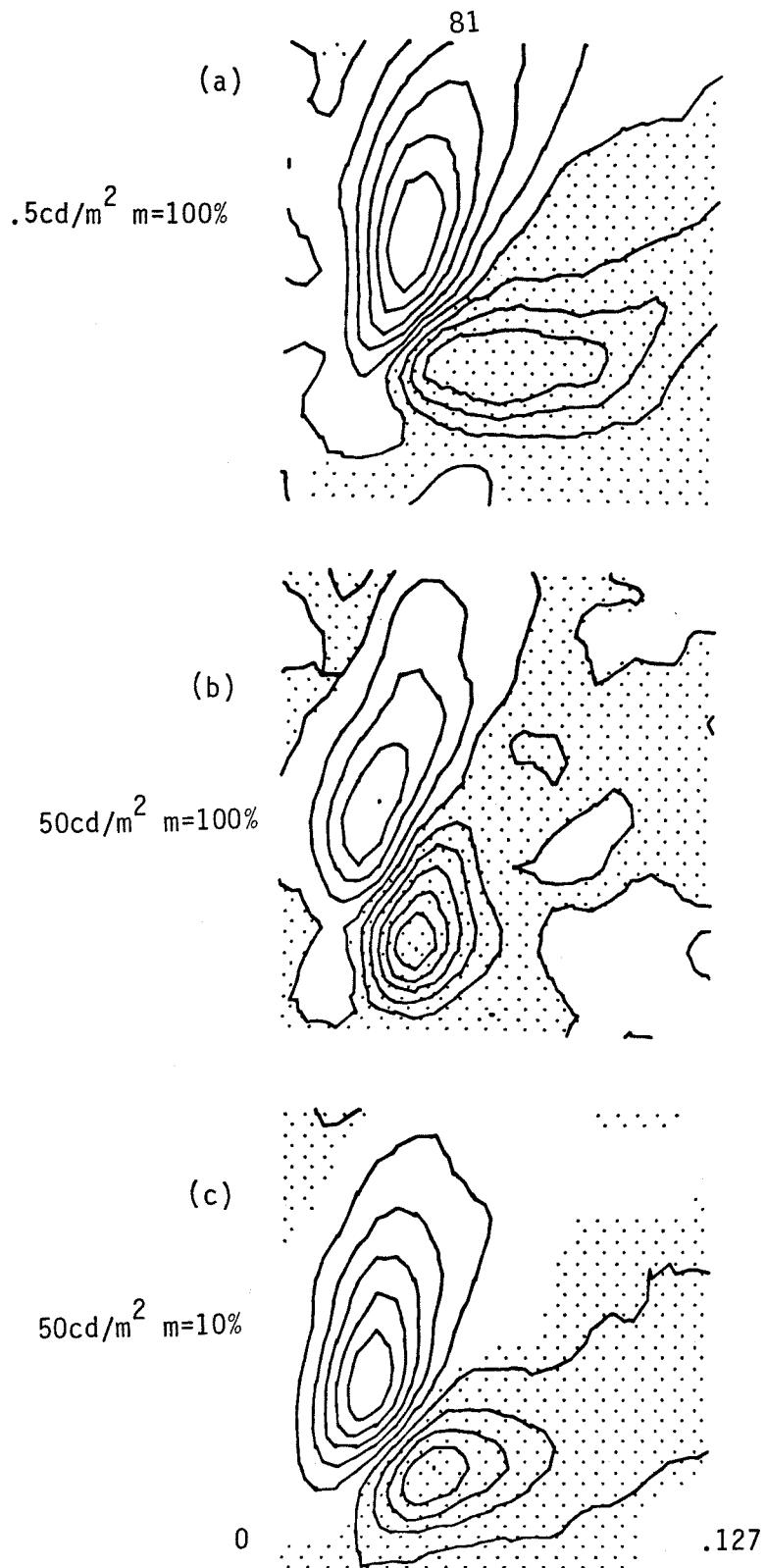50cd/m^2 m=100%

(c)

50cd/m^2 m=10%

0   .127

Fig. 4.15 Second order cross kernels with different intensities and modulation conditions. Each contour line represents a division of (a) 6.1 (b) 10 (c) 13.7 spikes/sec^3.
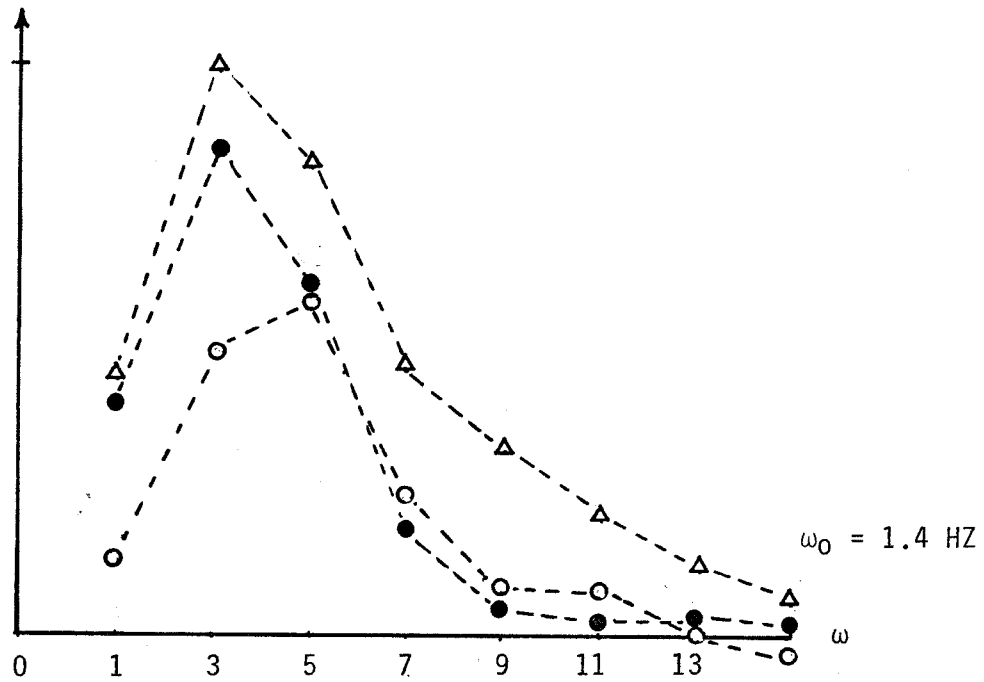
Fig. 4.16 Weight coefficients as the function of the contrast frequency, o denoting 50cd/m^2 m=100%, ● denoting .5cd/m^2 m=100%, △ denoting 50cd/m^2 m=10%.

As for fairly strong light in (b), there exists a negative peak near the diagonal line; this means the system has a mutual inhibition. This fits with the previous data in Fig. 4.12. To compare these kernels in the frequency domain, Fig. 4.16 shows their weight coefficients at 1.4 HZ contrast frequency. The frequency 1.4 HZ is the most effective value to elicit a motion response (H. Eckert, 1980). Among them (c) is the highest one, (b) is the lowest one. To show that at high frequency (a) is relatively smaller than (b) and (c), Fig. 4.16 also plots the weight coefficients from 1.4 HZ to 12.6 HZ. It is clearly shown that the 'weight' of (a) decreases faster with increasing frequencies, while the 'weight' of (c) does not.

A brief summary of this section is as follows:

(1) The mutual interaction has nonlinearity of second order as given by Marmarelis and McCann (1973).

(2) Within the cross kernel a positive peak occurs in the forward direction, a negative peak occurs in the backward direction.

(3) The memory of mutual interaction is about 100 msec.

(4) Under low intensity conditions the mutual interaction is slower.

(5) Under DC light conditions the mutual interaction is faster.

(6) At high intensity conditions, there is a mutual inhibition effect on each direction.

4.5 Relation between Kernel Peaks and the Sensitivity Gradient within Receptive Field

From previous data (Bishop, et al., 1968; Eckert, 1980), it was known that class-II cell has a sensitivity peak near 20 deg ventral

to the equator of the eye in the contralateral eye field. The sensitivity gradually drops to zero from a sensitivity peak at 20 deg in the contralateral eye field. How is the sensitivity gradient related to the contribution from self kernels and cross kernels? These contributions should provide other information about the site which causes the self nonlinearity (Sheby, 1978). Fig. 4.17 shows that kernel peak plots with respect to the receptive field coordinate. From these curves, the amplitude profile for the first order kernels matched that for the second order self kernels and also matched that for the second order cross kernels. It is possible that the sensitivity profiles arise from the density distribution of class-IIa1's dendritic tree which sums inputs fron neurons in the medulla. Fig. 2.4 shows that the area corresponding to the frontal eye region is covered by denser dendrites of the class-IIa1 cell, while the area corresponding to the lateral eye region is covered by fewer dendrites. Therefore, it is possible that both second order self and cross kernels arise from ganglion which preceds the lobula and the lobular plate. If the relative weight of each dendritic branch precedes a second order nonlinearity in class-IIa1, then the profiles for the second order self and cross kernels would not match with the profile for the first order kernel. As for the source of each kernel, this will be treated in chapter 7.

4.6 Conclusion

Several properties of the basic motion detection unit were observed by using transient type stimuli and white noise. Single
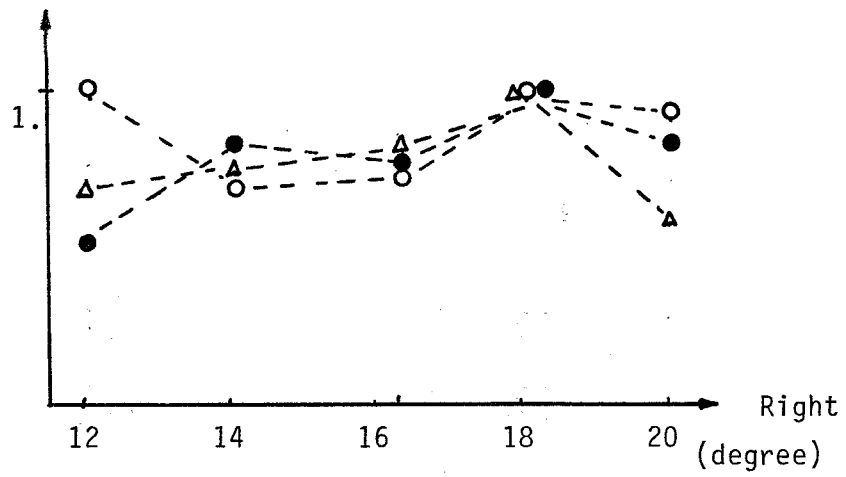
Fig 4.17 Scaled kernel peak plots. o denoting
the 1st order, ● denoting the 2nd order self
kernel, Δ denoting the 2nd order cross kernel.

channel studies revealed that the response of the single channel system consists of sustained on and transient on/off components. From section 4.3 we know that a constant light stimulating any one channel of the basic motion detection unit can change the property of the other channel. Thus, units which respond continuously to constant light are related to a neural circuit which causes this change. Both photoreceptors and on-fibers (Arnett, 1971) have this property. The on-fiber is the more likely candidate, because it carries information into the medulla, which is the place considered to have directionally selective interaction. The cross interaction of two channels has excitatory effect along the forward direction and inhibitory effect along the backward direction. This interaction could be modeled by a second order cross kernel. Self kernels and cross kernels under different light conditions show different features. The differences are the time delay of peaks and the kernel frequencies. Increasing the light intensity shortens the delay time of the kernel peaks and shows less temporal integration.

CHAPTER V

MULTI-INPUT STUDIES

UNDER LIGHT AND DARK ADAPTATION

5.1 Introduction

When we use temporal-spatial white noise as the stimulus pattern,

it is necessary to develop a method to make each stimulus light fall

within the acceptance angle of each physical channel. The method

Buchner (1976) used was to project the stimulus pattern onto the hexa-

gonal ommatidia array by a microscope objective and to align them

properly. However, this way the stimulus pattern would not have a one

to one relationship with receptors nor with lamina cartridges (i.e.,

there are seven receptors in one ommatidium, and one ommatidium sends

signals to seven lamina cartridges). Another way is to arrange the

stimulus pattern in front of the fly's eye with each single stimulus

falling within the acceptance angle of each lamina cartridge (or each

stimulus stripe falling within the acceptance angle of each lamina

cartridge column). There is no way to ensure this within an experiment.

However, the averaged error due to improper alignments of a large

number of experiments could be evaluated. Fig. 5.1a,b shows two examples

with physically neighbouring channels A, B, and C and stimuli a and b.

In case (a), the stimuli are properly aligned; A is mapped by a and

B is mapped by b. In case (b), the alignment is worse-case; each sti-

mulus pattern is located right at the boundary of two channels. To

simplify the evaluation, suppose that the spatial sensitivity distri-

bution of each physical channel is of rectangular shape instead of
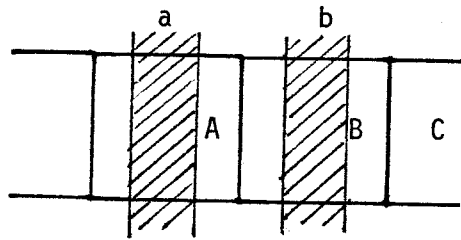
Fig. 5.1a   proper alignment of stimulus
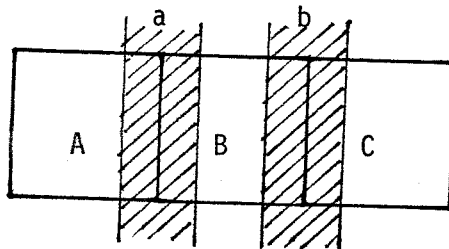stripes a,b with physical channel A,B,and C.

Fig. 5.1b Improper alignment of stimulus
stripe a,b with physical channel A,B,and C.

gaussian. Thus, the cross kernel H_{ab} of two neighbouring stimuli is equal to H_{adj1} (the kernel of two neighbouring channels) in case (a). The cross kernel H_{ab} is equal to the sum of $1/4 \, H_{AB}$, $1/4 \, H_{BC}$, $1/4 \, H_{BB}$, and $1/4 \, H_{AC}$ in case (b). Only the first two terms give the contribution to the kernel H_{adj1}. The next two terms are considered as error terms. By considering all possible stimulus positions, one finds that the averaged effect is that the computed kernel is the sum of 80% of H_{adj1} and 10% each of H_{BB} and H_{AC}. This accuracy is acceptable. The case of hexagonal array is similar to the square array, containing 80% of the desired kernel.

From Hardie's (1979) data on <u>Calliphora</u>, we know that under dim light the acceptance angle $\Delta\rho$ of R1-6 and R7/8 is 1.6^{o} and 1.3^{o}, respectively within the fovea (0-20 horizontal receptive field). With increasing illumination, $\Delta\rho$ is reduced by 20%. Compared with the interommatidia angle along the z axis $\Delta\phi_h$, which is 1.25^{o} within the fovea region, there is at most a 20% overlapped region between two adjacent ommatidia. The stimulus pattern used here is constructed by eight $.6^{\mathrm{o}} \times 9.6$ (or $1.2^{\mathrm{o}} \times 19.2^{\mathrm{o}}$) stripes with each two neighbouring stripes separated by $.6^{\mathrm{o}}$ (or 1.2^{o}). The stimulating field was concentrated in the region below the horizontal line and 10° to 20° ventral to the equator of the eye. By tilting the fly's eye 15°, the stimulus pattern and the receptor array could be ideally aligned as shown in Fig. 5.1a.

Before an experiment it is necessary to evaluate the experimental

time needed. The response of the system is a spike train, which is usually not a favored signal for computing kernels. (Usually it takes longer experimental time to get a clean kernel than the slow potential signal.) For such an eight-channel system there are a total of 28 second order cross kernels. A clean second order kernel needs an experimental time about 15 min. as mentioned in the last chapter. If the averaged spike rate of an eight-channel experiment is equal to that of an two-channel experiment, then in order to compute 28 clean kernels, seven hours experimental time is needed (this is a rough evaluation found by considering information quantity). In fact, the cell could not last such a long time and the computing cost is too high. Actually these 28 kernels could be reduced to 7 kernels by averaging the kernels of the same type. For example, the seven kernels contributed by every two neighbouring channels could be reduced to the one called H_{adj1}.

The next H_{adj2} is formed by six cross kernels contributed by every two neighbouring but one column channels, etc. Thus this averaging method shortens the experimental time down to 7/4 hours (105 min.).

5.2 Vertical-Stripe Experiments

The first experiment used eight $.6^o$ x 9.6^o vertical stripes each modulated by independent binary white noise at an intensity of 5×10^{-3} cd/m^2 (dim light), with modulation width 100%. Fig. 5.2 shows the computed kernels. From the positions of positive and negative peaks it could be noted that the first four cross kernels H_{adj1} to H_{adj4} have their directions the same as the selected direction of the cell.
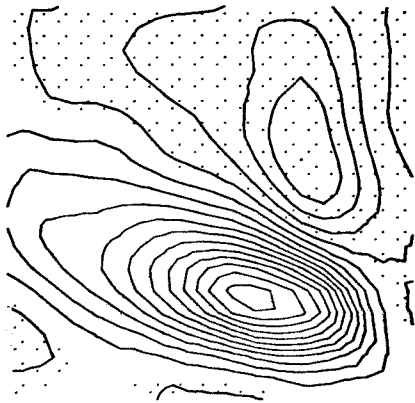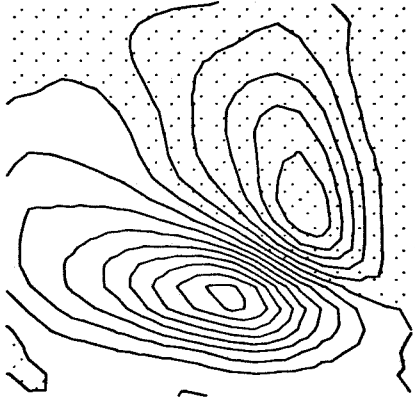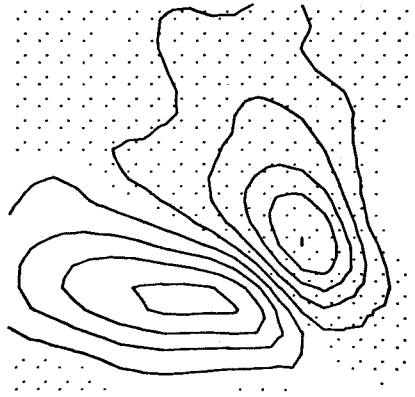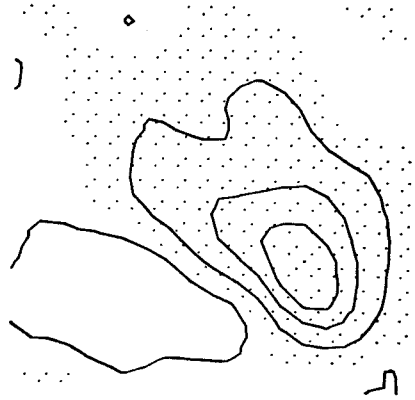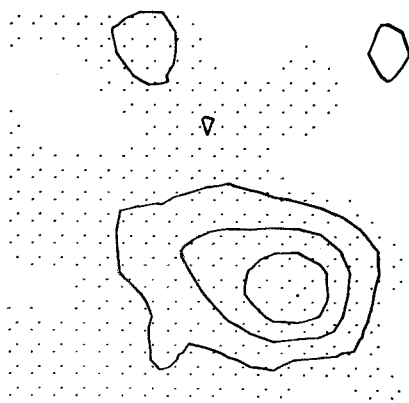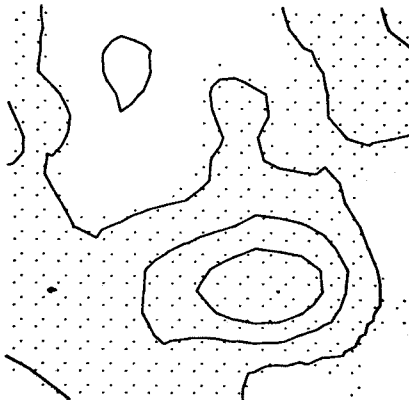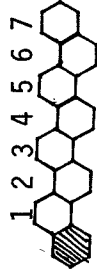
Fig. 5.2 Cross kernels under low intensity condition (.005cd/m^2). Each contour line represents a division of 1.484 spikes/sec^3.
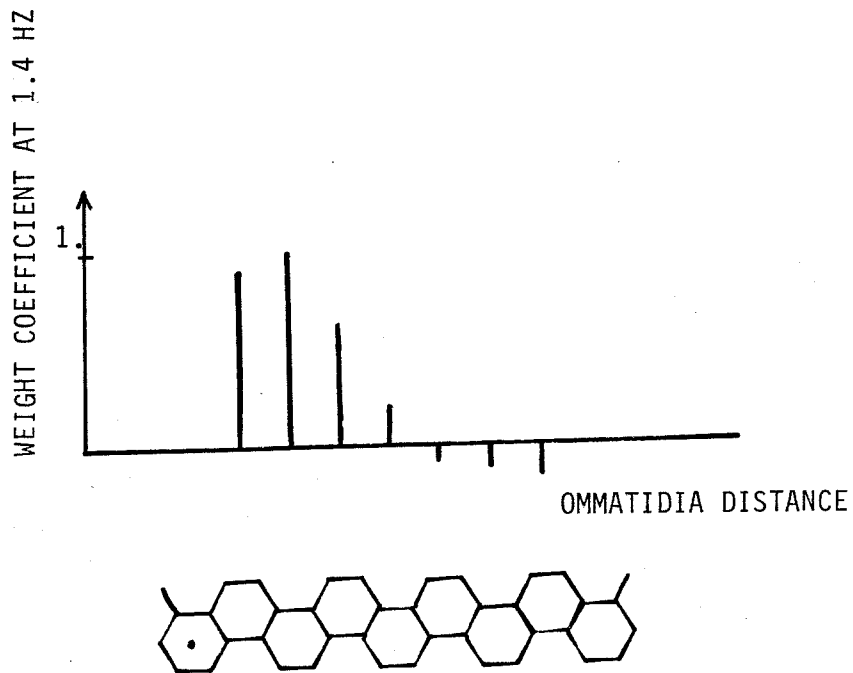
Fig. 5.3 Weight coefficients under low
intensity condition .005cd/m^2.
computed from Fig. 5.2.

Hadj2

Hadj4

Hadj6

Hadj8

Fig. 5.4 Cross kernels under low intensity condition (.005cd/m^2).
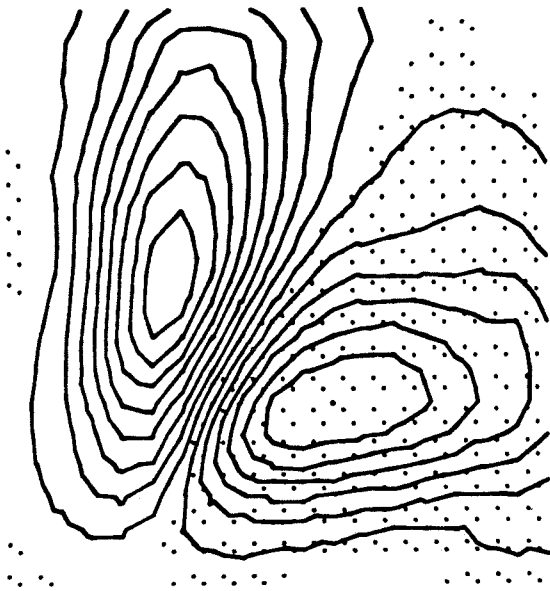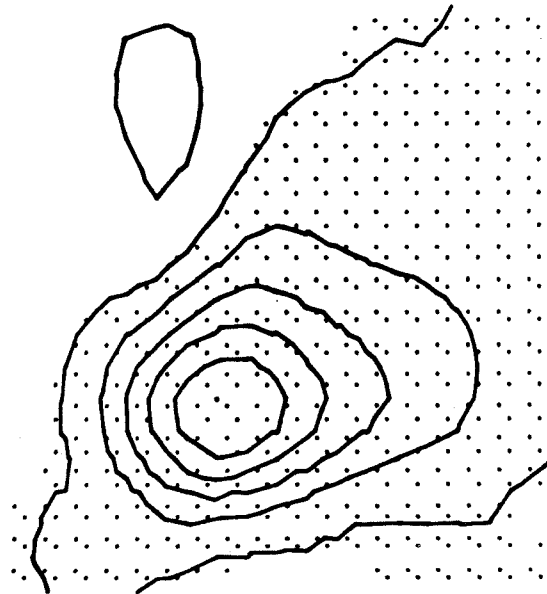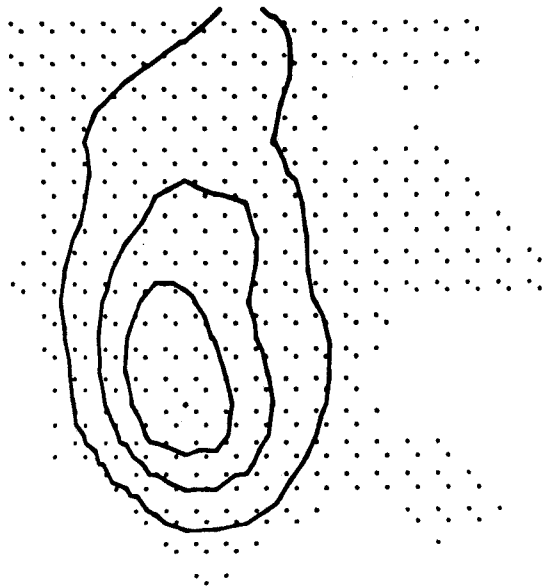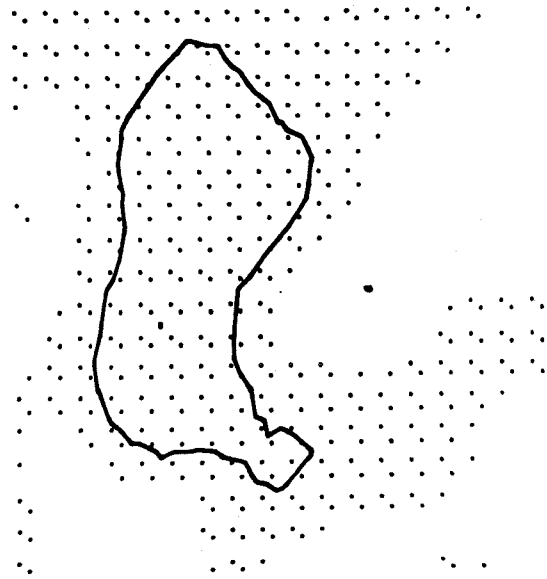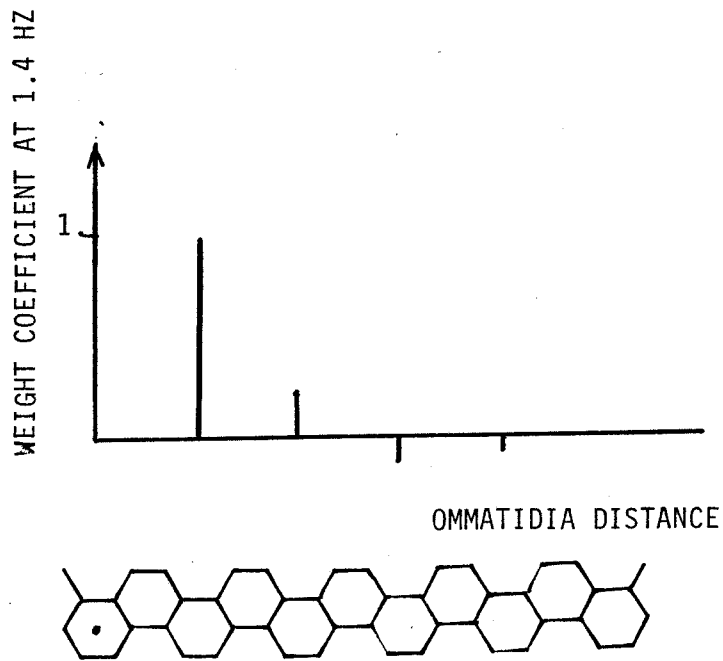
Fig. 5.5 Weight coefficients under low
intensity condition .005cd/m^2.
Computed from Fig. 5.4.
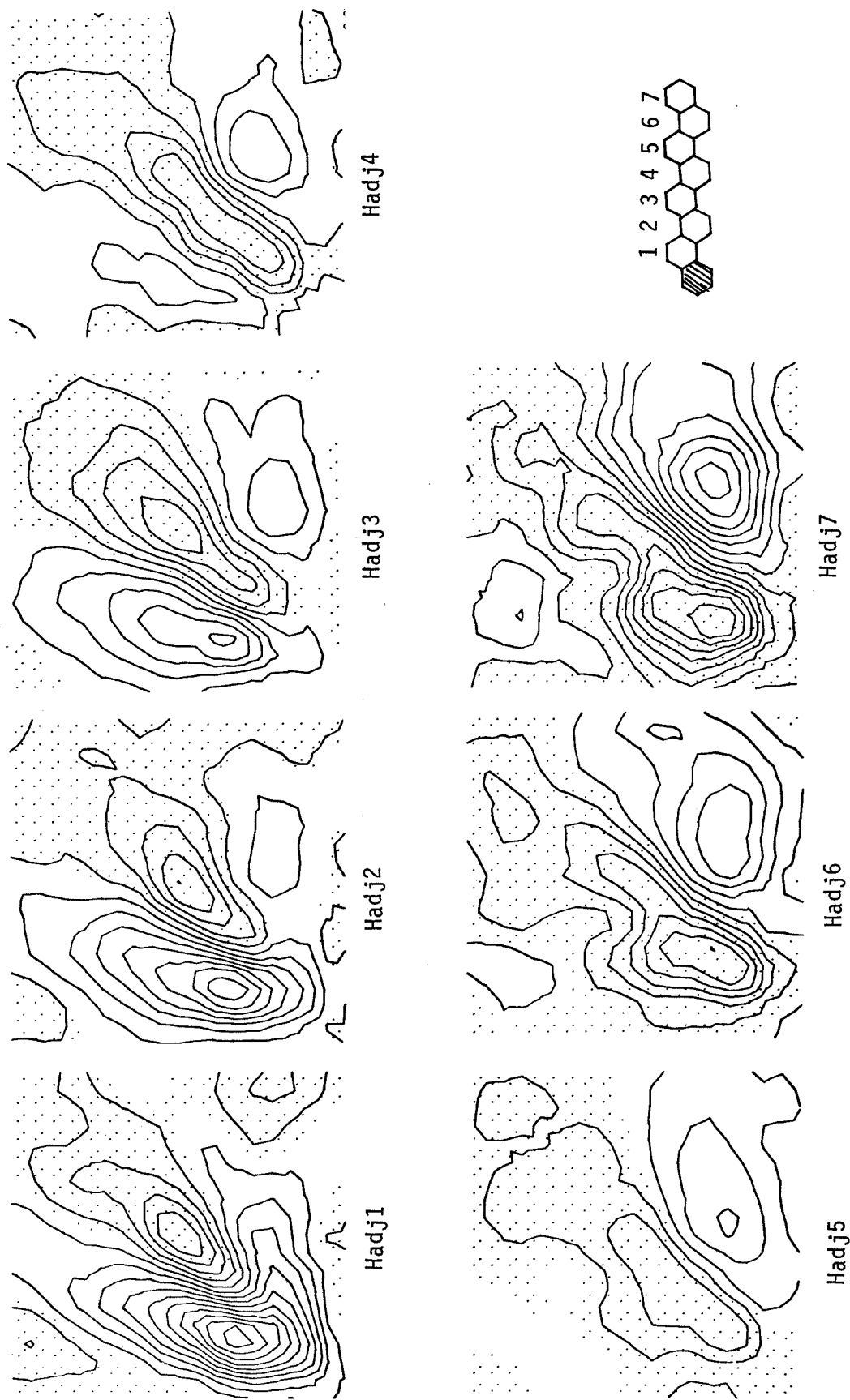
Fig. 5.6 Cross kernels under high intensity condition (50cd/m²). Each contour line represents a division of 2.122 spikes/sec³.

The next three cross kernels H_{adj5} to H_{adj7} have the reverse direction and their negative components are close to the diagonal line, which indicates a mutually inhibitory effect. The first cross kernel H_{adj1} has a positive component close to the diagonal which indicates a mutually excitatory effect. This may be due to: (1) a directionally insensitive component from cross interaction, (2) a facilitation effect at the postsynaptic site of class-II cell, (3) light artifact. The weight coefficients of these seven kernels at contrast frequency 1.4 HZ are shown in Fig. 5.3. The first three weight coefficients have about the same order of magnitude. This result matches those by Pick and Buchner (1979) done with Musca. But their data did not show the negative weight coefficients for the rest of the interactions.

The second experiment, using eight 1.2^o x 19.2^o stripes, was done to compare with the above result. This set was designed only for computing the kernels H_{adj2}, H_{adj4},...,etc. Fig. 5.4 shows that these kernels are consistent with Fig. 5.2. The weight coefficients plotted in Fig. 5.5 are also consistent with Fig. 5.3. This indicates that the function of the system does not change with the number of independent white noise inputs.

Increasing the light intensity the system shows a modification of the interaction scheme. This experiment was done at 50 cd/m^2 with 100% modulation width. Fig. 5.6 presents the kernels, of which only the first two have significant motion responses in the selected direction of the cell. The last four kernels all show the reverse directions compared with the first kernel and their magnitudes are greater than

those done with low light intensity. The weight coefficients at contrast frequency 1.4 HZ are plotted in Fig. 5.7. Only the first two coefficients have significant values, but the second coefficient is the largest instead of the first as shown by Pick and Buchner (1979). The significant negative values of the rest of the coefficients do not agree with their data obtained with a traveling sinewave. However, Pick and Buchner also obtained the same result (negative response) by another series of experiments done with two stripes and masking a number of vertical columns between those exposed to the stripe stimuli by black paint. One way to explain the unobserved negative response in traveling sinewave experiment is that because of saturation there are higher harmonic contributions from neighbouring columns and this contribution was added to the rest of the coefficients to cancel the negative value. However, this is unlikely because the magnitude from harmonics could not be so high. Another possibility is that a p-order 3 mechanism may be associated with the system at the high intensity condition, because according to Pick and Buchner this negative response is abolished if the black paint is replaced by a stationary background light of 30 to 100% of the mean stimulus luminance. A mechanism for the negative response suggested by Pick and Buchner was that an inhibition mechanism inhibits the leading channel of a pair of motion detection channels to make a 180° phase inversion (third order interaction).

The temporal integration mechanism in dim light has been shown in the last chapter. It is also confirmed by the kernels presented as Fig. 5.2 and Fig. 5.6.
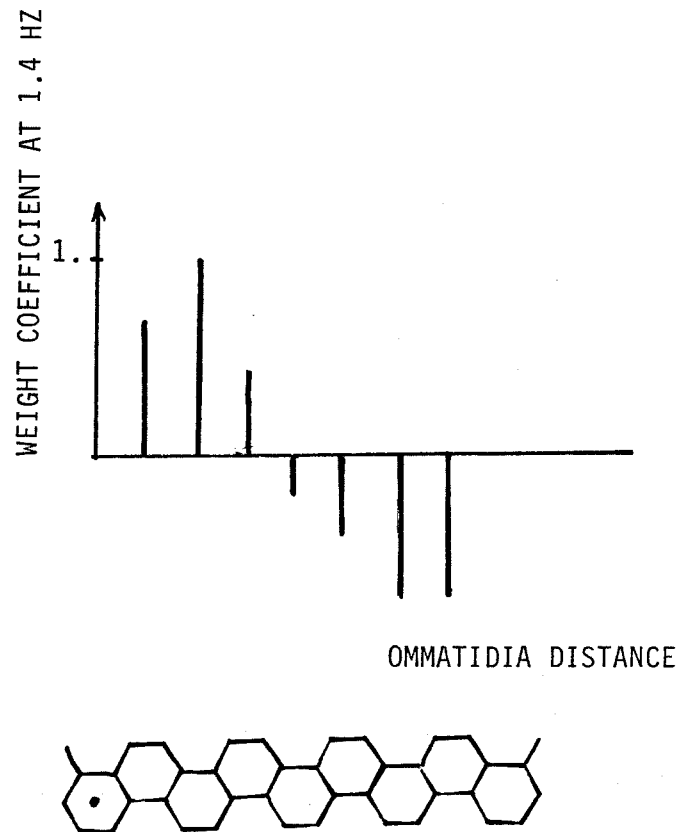
Fig. 5.7 Weight coefficients under high
intensity condition 50cd/m^2.
Computed from Fig. 5.6.

The results of this section could be summarized as follows:

1. Under dim light the number of effective interaction terms is at least three.

2. Under bright light the number of effective interaction terms is reduced, only the first and second weight coefficients dominate. The second coefficient is the largest.

3. There are negative interaction terms with channels separated by three to six (at least) columns of the receptor array.

4. The negative response mechanism is likely that suggested by Pick and Buchner. 'The inhibition has to act on the dark adapted unit, which is between the two channels stimulated, to create a 180° phase-shifted signal'.

5. A p-order 3 mechanism could be associated with the system.

Pick and Buchner (1979) indicated that two mechanisms may induce a change in spatial interaction pattern under scotopic and photopic light conditions. One of them is based on neural pooling, which is that under scotopic condition each receptor could increase the light sensitivity by summing the signals from neighbouring receptors. Another is neural recruitment, which is that the various sampling bases are recruited with different weights. They were not able to make a decision between the two alternatives from the methods based on measuring averaged turning response. Even for the cross kernels given us above, it is still not possible to tell which mechanism is the most likely one. It should be noted that the effect of neural pooling does not have to be along the axis of maximum motion response.

It is also effective along the axis perpendicular to the axis of maximum motion reaction, while the neural recruitment has to be along this axis. This suggests that we could determine which is the most possible mechanism by examining the cross kernels between adjacent rows.

5.3 Horizontal-Stripe Experiments

To evaluate the cross interaction between horizontal rows, the first experiment was designed with eight 1.2^O x 19.2^O horizontal stripes with neighbouring stripes separated by 1.2^O, the maximum light intensity is 50 cd/m^2 (high intensity) with 100% modulated binary white noise. The cross kernels of the results are presented as Fig. 5.8. The interaction of two neighbouring rows has a mutually excitatory effect. The rest of the cross kernels show a negative peak on the diagonal line. Since all these kernels are not direction sensitive, their function is not known clearly. The mutually excitatory effect of two neighbouring rows could be considered as a facilitation effect at the postsynaptic site of class-II cell or the cross interaction by the neural process before class-II cell or light artifact. Different interaction schemes under light and dark adaptations can be shown by comparing these kernels with the following kernels under scotopic light conditions. The next experiment was done by the same stimulus pattern but with low light intensity, 5 x 10^{-3} cd/m^2. The cross kernels are shown in Fig. 5.9. All the kernels reveal mutual excitatory interaction, which is different from those under photopic light conditions. This result could be explained if we constructed
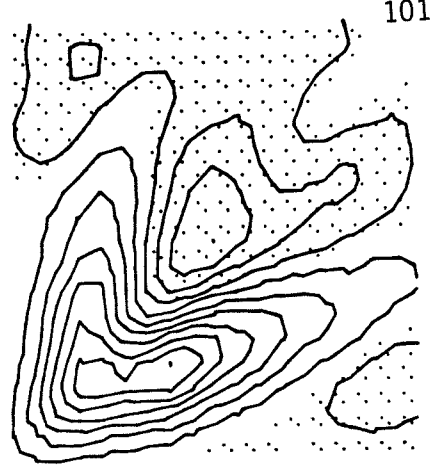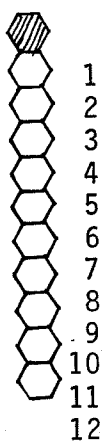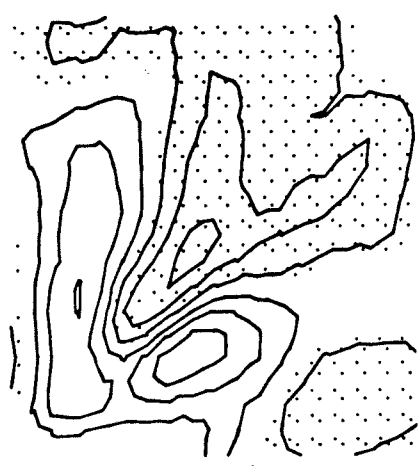
Fig. 5.8 Vertical cross kernels under high
intensity condition (50cd/m^2). Each contour
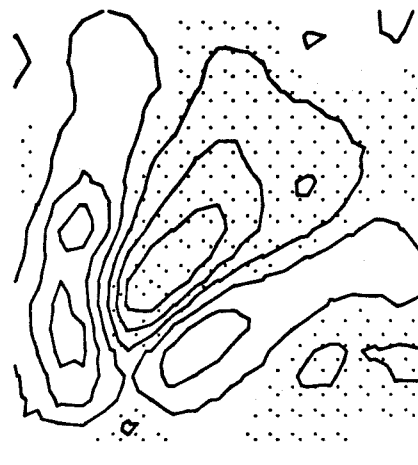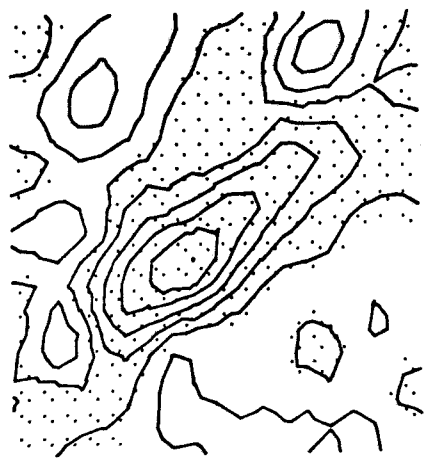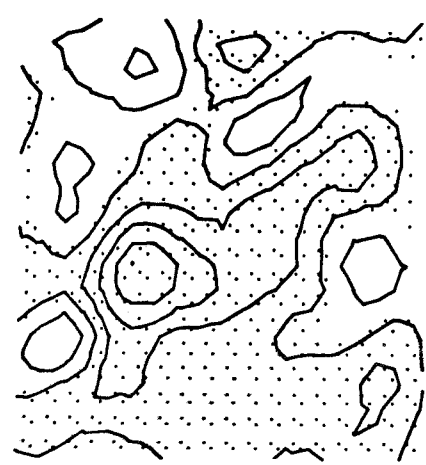line represents a division of 3. spikes/sec^3.

Hadj2

Hadj4

Hadj6

Hadj8
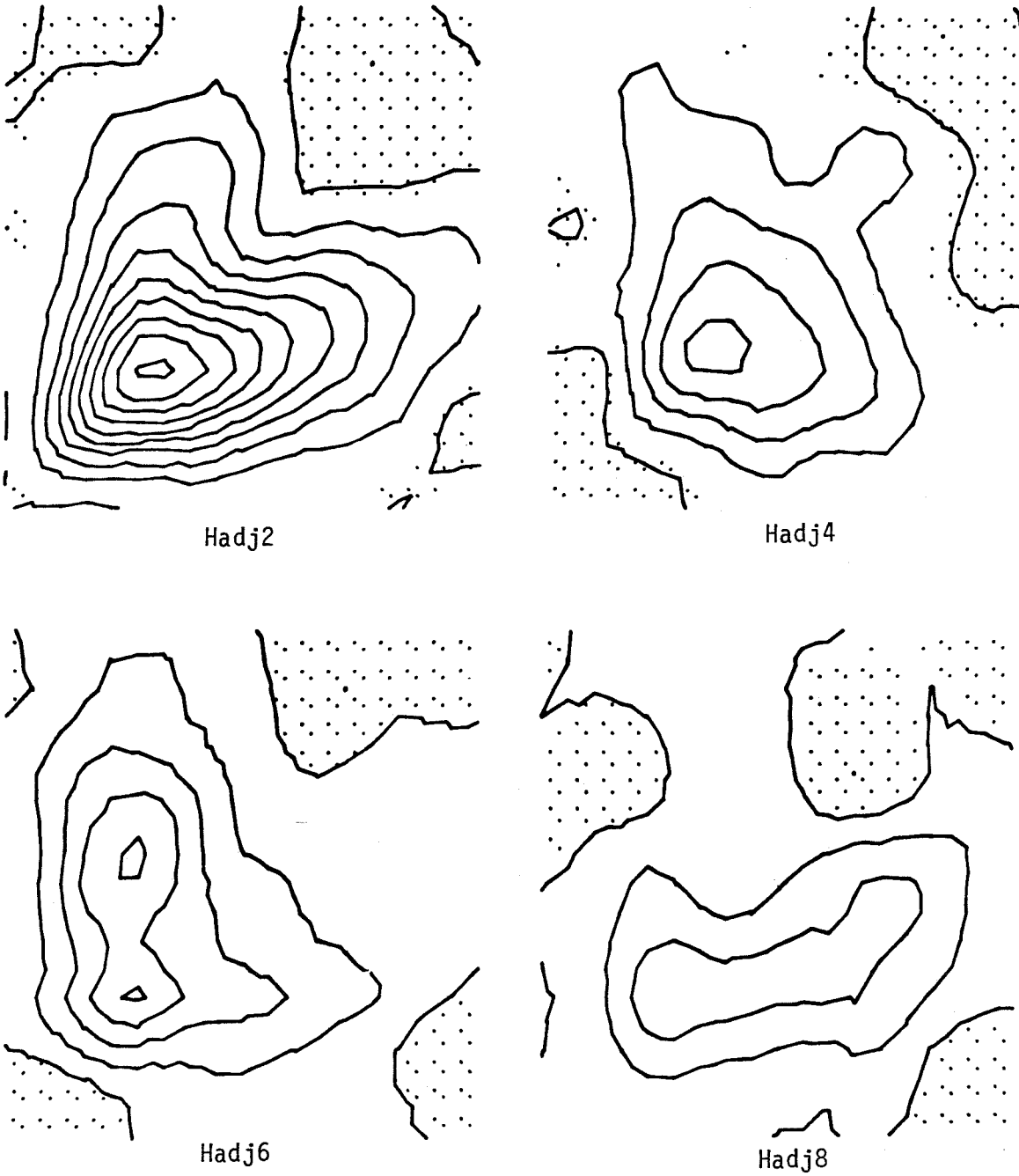
Fig. 5.9 Vertical cross kernels under low
intensity condition ($.005cd/m^2$). Each contour
line represents a division of .636 spikes/sec^3.

a circuit diagram (Fig. 5.10) by considering neural pooling mecha-
nism in front of the vertical interaction system of class-II cell.

5.4 Wide Angle Interactions

In section 5.2 it has been shown that the negative response
starts from two neighbouring but three vertical columns (4.8 deg).
The negative response reaches a maximum value by a separation of
6 columns. From Pick and Buchner (1979), the negative response ex-
tends to a separation of 12 columns. Although the interaction is
directionally sensitive it still could have a directionally
insensitive term (mutual inhibition) and this may provide a better
explanation of the negative response. Two stripes with variable
separations from 4° to 32° were used for this experiment. One stripe
was fixed at 20° laterally while the position of other stripe varied.
The stimulus was binary white noise with light intensity 50 cd/m^2,
100% modulated. Fig. 5.11 shows these cross kernels. The negative
direction response could be observed by the positive peak at the lower
right region of the cross kernel. However, the most significant
feature is the negative peak on the diagonal line. This is the same
as those shown in Fig. 5.6; 5.8a. Under photopic light condition
the mutual inhibition is an universal phenomena for two channels
having a separation of at least 2 horizontal columns or vertical
rows.

Fig. 5.12 presents the weights of negative responses induced
by two-stripe stimuli.
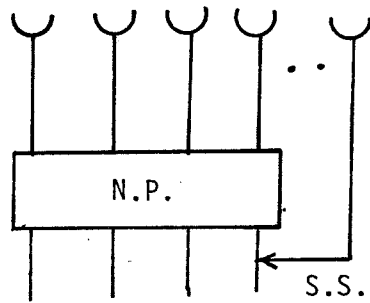
Fig. 5.10 Neural pooling circuit diagram.
S.S. denoting spatial specific interaction,
N. P. denoting neural pooling. The visual
element array shown above could be along
horizontal or vertical direction.
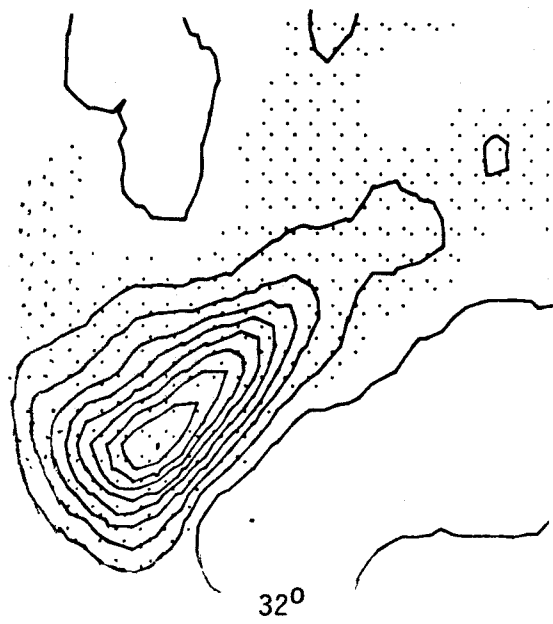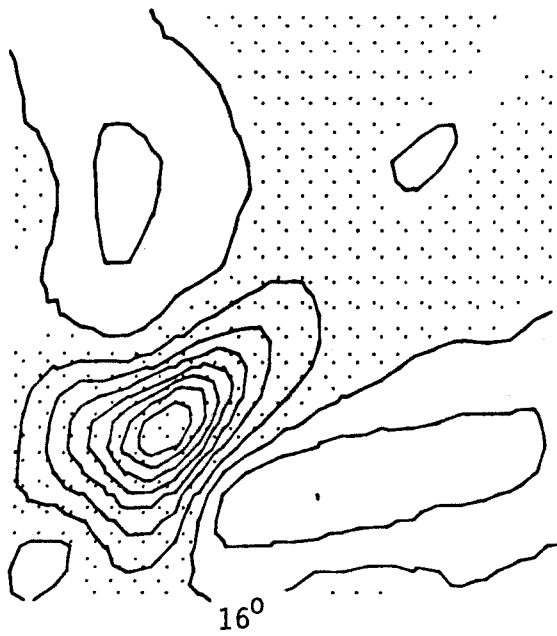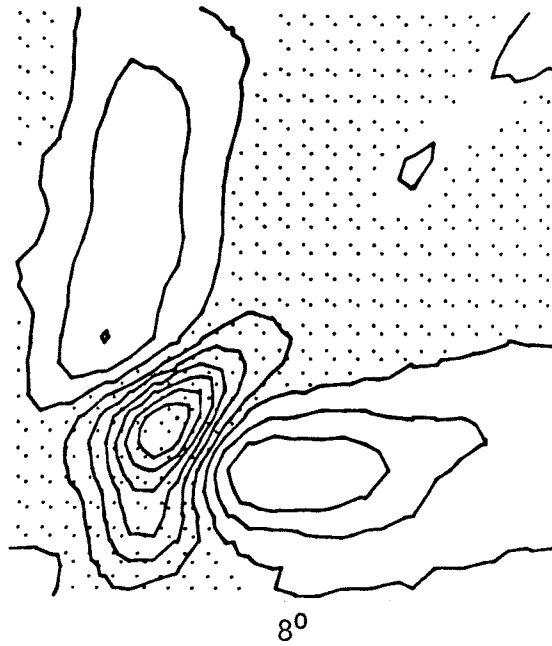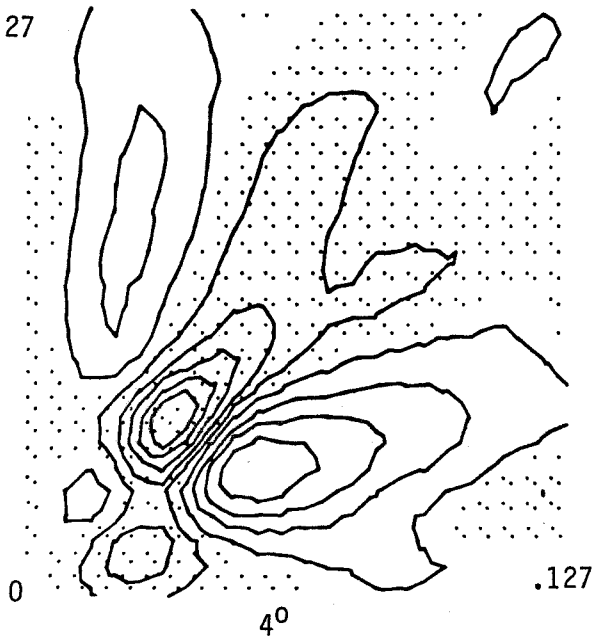
Fig. 5.11 Wide angle cross kernels.
Light intensity 50cd/m^2. Each kernel
was done by two stripes separately.
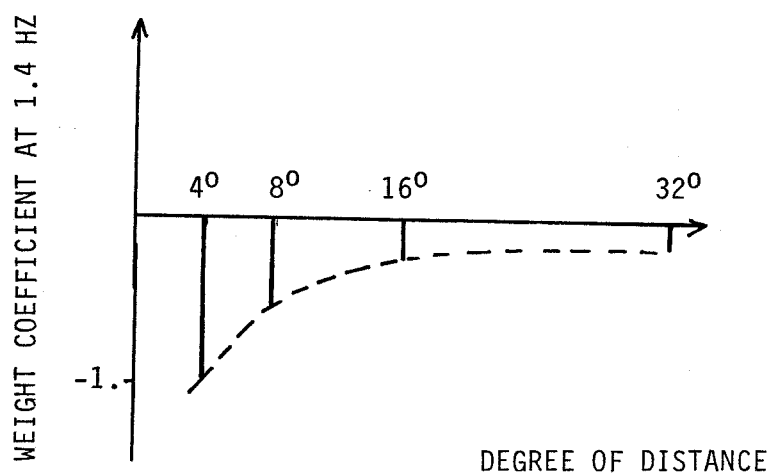
Fig. 5.12 Weight coefficients of wide
angle interaction.Light intensity was
50cd/m^2.

5.5 Conclusion

One of the advantages of using temporal-spatial white noise stimuli is the property of spatial independency. This allows the investigation of the interaction between any two inputs directly. Another advantage is that the receptive field are stimulated uniformly such that the underlying interaction of the receptive fields would not be biased as those by conventional stimuli (sinewave, pulse, etc.). One more advantage is the simplification of the procedure during the experiment. The main discoveries within this chapter are: (1) From dark adapted condition to light adapted condition the number of motion interaction subunits is decreased; the number of significant 'weights' is decreased from four to two as shown in section 5.2. (2) There is a negative response between two inputs separated by three to five columns. (3) There is a neural pooling effect among about five columns and rows under dark adapted conditions. (4) There is a mutually inhibitory effect under light adapted conditions. More discussion will be given in chapter 7.

CHAPTER VI

BINOCULAR INTERACTIONS

6.1 Introduction

From previous studies (Bishop, Keehn, and McCann, 1968) there are
four types of class-II contralateral motion detection cells with selec-
tive directions such as horizontal inward, vertical downward, horizon-
tal outward, and vertical upward. These cells carry information from
one optic lobe to the opposite one, and thus are expected to have
purposes such as depth perception, one of the known binocular inter-
actions. J. Dill (1970) worked on this problem by means of multiple
electrode techniques. By taking the responses from several sites in
the optic lobe and examining their cross-correlograms, the information
of peak polarity and time delay reflected inhibitory effect, excita-
tory effect, and source identification (common source or not). Hori-
zontal motion detection cells have been studied thoroughly. The main
results are:

1. The same unit was found in both optic lobes, which indicates
   that one cell sent its axon past the midbrain to the other
   lobe without synaptic junctions.

2. Two IIa-in cells, one in each lobe, have a mutually inhibitory
   effect.

3. One IIa-in and one IIb-in, both in the same lobe, have a mu-
   tually excitatory effect.

4. One IIa-in and one IIa-out, one in each lobe, have a mutually
   excitatory effect.

5. One IIa-in and one IIa-out, both in the same lobe, have a
   mutually inhibitory effect.

The inhibitory effect of case 2 could be summarized as Fig. 6.1.
Due to the limited information contained in the cross-correlograms
and lack of theoretical support, it is not certain that the inter-
action is simply mutual excitation and inhibition. This chapter at-
tempts to study this problem with experiments by using multi-input
white noise patterns stimulating both eyes or single eye to examine
their kernels.

6.2 Self Kernels of Binocular System

Chapter 4 has shown that three types of kernels exist in the recep-
tive field of a single eye, a first and a second order self kernel and
a second order cross kernel.

The first order kernel contains mainly a positive peak at a time
delay about 35 msec. This reflected the increase in response in pres-
ence of light (phototaxic). The second order self kernel has a positive
peak at roughly the same time as the first order kernel. The first
series of experiments were designed to examine the self kernels of input
channels within binocular regions, or outside it under normal conditions
(both eyes uncovered). An eight 1.2^o x 19.2^o vertical-stripe pattern
(same as in chapter 5) was placed in the contralateral field within $R0^o$
to 10°, 110° and modulated by binary white noise. The preparation was the
same as chapter 4 except that the ipsilateral eye was not covered by paint.

Fig. 6.2 presents the first order kernels from each channel. They
have all negative peaks instead of positive peaks. The time delay of

II-a1 Left   II-a1 Right

inhibition
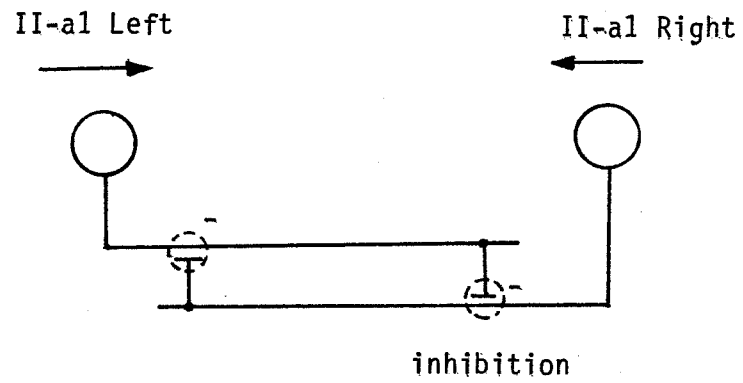
Fig. 6.1 Schematic drawing of binocular
interaction between two Class-IIa1 cells.

the peak is advanced. The first order kernel of channel 8 (close to the boundary of binocular field, see chapter 2) has a minor positive peak which indicates a tendency to return the positive peak outside the binocular region. This was confirmed by experiments with the stimulus pattern further away from the medial line. Fig. 6.3 is a set of first order kernels done under the monocular state with a stimulus placed in the same receptive field.

As for the second order kernels, the contour features are the same as those in the monocular state, but the magnitude can not be compared with them, because the above experiments were not done on the same cell. Binocular experiments followed by a monocular experiment have less chance of success due to the preparation difficulty. After a long binocular experiment, the electrode is shifted somewhat away from the cell; by this time painting the ipsilateral eye usually would miss the cell. However, short tests were successful for several preparations. It was found that although the kernels are noisier, they are still allowed for comparison. The increasing of spontaneous firing rate from the binocular state to monocular state could be learned just by the sound from the monitoring speaker. By these tests, the change of the first order kernel was confirmed. The magnitude of the second order self kernel decreased 10% for the binocular state. As for the second order cross kernel, it is similar to the second order self kernel, the contour features are unchanged; only the magnitude decreased about 10%.

The conclusion of this experiment is that the mutually inhibitory model in Fig. 6.1 is capable of identifying the kernel's char-

112
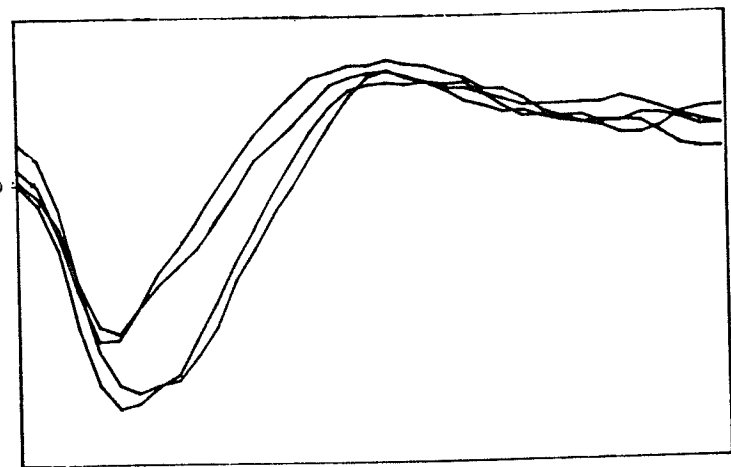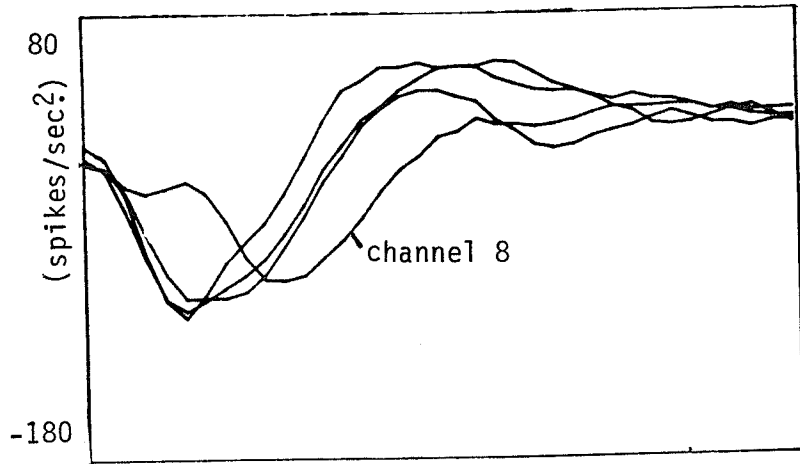
Fig. 6.2 First order kernel within
binocular visual field.
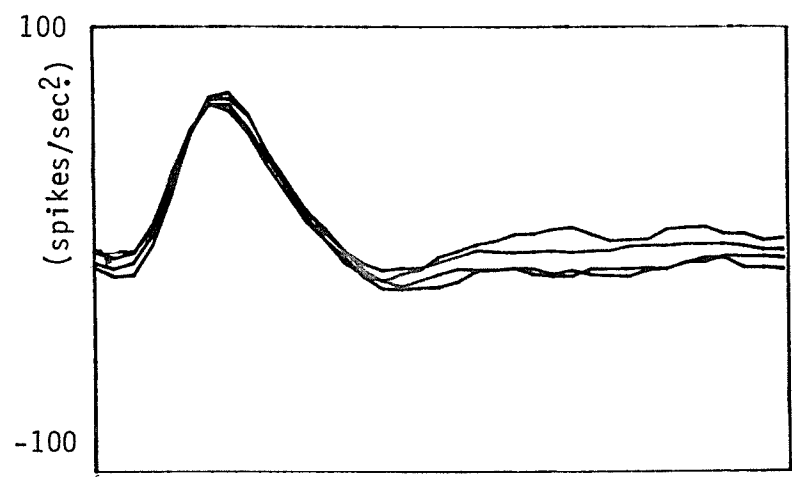
0 Fig. 6.3 First order kernel under   .2(second)

acteristics. Due to the nature of mutual inhibition the induced response of each IIa-in cell from an impulse of light in the binocular field would be diminished by each other. The second order (both self and cross) responses would be decreased 10% as well.

6.3 The Cross Kernel between Two Eyes

The second set of experiments was used to examine the mutual interaction of two inputs with each stimulating one eye. The stimulus pattern shown in Fig. 6.4 consists of four stripes, stripes A and B were placed at the ipsilateral eye field, the other stripes C and D were placed at the contralateral eye field. Each pair is just on the margin or outside the binocular field. The cross kernels of H_{AC}, H_{AD}, H_{BC}, and H_{BD} all have same contour features. The averaged result H_{LR} is shown in Fig. 6.5. The negative component on the diagonal line indicates an inhibition by channel A and B, the time delay is about 56 msec. The negative component below the diagonal line indicates that the impulse response of channels C and D would be instantaneously inhibited by an impulse added on channels A and B with a time delay of C and D at least 18 msec. The cross kernel H_{CD} shown in Fig. 6.6 is the same as Fig. 5.8a in chapter 5 mainly with a negative component on and around the diagonal line. The cross kernel H_{AB}, shown in Fig. 6.7 is unexpected with a positive component which indicates a mutual excitatory effect! Even for these kernels the model in Fig. 6.1 is still able to describe all of them. For kernel H_{AB} it could be built by a construction as shown in the
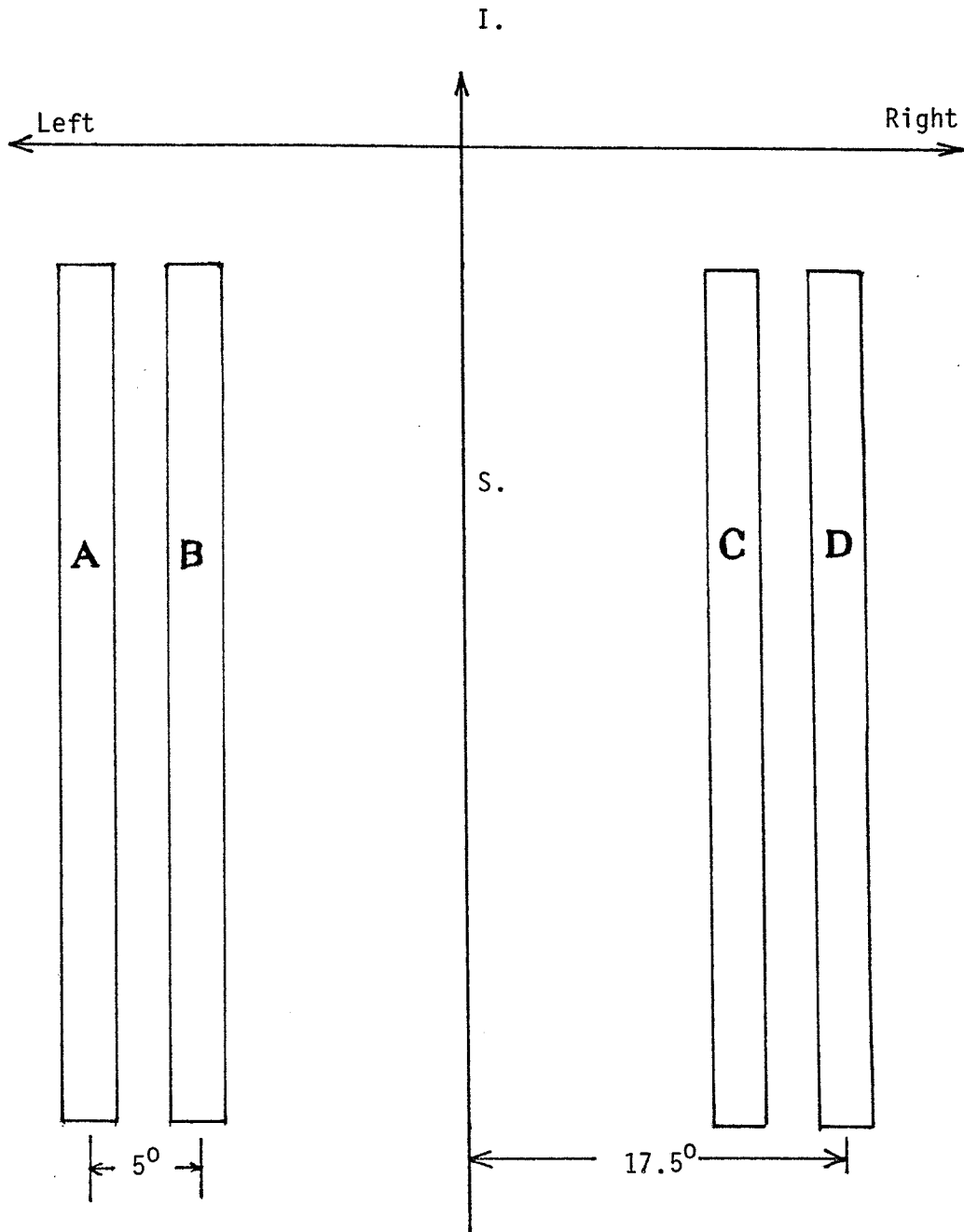
Fig. 6.4 Four stripes stimulus pattern.
A,B are located at left eye field, C,D
are located at right eye field.
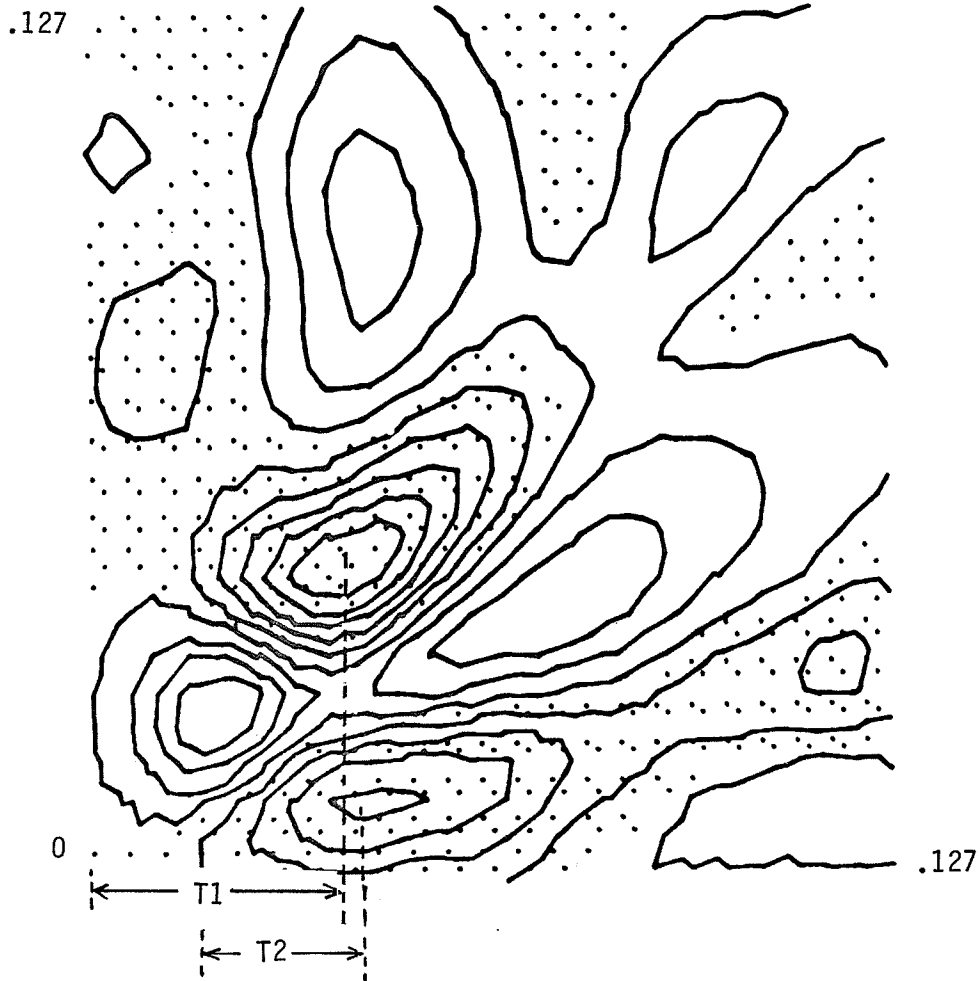
Fig. 6.5 Cross kernel H_{LR}. Each contour line represents a division of 1.51 spikes/sec^3.
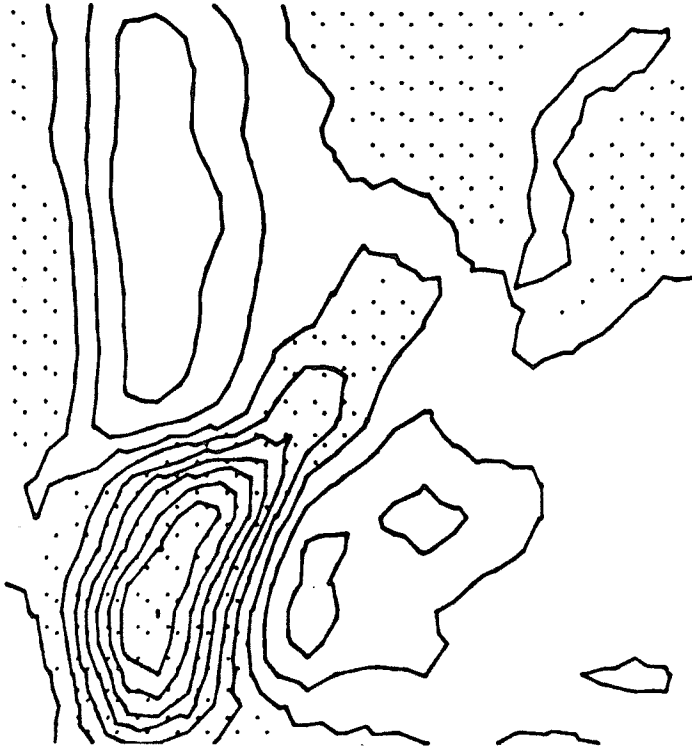
Fig. 6.6 H$_{CD}$. Each contour line represents a division of 1.52 spikes/sec^3.
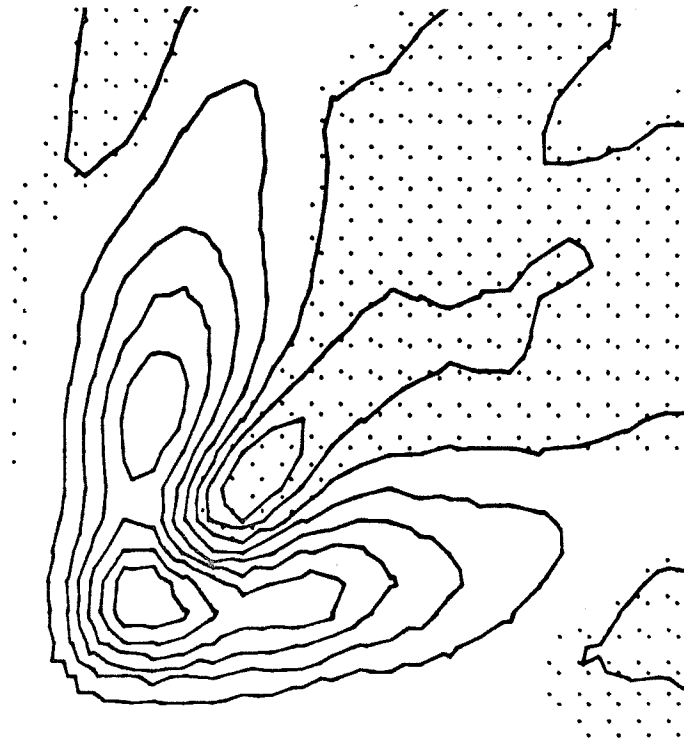
Fig. 6.7 H$_{AB}$. Each contour line represents a division of 2.03 spikes/sec^3.

block diagram Fig. 6.8. For the negative component below the diago-
nal line of kernel H_{LR} could be reasoned simply by considering the
propagation time of the response of the cell in ipsilateral lobe to
the presynaptic site in the opposite lobe, and the inhibitory effect
of the synapse. When two impulses stimulate the left and the right
eyes at the same time, because of mutual inhibition of equal weight,
the negative response delay time T_1 is longer than the two pulses peak
delay time T_2.

6.4 Conclusion

After all, the model is suggested without any modification, but
one thing was learned from these experiments. That is, via mutual
inhibition a nonlinear term is added to the binocular perception
system such that the part of the eye stimulated behind would have a
further decreasing response (due to negative component below the
diagonal line). This could possibly be used to advance the timing
of a turning reaction when one part of the eye received stimulus
(flick or motion) before the other eye. It is noted that the direc-
tion of stimulus sensed by this mechanism is the same direction
sensed by each eye. Furthermore, if we think the mutual inhibition
system like that on the vertebrate retina (which functions to
sharpen the image boundary), or a differential amplifier, then the
difference strength of the perceived responses from each eye would
be enhanced. By such a mechanism, a decision, the turning reaction
for example, could be made more easily. As for the function depth
perception, it has been ruled out by Burkhardt, et al., (1973) and
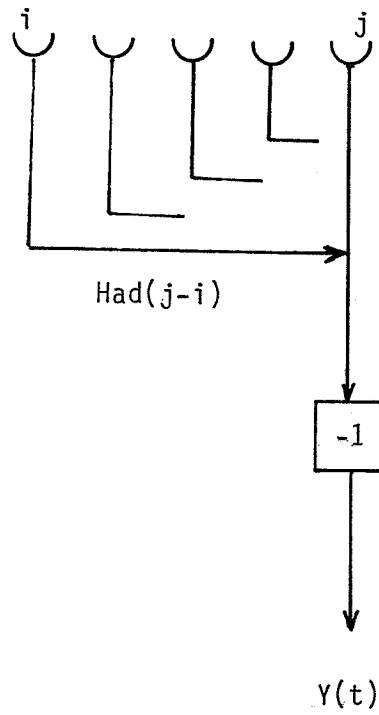
Fig. 6.8 Block diagram of spatial interaction
(ipsilateral field) of the Class-IIa1 cell.

Collett and Land (1975) by indicating that the acuity is too poor to enable them to do so.

Suggestions of other experiments are the mutual interaction of two inputs widely separated from the binocular field. The frequency of the stimulus needs to be increased to accurately measure the delay time T_2.

CHAPTER VII

CONCLUSION AND DISCUSSION

7.1 Introduction

One of the ultimate goals in the study of a neural system is to understand both its functions and architecture (neural circuitry). These two points in general are not independent, because both of them actually represent different views of a system. Thus it is common to ask what can we tell about the system architecture by the knowledge of the function.

Descriptions of the system functional by the Wiener kernels have their own characteristics. One is the order of nonlinearity in time domain and space domain, the other is the value on each point of a kernel. The order of nonlinearity in space domain (p-order) gives direct information about the number of channels involved with a particular interaction mechanism, while the order of nonlinearity in time domain of one channel is the product of the orders of its cascaded subsystems (if a feedback type system is not considered). By understanding the nonlinearity of part of the subsystems, we could break the system chain to figure out the order of nonlinearity of the rest of the subsystems. The value of the kernel indicates the excitatory or inhibitory effect of a set of impulses. By these schemes, all the information contained in the Wiener kernel could be factored out and be used to suggest the neural wiring step by step. But it has to be noted that many neural mechanisms could result in the same effect (excitatory or inhibitory). For example, an inhibitory effect

could be related to saturation, habituation, rectification, shunting, etc. Usually there is no way to tell which is the right mechanism by those kernels. Other information of the system is needed frequently.

For previous chapters the kernel data show that the system identification by Wiener kernels is an efficient method. Compared with a transient stimuli test, Wiener kernels have a higher signal to noise ratio for the same amount of experimental time. In addition they have the ability to accurately predict the system response to various stimuli. In the following sections there will be more considerations about the neural wiring between the retina and the class-II cells than in the previous chapters.

7.2 The Single Channel of the Basic Motion Detection Unit

The kernel model basic motion detection units studied in chapter 4 are consistent with those from Marmarelis and McCann (1973). The canonical kernel model of this two channel system consists of the first and second order self kernels and the second order cross kernels. The site which contributes the second order self kernel could be any place in the retina, lamina, medulla, and class-II cell, because all of these units have at least second order nonlinearity. But we also noticed that the response contribution of the second order term is as high as 65%. Thus, the retina could be ruled out first, for its second order nonlinearity (from photoreceptors) is very small (McCann and Fargason, 1977). Generally speaking the retina cell could be viewed as a wide bandpass filter which faithfully transduces the light signal into the electrical signal (Sheby, 1978). The temporal transfer

characteristic of the class-II cell, including the postsynaptic transfer function and the spike generation mechanism, appears likely to be linear. This has been shown in section 4.5 by considering the sensitivity profiles of the kernel peaks.

The medulla is usually considered as the place eliciting the motion detection response. If we consider that the lamina has the second order nonlinearity, then for same reason as the class-II cell the second order nonlinearity is not likely to arise from the medulla. The last candidate is the lamina. Arnett (1971) reported that there are two units named on-fiber and on-off fiber found in the first chiasma (distal end of lamina). Their PST due to pulse stimuli are very similar to the sustained and transient components of the class-II cell (Fig. 4.1;2). Furthermore, the first and second order self kernels of the on-fiber (McCann, 1974) resemble kernels of the class-II cell except for its being shifted to higher frequency.

Zettler and Autrum (1975) studied the responses of the retina cell (L1, L2 cells). They indicated that two properties are different between retina cell and monopolar cell: (1) The latency of monopolar cell is sensitive to the light level. (2) The hyperpolarization response of the monopolar cell is saturated only three log units higher than the threshold. The response of the class-II cell studied here also has these two properties. R. Powers (1979) computed the first and second kernels of monopolar cell in Drosophila. These kernels showed similar frequency properties as the class-IIa1 cell under three log unit light conditions. By the arguments above, it is concluded

that the single channel dynamic property of class-II cell arises mainly from lamina ganglion.

7.3 The Directionally Selective Interaction: A Model

Since no evidence from electrophysiology studies suggests that the motion detection unit exists before the medulla, it is suggested that medulla is the first portion which has motion detection ability. Its main function is to integrate signals from lamina and to provide spatial interactions.

From chapter 4 we know that the functional of the cross interaction of the basic motion detection unit is very complex. First, there are both excitatory and inhibitory components on either side of the diagonal line within the second order cross kernel. Second, either the forward response or the reverse response could be elicited by the four types of impulse stimuli (Fig. 3.2). For such a functional, the neural circuit is very likely to have a large number of cells or complex synaptic interactions. Indeed, the number of cells in the medulla is five times higher than that of the lamina (Strausfeld, 1976). However, in order to simplify the model, we only consider the minimum number of cells and develop a model which is primarily formed by synaptic interactions. The other simplification is that we consider the inhibitory effect only. There is no strong evidence that the excitatory effect has to arise from an excitatory postsynaptic mechanism, because this effect could also be due to the facilitation interaction. Besides, it is redundant to model the excitatory effect; the inhibitory effect is similar to the excitatory effect except for a negative sign and the reverse

synaptic direction. The inhibitory model suggested before was based on a single type of cell (on cell or off cell) and a single direction of synapse as shown in Fig. 7.1a (Barlow and Levick, 1965; Torre and Poggio, 1978). However, this model can not elicit a reverse (forward) response by the lower two pairs of impulse stimuli of Fig. 3.2b (Fig. 3.2a). To meet all the functional requirements of the inhibitory interaction, the inhibition model is suggested as that shown in Fig. 7.1b. There are on and off type cells and four different synaptic configurations. As mentioned before, this model only accounts for the inhibitory effect, a correlation model (functional model) has to consider the excitatory effect. Because of the homogeneous structure of the medulla of the fly, it is more possible to have a model with the modified geometry as shown in Fig. 7.1c. Within this model a pair of on and off cells are in one medulla bundle. The inhibitory network forms a hexagonal structure. The class 2 transmedulla cell has a similar dendritic configuration (Strausfeld, 1976). The existence of the on and off cells has been shown by intracellular recording within the medulla (Devoe and Ockleford, 1976). However, there are more types of cells than on and off cells. Therefore, Fig. 7.1c may not be a realistic neural circuit (based on only two types of cells), but the reverse direction dendrite is one of the necessary suggestions to fulfill its functional.

The change of cross kernel dynamics under scotopic light conditions and photopic light conditions could follow the dynamics of the lamina cell by the same mechanism as the self kernels. Due to still poor knowledge of the lamina and medulla, a complete neural model
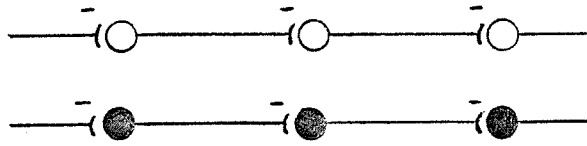
Fig. 7.1a Inhibition model.
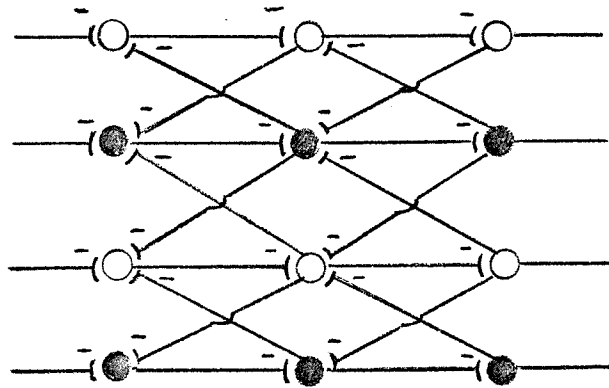
Fig. 7.1b Inhibition model with four types of
        synaptic interactions.
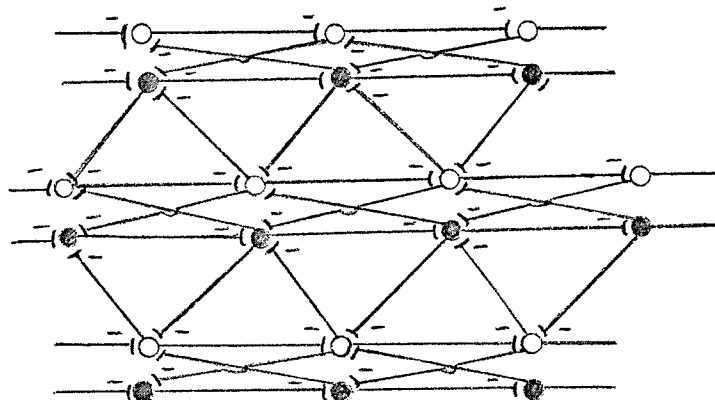
Fig. 7.1c Inhibition model suggested for the fly.

awaits further investigations.

7.4   Mechanisms of Light Adaptation of Class-II Cell

The results in chapters 4 and 5 privide evidence for intensity-
dependent spatial and temporal interaction. As already stated, the
dynamic change of temporal interaction between two channels has been
related to the dynamic properties of the lamina ganglion. The problem
left is the mechanism which controls the spatial interactions. The cross
kernel of two wide angle channels (horizontally and vertically separated)
appears as a mutual inhibition. This mutual inhibition is unlikely to
be due to the class-II cell itself, because the evidence of the reverse
direction responses indicates that the inhibition must exist before
the motion detection interaction. The lamina is the most likely place
subserving the spatial interaction. Zettler (1972) suggested that the
smaller receptive field of the monopolar cell compared to the recep-
tive field of the retina cell is because of the lateral inhibition mech-
anism. Besides, there was a morphological evidence (Strausfeld and Campos-
Ortega, 1977), which revealed that the interconnections between lamina
cartridges are possibly mediated by amacrine cells and L4 monopolar cells.
The spatial interactions processed by these cells mostly seem to be non-
linear. The reason that French and Jarvilehto (1978) did not find the
evidence of lateral inhibition of LMC cell could be due to their assump-
tion of linear interaction. Laughlin and Hardie (1978) suggested a sen-
sitivity control model to describe the LMC response under light adapted
conditions, the averaged voltage due to background intensity is sub-
tracted from retina cell response. This subtraction could arise by the

synaptic interaction between the L2 and receptors. The spatial inter-
action mechanism found here could be similar sensitivity control mech-
anism except that subtraction is by the neighbouring LMC cells via the
pathway of amacrine cells.

7.5 Conclusion

Through the class-II cell functional studied by the Wiener kernel,
three important factors could be abstracted, the temporal behaviour, the
spatial interaction, and the nonlinear term. Fig. 7.2 is a summarized
block diagram which presents a kernel model of the class-IIa1 cell asso-
ciated with all layers of ganglia. The retinular cells convert light
into electrical signals by a rather linear mechanism. The lamina controls
light sensitivity and has a second order nonlinearity. The acuity of the
class-IIa1 cell may be controlled within the retina by superposition or
in the medulla by a neural recruitment mechanism. Lateral interactions
have two functional types. The directionally independent interaction
arises from the monopolar cells in the lamina. The directionally depen-
dent interaction arises from the medulla and the second order cross
kernel models this interaction in a way which is very similar to a corre-
lation model.
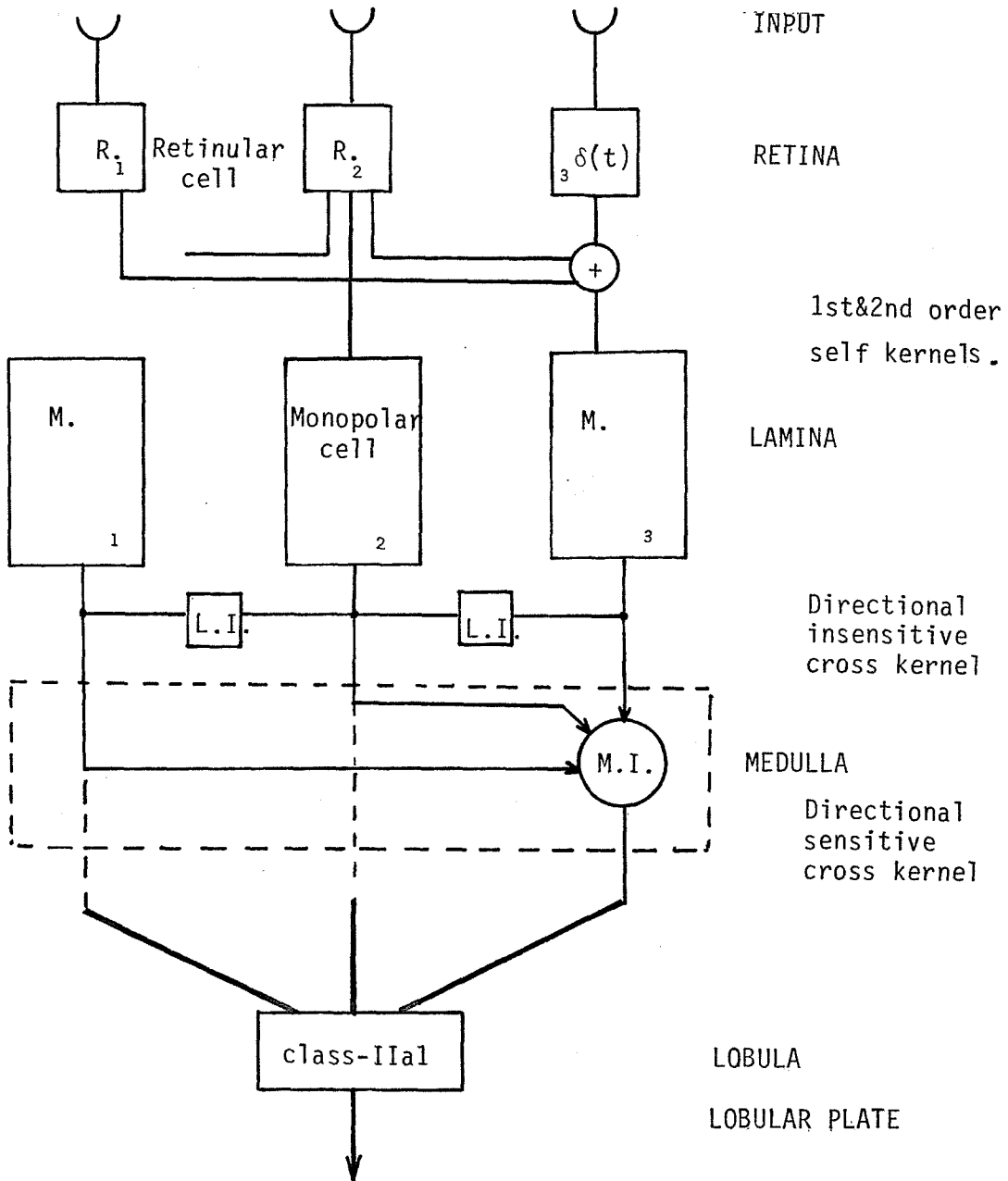
Fig. 7.2 Functional model of Class-IIa1 cell.
M.I. denoting motion specific interaction,
L.I. denoting lateral interaction.

REFERENCES

Abelson, H. (1977): Computational geometry of linear threshold. Information and Control. 34:66-92.

Arnett, D. W. (1971): Receptive field organization of units in the first optic ganglion of Dipterans. Science (Washington). 173:929.

Autrum, H. (1977): Concept and method in sensory physiology. J. Comp. Physiol. 120:87-100.

Barker, H. A. (1970): High-order autocorrelation functions of pseudorandom signals based on m-sequences. Proc. IEEE. 117:1857-1863.

Barlow, H. B. and Hill, R. M. (1963): Selective sensitivity to direction of motion in ganglion cells of the rabbit's retina. Science.139:412-414.

Barlow, H. B. and Levick, W. R. (1965): The mechanism of directionally selective units in rabbit's retina. J. Physiol. 178:477-504.

Barlow, H. B. (1972): Dark and light adaptation. Handbook of Sensory Physiology. V.VII/4:1-28.

Bedrosian, E. (1971): The output properties of Volterra systems. Proc. IEEE. 59:1688-1707.

Beersma, D. G. M., Starenga, D. G., and Kuiper, J. W. (1975): Organization of visual axes in the compound eye of the fly Musca domestica and behavioral consequence. J. Comp Physiol. 102:305-320.

Beersma, D. G. M., et al. (1977): Retina lattice, visual field and binocularities in flies. Dependence on species and sex. J. Comp. Physiol. 119:207-220.

Bishop, L. G. and Keehn, D. G. (1966): Two types of motion sensitive neurons in the optic lobe of the fly. Nature. 212:1374-1476.

Bishop, L. G. and Keehn, D. G. (1967): Neural correlates of the optomotor response in the fly. Kybernetic. 3:288-295.

Bishop, L. G., Keehn, D. G., and McCann, G. D. (1968): Motion detection by interneurons of optic lobes and brain of the flies Calliphora phaenicia and Musca domestica. J. Neurophysiol. 31:509-525.

Boschek, C. B. (1971): On the fine structure of the peripheral retina and lamina ganglionaris of the fly Musca domestica. Z. Zellforsch. 118:369-409.

Braitenberg, V. (1967): Patterns of projection in the visual system of the fly. I. Retina-lamina projections. Exp. Brain Res. 3:271-298.

Braitenberg, V. and Strausfeld, N. I. (1973): Principles of the mosaic organization in the visual system's neuropil of Musca domestica. Handbook of Sensory Physiology. VII/3:631-659.

Brillinger, D. R. (1976): Identification of synaptic interactions. Biol. Cybernetics. 22:213-228.

Burkhardt, D. (1964): Colour discrimination in insects. Advances in Insect Physiology. Vol. 2. Academic Press, New York.

Burkhardt, D., Darnhofer-Demar, B., Fischer, K. (1973): Zum binokularen Entfernungssehen der Insekten. I. Die Struktur des Sehraums von Synsekten. J. Comp. Physiol. 87:165-188.

Burkhardt, D. (1977): On the vision of insects. J. Comp. Physiol. 120:33-50.

Buchner, E. (1976): Elementary movement detector in an insect visual system. Biol. Cybernetics. 24:85-101.

Buchner, E. and Gotz, K. G. (1978): Elementary detector for
    vertical movement in the visual system of Drosophila.
    Biol. Cybernetics. 31:235-242.

Bussgang, J. J. and Ehrmann, L. (1974): Analysis of nonlinear
    system with multiple inputs. Proc. IEEE. 62:1088-1119.

Campbell, F. W. and Green, D. G. (1965): Optical and retinal
    factor affecting visual resolution. J. Physiol. 181:576-593.

Campbell, F. W. (1974): The transmission of spatial information
    through the visual system. In The Neuroscience: Third study
    program (Ed. by Schmidt, F. O. and Worden, F. G.), 95-103.
    M. I. T. Press, Cambridge, Mass.

Campos-Ortega, J. A. and Strausfeld, N. J. (1972): Columns and
    layers in the second synaptic region of the fly's visual
    system: the case for two super-imposed neuronal architectures.
    Information processing in the visual system of Arthropods.
    R. Wehner. (Ed.) Berlin, New York: Springer-Verlag.

Caughey, T. K. (1975): Nonlinear analysis, synthesis, and identifica-
    tion theory. Proc. First Symp. on Testing and Identification of
    Nonlinear Systems. (CALTECH).

Collett, T. S. and Blest, A. D. (1966): Binocular, directionally
    sensitive neurons, possibly involved in the optomotor response
    of insects. Nature. 212:1330-1333.

Collett, T. S. and Land, M. F. (1975): Visual control of flight
    behaviour in the hoverfly, Syritta pipiens L. J. Comp. Physiol.
    99:1-66.

Collett, T. S. and Land, M. F. (1978): How hoverflies compute
    interception courses. J. Comp. Physiol. 125:191-204.

Daitch, J. M. and Green, D. G. (1969): Contrast sensitivity of the
    human peripheral retina. Vision Res. 9:947-952.

Devoe, R. D. and Ockleford, E. M. (1976): Intracellular responses from cells of the medulla of the fly Calliphora erythrocephala. Biol. Cybernetics. 23:13-24.

Dill, J. C. (1970): A computer-aided investigation of motion detection units in the fly. PhD Thesis California Institute of Technology.

Doekele, G. S. (1975): The neural superposition eye and its optical demands. J. Comp. Physiol. 102:297-304.

Dvorak, D. R., Bishop, L. G., and Eckert, H. E. (1975): On the identification of movement detectors in the fly optic lobe. J. Comp. Physiol. 100:5-23.

Dvorak, D. and Snyder, A. (1978): The relationship between visual acuity and illumination in the fly. L. S. Z. Naturforsch. 33C:139-143.

Dvorak, D. et al. (1980): The contrast sensitivity of fly movement-detecting neurons. Vision Res. 20:397-407.

Eckert, H. E. (1978): Response properties of dipteran giant visual interneurons involved in control of optomotor behaviour. Nature. 271:358-360.

Eckert, H. (1980): Functional properties of the H1-neurons in the third optic ganglion of the blowfly, phaenicia. J. Comp. Physiol. 135:29-39.

Franceschini, N. (1975): Sampling of the visual environment by the compound eye of the fly: Fundamentals and applications. Photoreceptor Optics (Eds. A. W. Snyder, R. Menzel), 98-125. Berlin-Heidelberg, New York: Springer.

Franceschini, N. and Kirschfeld, K. (1976): Le controle automatique du flux lumineux dans l'oeil compose des Dipteres. Proprietes spectrales, statiques et dynamiques du mecanisme. Biol. Cybern. 21:181-203.

French, A. S. and Jarvilehto, M. (1978): The transmission of information by first and second order neurons in the fly visual systems. J. Comp. Physiol. 126:87-96.

Gafni, H. and Zeev, Y. Y. (1979): A model for processing of movement in the visual system. Biol. Cybernetics. 32:165-173.

Geiger, G. and Poggio, T. (1975): The orientation of flies towards visual patterns on the search for the underlying functional interactions. Biol. Cybernetics. 19:39-54.

Gordon, B. (1972): The superior corriculus of the brain. Scientific American. 227:72-82.

Gotz, K. G. (1968): Flight control in Drosophila by visual perception of motion. Kybernetic. 4:199-208.

Gotz, K. G. (1972): Principles of optomotor reactions in insects. Biol. Ophthal. 82:251-259.

Gotz, K. G. (1973): Visual control of locomotion in the walking fruit fly Drosophila. J. Comp. Physiol. 85:235-266.

Gotz, K. G. (1975): The optomotor equilibrium of the Drosophila navigation system. J. Comp. Physiol. 99:187-210.

Hamdorf, H., Paulsen, R., and Schwemer, J. (1973): Photogeneration of sensitivity control of photoreceptors of invertebrates. Proceedings of the Symoposium on the Biochemistry and Physiology of Visual Pigments. Springer-Verlag. Berlin.

Hardie, R. C. (1979): Electrophysiological analysis of fly retina. I. Comparative properties of R1-6 and R7 and 8. J. Comp. Physiol. 129:19-33.

Harper, T. and Rugh, W. (1976): Structural features of factorable Volterra systems. IEEE Autom. Control. 21:822-832.

Hartline, H. K. and Ratliff, F. (1957): Inhibitory interaction of
    receptor units in the eye of Limulus. J. Gen. Physiol.
    40:1357-1376.

Hausen, K. (1976): Functional characterization and anatomical
    identification of motion sensitive neurons in the lobula plate of
    the blowfly Calliphora erythrocephala. Z. Naturforsch. 31:629-633.

Heimburger, L., Poggio, T., and Reichardt, W. (1976): A special
    class of nonlinear interactions in the visual system of the
    fly. Biol. Cybernetics. 21:103-105.

Heisenberg, M. (1972): Comparative behavioural studies of two
    visual mutants of Drosophila. J. Comp. Physiol. 80:119-136.

Heisenberg, M. and Gotz, K. G. (1975): The use of mutations for
    the partial degradation of vision in Drosophila melanogaster.
    J. Comp. Physiol. 98:217-241.

Heisenberg, M. and Buchner, E. (1977): The role of retinula cell
    types in visual behavior of Drosophila melanogaster.
    J. Comp. Physiol. 117:127-162.

Hochstein, S. and Shapley, R. M. (1976): Linear and nonlinear
    spatial subunits in Y-cat retina ganglion cells.
    J. Physiology. 262:265-284.

Horridge, G. A. (1965): The physiology of the insect central neurons
    system.

Horridge, G. A. (1977): The compound eye of insects. Scientific
    American. 237:108-120.

Hubel, D. H. (1959): Single unit activity in striate cortex of
    unrestrained cats. J. Physiol. 147:226-238.

Hubel, D. H. and Wiesel, T. N. (1959): Receptive fields of single
    neurons in the cat's striate cortex. J. Physiol. 148:574-591.

Jarvilehto, M. and Zettler, F. (1971): Localized intracellular potentials from pre- and postsynaptic components in the external plexiform layer of an insect retina. Z. Vere Physiol. 75:422-440.

Jarvilehto, M. and Zettler, F. (1973): Electrophysiological histological studies on some functional properties of visual cells and second order neurons of an insect retina. Z. Zellforsch. 136:291-306.

Jarvilehto, M. (1976): Spectral and polarization sensitivity of identified retinual cells of the fly. Neural Principle in Vision. 214-226. F. Zettler (Ed.). Springer-Verlag. Berlin.

Julesz, B. (1975): Experiments in the visual perception of texture. Scientific American. 232:34-43.

Kien, J. (1975): Neuronal mechanisms subserving directional selectivity in the locust optomotor system. J. Comp. Physiol. 102:337-355.

Kirschfeld, K. (1972): The visual system of Musca. Optics structure and function. Information Processing in the Visual System of Arthropods. 61-74. R. Wehner (Ed.). Springer-Verlag. Berlin.

Kirschfeld, K. and Lutz, B. (1974): Lateral inhibition in the compound eye of the fly Musca. Z. Naturforsch. 29C:95-97.

Kirschfeld, K. and Snyder, A. W. (1976): Measurement of a photoreceptor's characteristic waveguide parameter. Vision Res. 16:775-778.

Krausz, H. (1975): Identification of nonlinear system using random impulse train inputs. Biol. Cybernetics. 19:217.

Krausz, H. I. (1977): The analysis of nonlinear synaptic transmission. J. Gen. Physiol. 70:243-265.

Kroeker, J. P. (1977): Wiener analysis of nonlinear systems using Poisson-Charlier cross correlation. Biol. Cyber. 89:331-357.

Laughlin, S. B. (1975a): Adaptation of the dragonfly retina for contrast detection and the elucidation of neural principles in the peripheral visual system. In: <u>Neural Principles in Vision</u>. F. Zettler (Ed.). 175-193. Springer-Verlag. Berlin.

Laughlin, S. B. (1975b): Receptor function in the opposition eye: An electrophysiological approach. In: Photoreceptor optics (Eds. Snyder, A. W. and Menzel, R.) 479-498. Berlin-Heidelberg-New York: Springer.

Laughlin, S. B. and Hardie, R. C. (1978): Common strategies for light adaptation in the peripheral visual systems of fly and dragonfly J. Comp. Physiol. 128:319-340.

Lee, Y. W. and Schetzen, M. (1965): Measurement of the Wiener kernels of a nonlinear system by cross correlation. <u>Int. J. Control</u>. 2:237-254.

Lettvin, J. Y., Maturana, H. R., McCulloch, W. S., and Pitts, W. H. (1959): What the frog's eye tells the frog's brain. <u>Proc. Inst. Radio Engrs. N. Y.</u>: 147:1940-1951.

Leutscher-Hazelhoff, J. T. and Kuiper, J. W. (1966): Clock spikes in the <u>Calliphora</u> optic lobe and a hypothesis for their function in object location in C. G. Bernhard (Ed.). <u>The Functional Organization of the Compound Eye</u>. Pergaman Press, New York.

Magleby, K. L. (1973): The effect of receptive stimulation on facilitation of transmitter release at the frog neuromuscular junction. <u>J. Physiol</u>. (Lond.). 234:327-352.

Mann, R. (1979): On identification of separable kernel systems. <u>Biol. Cybernetics</u>. 35:197-204.

Marmarelis, P. Z. (1971): Nonlinear Dynamics Transfer Functions for Certain Retinal Neuronal Systems. PhD Thesis, CALTECH.

Marmarelis, P. Z. and McCann, G. D. (1973): Development and application of white-noise modeling techniques for studies of insect visual nervous system. <u>Kybernetics</u>. 12:74-90.

Marmarelis, P. Z. and Naka, K. I. (1974): Identification of multi-input biological systems. IEEE Trans. Biomedical Engineering. BME-21:88-101.

Marmarelis, P. Z. and McCann, G. D. (1975): Optimization of test parameters in the identification of spike train response of biological systems through random test signals. Proc. of the First Symp. Testing and Identification of Nonlinear Systems. Marmarelis, P. Z. and McCann, G. D. Eds. Pasadena, Ca. CALTECH. 325-338.

Marmarelis, V. Z. (1977): A family of Quisa-White random signals and its optimal use in biological system identification. Biol. Cybernetics. 27:49-56.

Mastebroek, H. A. K., Zaagman, W. H., and Lenting, B. P. M. (1980): Movement detection: performance of a wide-field element in the visual system of the blowfly. Vision Res. 20:467-474.

Maturana, H. R. and Frenk, S. (1963): Directional movement and horizontal edge detectors in pigeon retina. Science. 142:977-979.

McCann, G. D. and MacGinitie, G. F. (1965): Optomotor response studies of insect vision. Proc. R. Soc. London. B163:369-401.

McCann, G. D. and Dill, J. C. (1969): Fundamental properties of intensity from, and motion perception in the visual nervous systems of Calliphora phaenicia and Musca domestica. J. Gen. Physiol. 53:385-413.

McCann, G. D. and Foster, S. F. (1971): Binocular interactions of motion detection fibers in the optic lobes of flies. Kybernetics. 8:193-203.

McCann, G. D. (1973): The fundamental mechanism of motion detection in the insect visual system. Kybernetics. 12:64-73.

McCann, G. D. (1974): Nonlinear identification theory models for successive stages of visual nervous systems of flies. J. of Neurophysiology. Vol. 37, No. 5, 869-895.

McCann, G. D., Fargason, R. D., and Shantz, V. T. (1977): The response properties of retinula cells in the fly Calliphora erythrocephala as a function of the wavelength and polarization properties of visible and ultraviolet light. Biol. Cybernetics. 26:93-107.

Meffert, P. and Smola, V. (1976): Electrophysiology measurements of spectral sensitivity of central visual cells in the eye of the blowfly. Nature. 260:342-344.

Mimura, K. (1972): Neural mechanism observing direction selectivity of movement in the optic lobe of the fly. J. Comp. Physiol. 80:409-437.

Mimura, K. (1974): Analysis of visual information in lamina neurons of the fly. J. Comp. Physiol. 88:335-372.

Mimura, K. (1976): Some spatial properties in the first optic ganglion of the fly. J. Comp. Physiol. 105:65-82.

Minsky, M. and Papert, S. Perceptrons. An introduction to computational geometry. Cambridge, Mass: MIT Press.

Nagano, T. and Fujiwara, M. (1979): A neural network model for the development of direction selectivity in the visual cortex. Biol. Cybernetics. 32:1-8.

O'shea, M. and Fraser-Rowell, C. H. (1975): Protection from habituation by lateral inhibition. Nature. 254:53-54.

Palka, J. (1969): Discrimination between movements of eye and object by visual interneurons of crickets. J. Exp. Biol. 50:723-732.

Palka, J. (1972): Moving movement detectors. Am. Zool. 12:497-505.

Palm, G. (1978): On representation and approximation of nonlinear systems. I. Biol. Cybernetics. 31:119-124.

Palm, G. (1978): On representation and approximation of nonlinear systems. II. Biol. Cybernetics. 34:49-52.

Palm, G. and Poggio, T. (1977): Wiener-like system identification in physiology. J. Math. Biology. 4:375-381.

Pick, B. (1974): Visual flicker induces orientation behaviour in the fly Musca. Z. Naturforsch. Teil C29:310-312.

Pick, B. (1976): Visual pattern discrimination as an element of the fly's orientation behaviour. Biol. Cybernetics. 23:171-180.

Pick, B. (1977): Specific misalignments of rhabdomere visual axes in the neural superposition eye of dipteran. Biol. Cybernetics. 26:215-224.

Pick, B. and Buchner, E. (1979): Visual movement detection under light and dark adaptation in the fly Musca domestica. J. Comp. Physiol. 134:45.

Pierantoni, R. (1973): An observation on the giant fiber posterior optic tract in the fly. Biol. Cyber. Congress. Leipzig.

Poggio, T. and Reichardt, W. (1973a): Consideration of models of movement detection. Kybernetics. 13:223-227.

Poggio, T. and Reichardt, W. (1973b): A theory of pattern induced flight orientation of the fly Musca domestica. Part I. Kybernetics. 12:185-203.

Poggio, T. and Reichardt, W. (1975): A theory of pattern induced flight orientation of the fly Musca domestica. Part II. Kybernetics. 18:69-80.

Poggio, T. and Reichardt, W. (1976a): Visual control of orientation behaviour in the fly. I. Q. Rev. Biophys. 9:311-375.

Poggio, T. and Reichardt, W. (1976b): Visual control of orientation behaviour in the fly. II. O. Rev. Biophys. 9:377-438.

Poggio, T. and Reichardt, W. (1980a): Characterization of nonlinear interactions in the fly's visual system. Recent Theoretical Developments in Neurobiology. MIT Press. (in press).

Poggio, T. and Reichardt, W. (1980b): Properties of polynomial algorithms multi-input systems. Biol. Cybernetics. (in press).

Pollen, D. A., Andrews, B. W., and Feldon, S. E. (1978): Spatial frequency selectivity of periodic complex cells in the visual cortex of the cat. Vision Res. 18:665-682.

Power, R. L. (1979): Iontophoretic studies of visual neurons in Drosophila melanogaster. PhD Thesis. CALTECH.

Reichardt, W. (1961): Autocorrelation, a principle for the evaluation of sensory information by the central nervous system. Sensory Communication. (W. A. Rosenblith Ed.) 303-317.

Reichardt, W. and Wenking, H. (1969): Optical detection and fixation of objects by fixed flying flies. Naturwissenschaften. 56:424-425.

Reichardt, W. (1972): Nervous integration in the facet eye. Biophysical Journal. 2:121.

Reichardt, W. and Poggio, T. (1979): Figure-ground discrimination by relative movement in the visual system of the fly. Biol. Cybernetics. 35:81-100.

Seelen, W. V. and Hoffmann, K. P. (1976): Analysis of neuronal networks in the visual systems of the cat using statistical signals. Biol. Cybernetics. 22:7-20.

Sekuler, R. (1974): Spatial vision. Ann. Rev. Physiol. 25:195-232.

Sheby, R. (1978): Wiener kernel analysis of the functional microstructure of a crustacean visual field. PhD Thesis. CALTECH.

Snyder, A. W. (1977): Acuity of compound eye, physical limitation and design. J. Comp. Physiol. 116:161-182.

Snyder, A. W. (1979): Physics of vision in compound eyes. Handbook of Sensory Physiology. VII/6A Vision in Vertebrate.

Strausfeld, N. (1971): The organization of the insect visual system (light microscopy) I. Projections and arrangements of neurons in the lamina ganglionaris of Diptera. Z. Zellforsch. 121:377-441.

Strausfeld, N. J. (1976): Atlas of an insect brain. Springer-Verlag Heidelberg, New York.

Strausfeld, N. J. and Campos-Ortega, J. A. (1977): Vision in insects: Pathways possibly underlying neural adaptation and lateral inhibition. Science. 195:894-897.

Torre, V. and Poggio, T. (1978): A synaptic mechanism possibly underlying directional selectivity to motion. Proc. R. Soc. London. B202:409-416.

Virski, R. and Reichardt, W. (1974): Tracking of moving objects by the fly Musca domestica. Naturwissenschaften. 61:132-133.

Virski, R. and Reichardt, W. (1976): Detection and tracking of moving objects by the fly Musca domestica. Biol. Cybernetics. 23:83-98.

Vowles, D. M. (1964): Models and the insect brain, in R. F. Reiss (Ed.) Neural Theory and Modeling. 377-399. Standford Univ. Press.

Vowles, D. M. (1966): The receptive fields of cells in the retina of the house fly Musca domestica. Proc. Roy. Soc. B164:552-576.

Wehrhahn, C. and Reichardt, W. (1975): Visually induced height orientation of the fly Musca domestica. Biol. Cyber. 20:37-50.

Wehrhahn, C. (1978): Flight torque and lift responses of the house fly Musca domestica to a single stripe moving in different parts of the visual field. Biol. Cyber. 29:237-247.

Wiener, N. (1958): Nonlinear problems in random theory. Cambridge, Mass. MIT Press.

Yoshiak, Washizu, and Burkhardt, D. (1964): Visual field of single retinula cells and interommatidial inclination in the compound eye of the blowfly <u>Calliphora</u>. <u>Zeitschrift für Vergleichende Physiologie</u>. 48:413-428.

Zaagman, W. H., Mastebroek, H. A. K., Buyse, T., and Kuiper, J. W. (1977): Receptive field characteristics of a directionally selective movement detector in the visual system of the blowfly. <u>J. Comp. Physiol</u>. 116:39-50.

Zaagman, W. H., Mastebroek, H. A. K., and Kuiper, J. W. (1978): On the correlation model performance of a movement detecting neural element in the fly visual system. <u>Biol. Cyber</u>. 31:163-168.

Zettler, F. and Jarvilehto, M. (1972): Lateral inhibition in an insect eye. <u>Z. Vergl. Physiologie</u>. 76:233-244.

Zettler, F. and Autrum, H. (1975): Chromatic properties of lateral inhibition in the eye of a fly. <u>J. Comp. Physiol</u>. 97:181-188.